Mechanistic Dissection of the Cop9 Signalosome's Deneddylation Activity on Cullin-RING Ligases

Thesis by

Ruzbeh Mosadeghi

In Partial Fulfillment of the Requirements

for the Degree of

Doctor of Philosophy

California Institute of Technology

Pasadena, California

2015

(Defended April 3rd, 2015)

Acknowledgements

The work in the following thesis is the culmination of a great deal of thought and sweat, only a portion of which was mine. Without the intellectual and physical help of the following people, as well as their mental support, this work would never have come to completion. I would first like to thank Dr. Raymond J. Deshaies, my thesis advisor for offering me a position in his lab and agreeing to mentor me as I started my scientific career. He had the difficult task of keeping me on track despite my deep desire to go on a variety of tangents with each new western blot. I learned a great deal through my interacts with him, particularly the art of designing a well controlled assay as well as how to critically assess the true meaning of data.

During my time in the Deshaies Lab, I also had the privilege of working with some of the most intelligent and accomplished scientists in the world. Rati Verma, taught me that nothing is to be taken at face value and the value of a critical eye and a dose of skepticism to new data. Proof is proof and there is no reason to settle for anything less. Senthil Radakrishnan, Min-Kyung Sung, Thang Nguyen, Xing Liu, Jing Li, and Gary Kleiger have been good friends with whom I have had the privilege to share scientific ideas and more than a few laughs. I would really like to thank all my fellow graduate students who have also endured the worthwhile trial by fire that is working in such an elite lab. Helen Yu and Emily Blyth, thank you for the many conversations about science and life. Michael Rome, Nathan Pierce and Kuang-Jung Chang taught me many of the basics of being a graduate student.

Tara Gomez has been a friend long since leaving the lab and taught me about the ins and outs of being a graduate student beyond the classes and experiments,

and being a perfect example of balancing life and school. Natalie Stone was never one to let me rant unchallenged and through our many debates and sessions commiserating about graduate school has become a life long friend, much like the older sister I never had. Robert Oaina, the gateway to the Deshaies Lab, is a large part of why anything is accomplished in the lab. His experimental experience is immense and was critical in my learning how to perform experiments. Outside of lab, Rob has been my partner in crime for the last five years and really made my time in the Deshaies Lab such an enjoyable experience. Justin Reitsma, I would like to thank for reinvigorating my love of science when it had reached its lowest and for showing me that through collaboration, scientific research really is a worthwhile endeavor.

Junyue Cao was an excellent rotation student and set up several assays that reall helped our understanding our how the CSN works. Minsoo Kim was a SURF student for several summers who help me make some of the most difficult proteins I have ever worked with.

Willem (Pim)den Besten and Kurt Reichermeier, Team Europe. I can't possibly thank you two more. I would like to thank Kurt for being a great friend, workout partner and mentee. His enthusiasm for science is contagious and really motivated me at the end of time here. Pim was my second mentor, whom I would like to thank for lending me an ear whenever I needed it for any concern I had in or out of lab. His depth of knowledge and scientific expertise are unrivaled and were a great help in the development of this project.

I would also like to thank Daphne Shimoda and Heenam Park for all of their support throughout my five years at Caltech. Ethan Emberley and Frank Parlati were my first mentors in the lab and were instrumental in helping me start my research on the mechanisms of the Cop9 Signalosome. I would also like to thank my committee Shu-ou Shan, Sarkis Mazmanian and David Chan for their guidance throughout the years.

Finally, I would like to thank all of my family and friends for all of your love and support throughout my studies. You made my life outside of lab immensely enjoyable and made me forget about all of the struggles. In particular, I would to thank my parents Jabbar and Parvaneh for giving up so much to give my brother and me opportunities that they never had and for always pushing us to maximize our potential. I owe a great deal of gratitude to my brother Sasan. He has been my mentor my entire life and the trailblazer who paved the path for me. His relentlessly driving me to be the best that I could be when I wanted to slow down and his refusal to accept mediocrity always replenished my willpower. Lastly, I would like to thank the love of my life, my wife, Lauren. I could not have endured all of the long years of this program without you. You were my cheerleader when I needed a pick-me-up. You were there to console me when I was in despair. You held me accountable when I wanted to slack and believed in me when I was skeptical. Thank you for always reminding me of the prize at the end and for supporting me the whole way there.

Abstract

We set out to understand the precise mechanisms that regulate the activation and deactivation of Cullin-RING Ligases (CRLs). While a great deal of work has already gone into identifying the players involved in these pathways and the cellular consequences associated with the loss of each, the biochemical mechanisms regulating these steps have remained elusive. In this work we sought to gain a better understanding of the mechanisms behind these steps by teasing apart specific their biochemical reactions. By measuring the individual microscopic rate constants of the reactions we have shed light on both the proper sequence of events in the regulation of CRLs as well as how they are in fact controlled.

Prior to this work, it was believed that CSN deactivated CRLs by binding them and enzymatically removing the activating post-translation modification Nedd8. It was believed that CSN could not bind to CRLs while they were active due to the steric hindrance by the CRL substrates, and that they would remain bound to deneddylated CRLs as a sequestering agent until a new substrate could displace it. We now have some insight that substrates themselves cannot inhibit CSN very well, but that the active ubiquitination by an E2 enzyme precludes CSN binding and activity. When the substrate for a CRL becomes depleted, CSN then binds to the CRL in a low affinity, low activity conformation. This triggers a conformational change that pulls the autoinhibitory Ins-1 loop away from the active site in the catalytic subunit Csn5, resulting in a large increase in affinity and cleavage of the isopeptide bond between CRLs and Nedd8. Upon dissociation of Nedd8, CSN rapidly returns to the low affinity state and dissociates from the CRL, allowing it reenter its activation cycle.

Table of Contents

Chapter 1: Introduction to the Ubiquitin Proteasome System and Cullin-RING Ligases

Ubiquitin Proteasome System

The cell, regardless of being a complete organism or part of one, comprises several basic components. The simplistic view of biologists midway through the last century was that these basic components were 1) nucleic acids, records and messages of the genetic code; 2) proteins that provide the internal skeleton of a cell, transmit messages, and carry out catalytic functions; and 3) lipids, which serve as boundaries of the cell and hold the contents within a structure separated from the outside world. Although these early functions of the basic components have been validated, the true complexity of the cell has turned out to be much more complicated than early biologists could have imagined.

One cataclysmic change that occurred in the field was in our understanding of the fate and stability of cellular proteins. It was thought that proteins within a cell were subject to regulation by transcription, and that once they were made they were relatively stable. The common belief at this time was that these newly transcribed proteins would remain stable in the cell until they were damaged. This of course, could not be the way that things function, given our current understanding of cell biology. There are many proteins, such as the cyclins, that directly regulate the cell cycle. When they are present they allow certain activities to occur which help progress the cell to the next stage of the cell cycle. We understand now that such signals, if left uninhibited, would cause the cell to replicate and divide over and over, and result in an uncontrolled expansion of cell number. This would either result in the organism growing exponentially throughout its life or, through a mechanism controlled by chromosomal telomeres, lead to premature senescence of cells and a shortened life span. Of course, cells do not replicate ad

infinitum, a process regulated by both controlling the activity of such proteins, as well as degrading them entirely.

In Eukaryotic cells, one mechanism that carries out the function of degrading proteins is the ubiquitin–proteasome system (UPS) (Deshaies and Joazeiro 2009). The UPS constitutes an elegant cascade of events, which target specific proteins within the cellular milieu for destruction by the covalent conjugation of the small protein ubiquitin. Ubiquitinated proteins are recognized by a massive protein complex, the proteasome, which degrades the said protein into its constituent amino acids. The UPS can be readily be broken down into two processes: 1) Ubiquitination, in which a ubiquitin molecule is covalently attached to a protein, and 2) proteasomal degradation, which uses three different protease active sites encased within a cylindrical chamber to degrade the specific subset of the ubiquitinated proteinz. The most universally accepted definition of a proteasome substrate is a protein tagged with a chain of four or more ubiquitins connected to each other through lysine 48 or lysine 11 of one ubiquitin and the C-terminus of another.

Ubiquitin

The ubiquitin molecule is a very simple yet extraordinary precise signal that is utilized by the cell for a variety of functions. Ubiquitin is a 76 amino acid protein expressed from four different genes as polyubiquitins or ribosomal protein fusions . Through the function of USPs free ubiquitin is formed from these polyproteins. The free ubiquitin can then be conjugated to an acceptor lysine’s ε-amino group on the target protein through its C-terminal glycine’s carboxylic acid group forming an isopeptide

bond. The result of this reaction will be a monoubiquitinated protein (Komander and Rape 2012).

Analogous to phosphorylation, many signaling functions of the cell are carried out by the attachment of a single ubiquitin molecule. In addition, more ubiquitin molecules can be attached to the first ubiquitin on a variety of lysines to form a chain. Chain formation through different lysines on ubiquitin can yield topologically distinct signals. Chains formed by linkages through specific lysines have been shown to carry out unique signaling functions by binding different classes of receptors (Komander and Rape 2012). For example, proteasomal degradation is thought to depend on proteasome receptors binding to K48- or K11-linked ubiquitin chains, whereas K63-linked chains have been shown to functions as nondestructive signals for a variety of cellular processes.

Although ubiquitin has been implicated in a variety of diseases, ubiquitin itself has not been shown to be a causative agent. There is, however, some evidence that the UBB+1 form of ubiquitin has been associated with tauopathies and polyglutamine diseases. The UBB+1 protein is formed by the molecular misreading that yields a frame shift mutation in the translated protein (Dennissen, Kholod et al. 2011).

In addition to ubiquitin, there are a variety of other ubiquitin-like molecules that use very similar mechanisms as the ubiquitin cascade. Under certain conditions, these proteins can replace each other and enter each other's cascades. It remains to be determined whether or not this phenomenon is physiologically relevant.

E1 – Ubiquitin Activating Enzyme

After the formation of monomeric ubiquitin molecules, the initial step in activating the ubiquitination cascade starts with an E1 enzyme. E1 proteins are known as

ubiquitin activating enzymes because they utilize the energy of ATP to form a covalent thioester bond to the C-terminal carboxyl group of the ubiquitin. This newly activated ubiquitin can now be moved along the cascade using the energy of its thioester to be conjugated to proteins (Schulman and Harper 2009).

In mammalian cells, there are at least two E1 enzymes capable of activating ubiquitin *in vitro*, implying that there is some degree of redundancy. Ube1 is the main gene thought to carry out this function *in vivo*, since many of the other related proteins have been shown to predominantly carry out their functions on other ubiquitin-like proteins. Uba6 is another E1 enzyme has been proposed to be an E1 under certain conditions, although later work showed that its preferred substrate is the Ubl FAT10. It remains to be seen which other E1s are true ubiquitin activating enzymes *in vivo* and what roles they play in cellular biology.

To date, genetic analysis of Ube1, the sole strict ubiquitin E1 enzymes, has revealed a role in one disease. Three separate mutations in exon 15 of UBE1 have been shown to cause X-linked Infantile Spinal Muscular Atrophy (XL-SMA) (Nouspikel and Hanawalt 2006). The fact that these mutations are fatal during the infantile period shows that, despite the possible redundancy, the activation of the ubiquitination cascade by Ube1 is critical to human development.

E2-Ubiquitin Conjugating Enzymes

After activating an ubiquitin molecule with ATP, the E1 enzyme will pass the ubiquitin along to a variety of E2 ubiquitin conjugating enzymes. This is accomplished by transferring ubiquitin from the E1 to the active cysteine of the E2. Once the ubiquitin has been loaded onto the E2 enzyme, the E2 can interact with a partner E3 to transfer the

ubiquitin to a substrate. See below for more detail about the interaction between E2s and E3s. This cycle can occur once or be repeated many times and lead to a polyubiquitinated substrate (van Wijk and Timmers 2010).

Although many known E2 enzymes form K48 linked chains, E2s can facilitate other types of linkages. For example, Ubc13 is known to form K63 linked ubiquitin chains. All in all, mammalian cells have at least 35 active E2 proteins to carry out conjugation of ubiquitin as well as the other UBLs.

E3 – Ubiquitin Ligases

A common theme in the ubiquitination cascade is that the further you move along, the more players are involved. Moving from a single E1 to initiate the activation of ubiquitin molecule to its final attachment as a post-translation modification on a large number of proteins within a cell requires a great deal of specificity. Much of this specificity is derived from the E3 ubiquitin ligases. The E3 ligases can be subdivided into two groups based on domain homology: HECT domain E3 ligases and RING-finger, or RING domain, E3 Ligases. Because E3 ligases serve to deliver ubiquitin to terminal substrates, some of which are non-essential, they tend to be intricately involved in many diseases when they are deleted or functionally impaired. In the absence of E3 ligases, proteins can accumulate inappropriately and impair the cell's ability to signal, or in some cases, form insoluble aggregates within cells (Popovic, Vucic et al. 2014).

When one thinks of the typical ubiquitination cascade in which the ubiquitin is sequentially passed along the E1, E2, E3, and finally to the substrate, it is typically one that involves a HECT domain E3 Ligase. HECT domain ligases, (HECT: Homologus to E6-AP Carboxyl Terminus), accept the ubiquitin molecule to form a third thioester from

their cognate E2. The ubiquitin molecule is then transferred to the lysine of a substrate bound directly to or in a complex with the E3 enzymes. Through this direct transfer of ubiquitin, the specificity of the ubiquitin chain linkage can be decided by the E3 ligase since the E2 protein is not involved in the process after the thioester transfer to the E3 (Kim and Huibregtse 2009).

RING domain E3 ligases, in contrast, never covalently bind the ubiquitin molecule. RING domain E3s serve two distinct functions in the final conjugation of ubiquitin to their substrates: 1) they activate the E2 enzyme to more readily transfer its covalently bound ubiquitin to the substrate, and 2) they bring the substrate in close proximity to the E2 so that the transfers can readily occur. As opposed to being an active intermediate in the chemical reaction, RING domain E3 ligases serve as scaffolds between E2s and substrates to mediate the transfer of ubiquitin.

RING (Really Interesting New Gene) domain proteins, were first described in the early 1990's as a class of proteins with conserved cysteine and histidine residues organized in semi-symmetric units, which selectively bind two zinc atoms. Although proteins of the RING domain family appeared to look very much like zinc finger proteins and were postulated to be involved in DNA binding, the length of the loop between the two zinc binding domains excludes this possibility. In the time since, the family of RING proteins has grown from the 27 originally defined to over 300 members in the human genome (Deshaies and Joazeiro 2009).

Although RING domains are fairly heterogeneous and one cannot make hard and fast rules, the RING domain appears to be the predominant binding site for the incoming E2 ubiquitin conjugating enzymes. Further studies have show that RING domains do not

just serve as the binding domain for E2s, but can in fact increase the activity of E2s (Deshaies and Joazeiro 2009).

A large number of diseases are caused by mutations in E3 ligases, and it is beyond the scope of this thesis to list them all. Whereas we see very few diseases caused by mutations in the early steps of the ubiquitination cascade, the phenomenon of E3 proteins being directly linked to diseases probably occurs because they are more specific for smaller subsets of substrates than E1, E2s, or ubiquitin itself. This is evidenced by the fact that not all E3s are essential to life and there can be a certain level or redundancy for the degradation of very critical substrates, such as c-myc, a powerful proto-oncogene when not properly regulated (Skaar, Pagan et al. 2013).

Cullin-RING Ligases

Within the larger family of RING domain ligases there is a subset of E3 ligases defined by a scaffold protein containing cullin homology repeats that functions as a heterodimer with one of the RING domain protein, Rbx1 or Rbx2. Cullins 1, 2, 3, 4A and 4B are always found as a stable heterodimer with Rbx1 bound to their C-terminal domain, while Cul5 is always bound to Rbx2. The cullins are typical RING ligases in the sense that they use their RING subunit to recruit and activate the E2 enzymes to directly transfer ubiquitins to the substrate. They also function like other RINGs E3 ligases because they essentially serve as a scaffold to organize substrates and E2 proteins to come within close proximity to enable ubiquitin transfer (Deshaies and Joazeiro 2009).

The first Cullin-RING Ligase family member to be reconstituted was that consisting of Cullin 1 (Cul1), Skp1 and the Fbox protein Cdc4, collectively referred to as an SCF complex. With the exception of Cul3 proteins, each cullin has a single adaptor to

which it binds. For Cul1, the adaptor protein is the s-phase kinase-associated protein 1 (Skp1). Adaptor proteins bind cullins near the N-terminus, the opposite end of the scaffold from where the RING finger protein and the E2 bind (Deshaies and Joazeiro 2009). Skp1 recognizes its binding partners through what is referred to as an F-box motif.

Although each cullin associates with a single adaptor, they have the capability to ubiquitinate hundreds of substrates each. This massive expansion in the repertoire of cullin substrates is due to the ability of each cullin adaptor to bind many substrate receptors. There are nearly 70 F-box containing proteins, which serve as the substrate receptors for Cul1 through their interaction with Skp1. Each of these F-box proteins contains substrate recognition domains, which have evolved to bind substrates with great specificity. The recognition motifs of the F-box domains vary greatly and, depending on the specific F-box protein, can recognize degrons comprising of phosphorylation, binding co-factors, glycosylation, small molecules and protein interactions accessible only when the target protein is not bound to its natural partner (Skaar, Pagan et al. 2013). Each substrate receptor can potentially bind multiple substrates provided that they contain similar degrons. Two exceptions should be noted: 1) Cul3 does not have a single adaptor protein and directly binds all of its substrate receptors (BTB domain proteins) (Deshaies and Joazeiro 2009) and 2) DDB2, a substrate receptor of Cul4, is known to bind damaged DNA and facilitate the ubiquitination of proteins in vicinity of the damage rather than the DNA itself (O'Connell and Harper 2007).

The F-box proteins can be subdivided into three broad categories based on additional domains that they possess. The first group is the Fbl proteins, which bind their substrates via a luecine rich repeat (LRR) domain. LRR domains tend to be shaped like a

scythe and known to be involved in protein binding. In this work, we will discuss Skp2, which is the best-studied Fbxl. Skp2 is special because it is known to function with an accessory protein, Cks1, which helps mediate binding to its substrates. The best studied of these substrates is the cell cycle inhibitor p27. p27 carries out its function by binding the heterodimer of a Cyclin-dependent Kinases (CDK) and its activating cyclin. p27 is thought to be a substrate of SCF^{Skp2} while it is bound to it to the cyclin-CDK dimer, although only p27 is ubiquitinated and destroyed (Skaar, Pagan et al. 2013).

One particular target of p27 is cyclin E, or rather, the cyclin E-Cdk2 (EK2) heterodimer, which itself is a substrate of an SCF complex that contains the F-box protein Fbw7. Fbw7 belongs to the WD-containing class of Fbxw proteins. This class of proteins contains a WD domain, which forms a beta-propeller structure that serves as their substrate recognition domains. Many also contain D-domains allowing them to form homodimers. Some of the substrates for Fbw proteins, such as cyclin E, are known to have multiple degrons and it is thought that homodimerization of Fbw7 allows for more efficient ubiquitination of cyclin E and other target substrates by binding them in multiple locations (Welcker and Clurman 2008). It should be noted that since EK2 is part of two separate SCF complexes with each one degrading only a single protein, SCF^{Skp2} degrades p27 and SCF^{Fbw7} degrades cyclin E, the implication of this finding is that the orientation of substrates can be a determining factor for which free lysine residues are covalently modified by ubiquitin.

The third and final group of Fbox proteins is that of the Fbx “other”, or Fbxo, family. This category is more of a catch-all for non-LRR or non-WD-40 domain-

containing F-box proteins, and some members of this class have very specific binding domains (Skaar, Pagan et al. 2013).

Mutations in substrate receptors for every cullin have been linked to a number of diseases, particularly cancer. Those linked to cancer have been classified either as oncogenes or tumor suppressors. The full lists of these mutations have been widely published and specifics have been worked out for many of these proteins. For the purposes of our experiments, it should be noted that Skp2 is an oncogene and Fbw7 is a tumor suppressor. The mechanism of Skp2's oncogenic activity appears to be by its overexpression leading to a reduction of its substrate p27. Since p27 is a cell cycle inhibitor, its reduction is thought to lead to an increase in cellular replication and a poor prognosis in cancer. Fbw7, on the other hand, is a major tumor suppressor, and when the substrate binding sites within its WD-40 domain are mutated there is a robust expression of its substrate, the well-known oncogenes, c-myc and Notch (Welcker and Clurman 2008).

Regulation by Cand1

For a long time it had been known that cullins bind numerous Fboxes that are all competing for the same binding site with fairly high affinity, since the entire SCF complex could survive being expressed in baculo cells, immunoprecipiated and purified by size-exclusion chromatography. It was also known that cullins could bind to a protein known as Cullin-associated Nedd8 dissociated 1 (Cand1). Cand1 was thought to play a role in sequestering cullins away from active ubiquitination by binding a large portion of the cullin near both termini. One of Cand1's binding sites near the C-terminus of Cullins blocks the conjugation site of an activating modification by the Ubl Nedd8 discussed

below. Paradoxically, there has never been any clear evidence of Cand1 negatively regulating CRLs *in vivo*. In fact, as will become clearer with the data that has been recently published, as well as that which will be presented within this work, many "negative regulators" of the CRL pathway function to make the entire system quicker and more efficient (Lydeard, Schulman et al. 2013).

For the case of Cand1, it turns out that when a more complete set of CRL interactors are introduced to the system, its binding to Cullins is anything but static, and thus its proposed role as a sequestering agent is obsolete (Pierce, Lee et al. 2013). As it turns out, Fboxes and Cand1 can both bind to cullins with incredibly high affinity, as long as they are in isolation of one another. When the off-rate of the Fbw7-Skp1 complex from Cul1 was measured with and without the presence of Cand1, Cand1 was found to increase the rate by approximately one million-fold while having a mere two-fold effect the on-rate. The data very clearly showed that Cand1's role in regards to SCFs was to act as an exchange factor, replacing substrate receptors and allowing the SCF to degrade a variety of substrates within a short period time. This showed that a protein which can both stably bind a Cullin, as well dissociate the CRL complex, can in fact help unbound substrate receptors gain access to the cullin. Moreover, it provided a rationale for why researchers were unable to find convincing evidence for Cand1 as a negative regulator of CRLs *in vivo.*

Nedd8

During the mid to late 90's, people had discovered the gene for Nedd8. Although they did not quite understand its function, they knew that it was a Ubl and that it appeared in two forms, one as small monomeric Nedd8 as well as a second larger form which

migrated around 90 kDa (Kawakami, Chiba et al. 2001). Early biochemical studies revealed the E1, NAE1 (a heterodimer of Uba3 and APPBP1) and E2 (Ubc12) enzymes that are required for the neddylation of proteins. Interestingly, despite being the closest homolog of ubiquitin, Nedd8 was only found conjugated to proteins as a monomer. In fact, under normal physiological conditions one cannot readily see Nedd8 chains. Also, in the absence of over-expression, Nedd8 has only been found as a post-translation modification on Cullin family proteins. To this day, Cullins are the only validated targets of Nedd8 despite numerous reports of Nedd8 conjgation to other proteins. Later the Dcn family of E3 proteins (Defective in cullin neddylation) was found to facilitate the neddylation of cullins. In human cells these proteins appear to be partially redundant, and the exact function for each has not yet been differentiated (Lydeard, Schulman et al. 2013).

Even today, the exact function of Nedd8 is not clearly understood. However, it has been known for a long time that Nedd8 acts as an activator of CRLs. Prior to the recent findings on the function of Cand1, it was thought to be a signal to inhibit Cand1's function as a sequestering agent, thus allowing for more ubiquitination. Separately, Nedd8 has been shown to activate the transfer of ubiquitin by SCF in the absence of Cand1. Thus, Nedd8 provides at least two separate functions for the activation of cullins. Saha et al found that the modification of Nedd8 could activate almost every single aspect of E2 recruitment and ubiquitin transfer during the process of ubiquitination. Notebly, they found that Nedd8 enhances E2 recruitment to the SCF, brings the E2 in closer proximity to the substrate thus helping to bridge a 50 angstrom gap seen the crystal structures between substrate and E2, and increases the k_{cat} of Ubiquitin transfer.

Concurrent with the biochemical data that showed the effect of neddylation on the kinetic parameters of ubiquitination, the crystal structure of neddylated Cul5 was published. The crystal structure showed, in two asymmetric conformations, that the RING domain protein, Rbx1 in this case, did not have a large surface buried against the cullin as in the case of unneddylated Cul1. The attachment of Nedd8 appears to dramatically alter the C-terminus of cullins and allow the RING protein to pop up like a spring. This, along with the biochemical data, implied that one of the roles of Nedd8 is to alter the conformation of cullins to release its RING protein, which would allow the RING domain and its bound E2 to move closer to the substrate bound to the substrate receptors via the N-terminus of cullin. This can readily explain the shift in kinetic parameters seen upon neddylation.

It should be noted however that there is another explanation for the crystal structure and the effects of neddylation. Around this same time, there was an observation published by Singer and colleagues that Nedd8 allows for the dimerization of Cul3 *in vivo* . This model, albeit controversial, does have some precedence because other RING domains are known to function in dimers through their RING domains (Dou, Buetow et al. 2012). In the family of RBR proteins (RING in-between RING), two of the RING domains fold and bind one another (Koyano, Okatsu et al. 2014). However, Singer's hypothesis was not thoroughly proven for two reasons: 1) the lysate assays were not done in the presence of neddylation or deneddylation inhibitors (the former was not first described until two years after this work was published) and 2) Many BTB proteins form homodimers similarly to Fboxes (Skaar, Pagan et al. 2013).

One striking effect that neddylation is now known to have is its ability to inhibit Cand1 mediated Fbox exchange. Through a series of powerful biochemical assays, Pierce et al. were able to show that neddylation can eliminate the ability of Cand1 to alter the off-rate of Fboxes. In essence, their data implied that when a cullin is bound to a substrate and neddylated, Cand1 could not perturb its ability to transfer ubiquitin molecules to its substrate (Pierce, Lee et al. 2013).

Nedd8 is essential in almost all eukaryotes besides *S. cerevisiae*, which does not require its homolog, Rub1, under normal conditions. The role of cullins has been thoroughly noted in human diseases as described above, and there are currently neddylation inhibitors (MLN4924) being tested in clinical trials for the treatment of hematological tumors (Soucy, Smith et al. 2009). One association of the Nedd8 protein to human disease comes from a post-translation modification in *Burkholderia pseudomallei and* Enteropathogenic *Escherichia coli* (EPEC) by the protein cyclomodulin cycle inhibiting factor (CIF). CIF is known to deaminate both ubiquitin and Nedd8. The mechanistic specifics of the deamiation of Nedd8's Gln40 to glutamate are still being worked out, but it appears that the alteration inhibits the activity of cullins and is directly responsible for some of pathogenesis found in EPEC infections (Morikawa, Kim et al. 2010).

Cop9 Signalosome (CSN)

The first subunit of the Cop9 Signalosome, CSN, was discovered in Arabidopsis during the early 90's when Deng and colleagues were screening for mutations that produced a constitutive photomorphogenic phenotype. A mutation in the Cop9 protein, which has since been named Csn8, was found to allow for photomorphogensis, the

response of seedlings in light, under both light and dark conditions. Thus the original phenotype of loss of function of the Cop9 Signalosome was the inability of seedlings to not sprout under dark conditions. Through some diligent work, it was discovered that CSN is 350 kDa, eight-subunit, heteromeric metalloprotease. To date, the only proven function of CSN is removal of Nedd8 from CRLs so as to return them to a state where they are less likely to engage in substrate ubiquitination and be more susceptible to Fbox exchange by Cand1. CSN shares considerable homology with both the lid complex of the 19S regulatory cap of the proteasome as well as the translation initiation factor 3 (eIF3). All three of these complexes are made up of proteins that carry either a PCI domain (Proteasome, Cop9, Initiation Factor 3) or an MPN domain (Mpr1p and Pad1p *N*-terminal). The MPN domains can be further subdivided into MPN+ or MPN- proteins depending on whether or not they contain a JAMM domain (Jab1/MPN Metalloprotease) capable of chelating the catalytic zinc ion. The JAMM domain proteins are a class of metalloenzyme, many of which play a role in ubiquitin or Ubl cleavage, such as the proteasome lid subunit Rpn11, the K63-linked DUB AMSH, as well BRCC36, the DUB in the BRCA1-RAP80 complex. Functionally, the JAMM domains chelate a zinc molecule using two histidines and an aspartate. The catalytic water molecule that is activated by a glutamate on a different loop offers the fourth chelation site for the zinc. CSN contains two MPN proteins as well as six PCI domain proteins. Of the two MPN domain proteins, Csn5 is the only active metalloprotease and carries out the only validated catalytic function of the Cop9 Signalosome. Csn5 catalyzes the removal of Nedd8 from cullin-RING ligases (Wei, Serino et al. 2008). The other MPN domain subunit, Csn6 does not have an active JAMM domain, but is thought to play a role in

regulating Csn5 activity (Lingaraju, Bunker et al. 2014). The remaining subunits all contain a PCI domain.

Recently, the crystal structure of CSN was published shedding a great deal of light onto its organization and potential regulation. The core of CSN is formed by two distinct organizational centers. The first is formed by the interdigitation of the winged-helix domains (WH) of all eight subunits. A second organization center is formed on one side of the WH domains by the PCI domains of the six proteins that contain them. The remaining portions of the PCI domain subunits fan out into a horseshoe shape. On the opposite side of the WH domains rests the dimer of CSN5 and CSN6, which point toward the neddylated surface of the Cullin. The majority of the contact between the SCF and CSN appears to come from the N-terminus of Csn2 and potentially some from Csn4 contacting the Rbx1 protein as well as Cul1. The data for Csn4 is implied by conformational shifts, but biochemical proof is still missing. N-terminal deletions mutants of Csn2, on the other hand have been show to be defective in deneddylating Cul1 (Lingaraju, Bunker et al. 2014).

JAMM domains share a large amount of homology, which is not surprising given that they all act on similar substrates. However they all contain one loop that is widely divergent. The Ins-1 loops of the different JAMM domains tend to be very different from each other, but are highly conserved among the same proteins in different species. What is clear is that a large amount of specificity for substrates is derived from difference in Ins-1. In the case of Csn5, there appear to be four highly conserved residues that are all capable of hydrogen bonding, 103-TETR-106. As opposed to many other isopeptidases,

CSN appears to be autoinhibited and incapable of cleaving a model reagent consisting of a fluorophore attached to the C-terminus of ubiquitin or other UBLs. Although CSN can readily cleave Nedd8 off of CRLs, another interesting fact is that CSN requires an intact complex to carry out its isopeptidase activity, i.e., Csn5 alone cannot cleave Nedd8 from Cul1. Recently, two papers have shed some light on the role of the Ins-1 in the autoinhibition of CSN. They have each made a single point mutant in either E104 or R106 that exhibit deregulated activity. In the case of the E104A mutation, the researchers were able to show that their CSN complex could cleave the fluorophore rhodamine from the C-terminus of ubiquitin. The results from the R106A mutation were less convincing, but implied that mutation of the arginine alleviates autoinhibition and this allows monomeric Csn5 to cleave Nedd8 from Cul1 (Echalier, Pan et al. 2013). More work is required to fully understand the functional role and regulation of CSN by Ins-1.

As has been the case many times in the study of Cullin-RING- Ligases, the *in vitro* biochemical result that CSN inhibits CRL activity does not hold in the context of an intact cell. In fact, the result of either knocking down Csn5 in human cells or *S. pombe* was a stabilization of CRL substrates with a concomitant loss of Fboxes. Thus it appears that losing the negative regulatory function of CSN allows for ubiquitination by a CRL to run rampant and cannibalize its own substrate receptors. Originally, this was a rather confusing results but since the function of Cand1 has now been elucidated, it is clear that in the absence of neddylation, substrate receptors are incapable of being removed after the ubiquitination of their substrates and thus become targets of the E3 ligases themselves. This then can then potentially lead to the buildup of substrates in two distinct ways 1) new substrates will not be able to gain access to a cullin or 2) the rate of

degradation of substrate receptors will outstrip their rate of synthesis and thus the steady-state levels of receptors will be insufficient to sustain recruitment and ubiquitination of CRL substrates. With almost every mechanistic insight that is discovered in the field of Cullin-RING Ligases, it appears that all of the players in the system are designed to make the system more efficient.

A major focus of work in this thesis and in the future will be determining precisely how the timing of each piece of the system is controlled. The current theory for the regulation of deneddylation by CSN is that substrates inhibit deneddylation (Enchev, Scott et al. 2012). Unfortunately, this result has never been fully tested. A second major focus of this dissertation will be on the functional regulation of deneddylation of CRLs by CSN. The two primary mechanisms we sought to understand are what regulates the binding of CSN to its neddylated-CRL substrate and what role does Ins-1 play in regulating the isopeptidase activity of CSN.

Chapter 2: Deconjugation of Nedd8 from Cul1 is directly regulated by Skp1–F-box and substrate, and CSN inhibits deneddylated SCF by a non-catalytic mechanism

The following chapter was published in the Journal of Biological Chemistry.

This is the accepted draft prior to formatting to standards of JBC.

Emberley, E. D., R. Mosadeghi and R. J. Deshaies (2012). "Deconjugation of Nedd8 from Cul1 is directly regulated by Skp1-F-box and substrate, and the COP9 signalosome inhibits deneddylated SCF by a noncatalytic mechanism." J Biol Chem 287(6): 9.

A majority of the work was carried out by Dr. Ethan Emberley, so devised the project.

My contributions were figures: Figure 2A-E), Figure 5A and B, Supplemental Figure 1C and D, Supplemental Figure 3 andSupplemental Figure 4.

Deconjugation of Nedd8 from Cul1 is directly regulated by Skp1–F-box and substrate, and CSN inhibits deneddylated SCF by a non-catalytic mechanism

Ethan D. Emberley[1,2], Ruzbeh Mosadeghi[1,2], and Raymond J. Deshaies[2,3,4]

[1]These authors made equal contributions to this work

[2]Division of Biology

[3]Howard Hughes Medical Institute

California Institute of Technology

Pasadena, CA 91125

[4]Corresponding author, Deshaies@caltech.edu (626) 395-3162

Abstract

COP9-Signalosome (CSN) mediates deconjugation of the ubiquitin-like protein Nedd8 from the cullin subunits of SCF and other cullin–RING ubiquitin ligases (CRLs). This process is essential to maintain the proper activity of CRLs in cells. Here, we report a detailed kinetic characterization of CSN-mediated deconjugation of Nedd8 from SCF. CSN is an efficient enzyme, with a k_{cat} of ~1 sec^{-1} and K_M for neddylated Cul1–Rbx1 of ~200 nM, yielding a k_{cat}/K_M near the anticipated diffusion-controlled limit. Assembly with an F-box–Skp1 complex markedly inhibited deneddylation, although the magnitude varied considerably, with Fbw7–Skp1 inhibiting by ~5-fold but Skp2–Cks1–Skp1 by only ~15%. Deneddylation of both SCF^{Fbw7} and $SCF^{Skp2\text{-}Cks1}$ was further inhibited ~2.5-fold by the addition of substrate. Combined, the inhibition by Fbw7–Skp1 plus its substrate cyclin E was greater than 10-fold. Unexpectedly, our results also uncover significant product inhibition by deconjugated Cul1, which results from the ability of Cul1 to bind tightly to CSN. Reciprocally, CSN inhibits the ubiquitin ligase activity of deneddylated Cul1. We propose a model in which assembled CRL complexes engaged with substrate are normally refractory to deneddylation. Upon consumption of substrate and subsequent deneddylation, CSN can remain stably bound to the CRL and hold it in low state of reduced activity.

Introduction

Cullin–RING ubiquitin ligases (CRLs) are heteromeric enzymes comprising cullin, RING domain, and substrate receptor subunits (Petroski and Deshaies 2005, Deshaies and Joazeiro 2009). The cullin subunit serves as the backbone of the enzyme, displaying on one end a substrate receptor complex that recruits substrates for ubiquitylation, and on the other end a RING domain subunit (Rbx1/Roc1/Hrt1) that recruits a ubiquitin-conjugating enzyme that transfers ubiquitin to substrate.

CRLs comprise a family of up to 240 enzymes that exert a profound effect on eukaryotic cells and organisms. CRLs, in aggregate, appear to account for ~20% of total protein degradation by the ubiquitin-proteasome system (UPS)(Soucy, Smith et al. 2009), and have been implicated in myriad processes that underlie normal development and physiology (Cardozo and Pagano 2004). CRLs and the pathways they control are also prominent targets of mutation in human diseases. For example, the most common genetic defect observed in colon cancer is of the APC pathway, which mediates degradation of b-catenin via the CRL known as $SCF^{b\text{-}TrCP}$ (Frescas and Pagano 2008). Likewise, the CRL subunit Fbw7/Cdc4 is a prominent human tumor suppressor gene (Crusio, King et al.). Given their central roles in controlling numerous cellular processes, there is considerable impetus to understand how CRLs work and how they are regulated. Although much of the regulation in CRL pathways is focused on the substrates, the CRLs themselves are well-documented to be regulated by conjugation of the cullin subunit with the ubiquitin-like protein, Nedd8 (Bosu and Kipreos 2008, Deshaies, Emberley et al. 2010).

The Cop9 Signalosome is an 8-subunit complex that was originally discovered based on its role in controlling light-regulated development in *Arabidopsis thaliana* (Wei,

Serino et al. 2008). Insight into the molecular basis of CSN action began to emerge with the finding that in human cells CSN forms a stable complex with a particular subfamily of CRLs known as SCF ubiquitin ligases (Lyapina, Cope et al. 2001). A similar interaction was also detected in *Arabidopsis* (Schwechheimer, Serino et al. 2001). Importantly, CSN was shown to control Nedd8 modification of the Cul1 subunit of SCF (Lyapina, Cope et al. 2001). Whereas ~10-20% of Cul1 is typically modified with Nedd8 in wild type *Schizosaccharomyces pombe*, in CSN-deficient cells the entire population of Cul1 is neddylated. The reason for this is that CSN-deficient cells lack an enzymatic activity that deconjugates Nedd8 from Cul1 (i.e. deneddylates). Subsequently, it was shown that this enzymatic activity resides within the Csn5 subunit of CSN and is specified by a novel metalloenzyme motif referred to as the 'JAMM' domain (Cope, Suh et al. 2002). It is now widely appreciated that CSN mediates deneddylation of all cullins, and appears to be the only enzyme capable of doing so with good efficiency (Bosu and Kipreos 2008, Deshaies, Emberley et al. 2010).

In vitro, CSN inhibits CRL activity (Yang, Menon et al. 2002). This can be readily understood, because conjugation of Nedd8 to Cul1 stimulates the activity of SCF (Read, Brownell et al. 2000, Kawakami, Chiba et al. 2001, Duda, Borg et al. 2008, Saha and Deshaies 2008). But, multiple lines of genetic evidence indicate that CSN is required to sustain CRL activity in cells (Bosu and Kipreos 2008). This apparent paradox is resolved by the observation that CSN-mediated inactivation of CRLs counteracts autocatalytic breakdown of substrate receptor subunits (Wee, Geyer et al. 2005, Cope and Deshaies 2006, Denti, Fernandez-Sanchez et al. 2006). Thus, the principal physiological function of CSN appears to be to sustain optimal levels of CRL activity.

Several lines of evidence point toward CSN playing an important role in human cancer, and potentially being a novel molecular target for cancer therapy. The catalytic subunit of CSN, Csn5, is overproduced in many human cancers, and its overproduction often correlates with poor survival (Shackleford and Claret 2010). Interestingly, the coding region for Csn5 is co-amplified along with that for c-Myc in some aggressive human breast cancers (Adler, Lin et al. 2006). Simultaneous overexpression of the two proteins synergistically activates c-Myc target genes, implicating Csn5 as a positive regulator of c-Myc. Moreover, expression of a catalytically-inactive mutant of Csn5 greatly attenuates growth of a c-Myc-driven tumor in mice (Adler, Littlepage et al. 2008). Likewise, knockdown of Csn5 suppresses growth of hepatocellular carcinoma in mice (Lee, Judge et al.). Finally, four subunits of CSN were shown to be required for the growth of human colon cancer cells that express GTPase mutant K-Ras, but not of isogenic cells in which the oncogenic *KRAS* allele was deleted (Luo, Emanuele et al. 2009). Taken together, these results suggest that CSN promotes cancer, and nominate Csn5 as a target for cancer therapy.

To successfully target CSN in cancer will require a better understanding of how CSN works in cells, which in turn will require a better quantitative understanding of CSN's biochemical properties. Although it has been known for ten years that CSN catalyzes the removal of Nedd8 from Cul1, the quantitative parameters for this reaction have yet to be described, due to the complexity of both the enzyme and its substrate. Here, we establish enzyme and substrate preparations and quantitative biochemical assays that allowed us to measure the steady-state kinetic parameters for substrate deneddylation by CSN. Our most important finding is that different F-box proteins can

directly inhibit deneddylation of their Cul1 partner to variable extents, and this inhibition is potentiated upon binding of substrate. We also find that CSN has unusually high affinity for its reaction product, unmodified Cul1–Rbx1. Finally, we document that CSN can also inhibit the ubiquitin ligase activity of purified, unmodified SCF, pointing to a new and unexpected role of CSN as a stoichiometric inhibitor of the activity of deneddylated CRLs.

Results

We set out to characterize in-depth CSN's deneddylating activity by developing an *in vitro* assay in which the conversion of neddylated Cul1 to Cul1 could be quantitatively measured. CSN was purified from HEK293 cells that stably express the Csn2 subunit modified with an N-terminal FLAG tag (Wu, Yamoah et al. 2003). CSN recovered from an anti-FLAG affinity column was further enriched by gel filtration prior to being used for the experiments described here. All eight subunits were found to be present in the purified material, in apparently stoichiometric amounts (Fig. 1*A*). Mass spectrometry analysis of purified CSN identified two co-fractionating proteins (Ddb1 and Hsp70) that could not be totally removed by conventional methods such as high salt or treatment with ATP and Mg^{2+} (data not shown).

To develop a quantitative, multi-turnover assay for deneddylation, we first sought to generate a labeled form of Nedd8. To this end, we fused a sequence encoding eight histidines followed by a protein kinase A phosphorylation site to the N-terminus of Nedd8 to generate His-PKA-Nedd8 (HPN8). When Cul1 was neddylated with HPN8 (HPN8-Cul1) and subsequently purified by gel filtration and nickel-NTA

chromatography, the resulting CSN substrate was 98% neddylated as determined by SDS-PAGE (Supplemental Figs 1*A*, *B*). After radioisotope labeling with [^{32}P]-ATP and cAMP-dependent protein kinase, >97% of the total signal from Nedd8 was attached to Cul1 as determined by phosphorimaging (Fig. 1*B,* time=0*)*. When CSN (1 nM) was added to HPN8-Cul1 (50 nM) and the reaction progress analyzed, deneddylation proceeded at a linear rate (Fig. 1*B*, *C*).

Prior to performing kinetic analyses, we carried out a series of control experiments. First we confirmed that the phosphorylated His-PKA tag had little to no effect on the rate of deneddylation of Cul1 (Supplemental Fig. 1*C*). Second, we compared rates of deneddylation by our FLAG-tagged CSN prepared from 293 cells with untagged CSN expressed in insect cells from recombinant baculoviruses (Supplemental Fig. 1*D*) and untagged CSN expressed in *E. coli* (Sharon, Mao et al. 2009) (Supplemental Fig. 1*E*). The FLAG tag had no discernable effect on the activity of CSN isolated from eukaryotic cells. Meanwhile, the enzyme purified from *E. coli* was ~2-fold less active, possibly due to removal of terminal sequences from some subunits to facilitate expression.

To obtain enzymological metrics for CSN-mediated deneddylation, we evaluated reaction rate as a function of substrate concentration. CSN was held constant at 0.8 nM and the initial rates of deneddylation at varying concentrations of HPN8-Cul1–Rbx1 were determined (Supplemental Fig. 1*F*). The rates for each concentration of substrate were plotted and fitted to the Michaelis-Menten equation, which yielded a K_M of 212 nM and k_{cat} of 1.1sec^{-1} (Fig. 1*D*).

Within cells, the fraction of Cul1 that is modified by Nedd8 is higher for Cul1 bound to F-box proteins (Read, Brownell et al. 2000, Kawakami, Chiba et al. 2001, Chew

and Hagen 2007). We reasoned that this might arise from differential rates of deneddylation of Cul1, depending upon its assembly status. To test this possibility, we compared rates of deneddylation for HPN8-Cul1–Rbx1 versus three different HPN8-conjugated SCF holoenzyme complexes. Deneddylation of HPN8-SCF^{Fbw7} and HPN8-$SCF^{b\text{-}TrCP}$ was assayed at 500 nM. Strikingly, Fbw7–Skp1 had a major effect, reducing the rate of deneddylation by 5.8-fold (Fig. 2*A*). b-TrCP–Skp1 had a weaker effect, reducing the rate by 2.2-fold. However, the recombinant b-TrCP used for this experiment lacks the N-terminal 138 amino acids, which were removed to facilitate efficient expression (Wu, Xu et al. 2003). Interestingly, not all F-box proteins were inhibitory. Addition of Skp2–Cks1–Skp1 reduced the rate of deneddylation by <20% (Fig. 2*B*). We do not understand the basis for this difference in behavior but note that endogenous Cul1 co-precipitated with transiently expressed F-box proteins was ≥50% neddylated in b-TrCP and Fbw7 immunoprecipitates, but considerably less modified in Skp2 immunoprecipitates (Supplemental Fig. 2*A, B* and data not shown).

In other work we have shown that a mutant of Skp1 (Skp1ΔΔ) used for crystallography (Schulman, Carrano et al. 2000) that lacks two acidic internal loops was able to bind Cul1–Rbx1 and assemble an active SCF complex, but was unable to promote displacement of Cand1 from Cul1–Rbx1 (Goldenberg, Cascio et al. 2004) (N. Pierce and R.J.D., unpublished data). Because Fbw7–Skp1 had the most potent effect on deneddylation, we tested the impact of the Skp1 loops in this context. Interestingly, the loop deletions reduced the inhibitory effect of Fbw7–Skp1 by ~2.5-fold (Supplemental Fig. 3). However, the acidic loops of Skp1 were not sufficient to specify inhibition of deneddylation, because our Skp2–Cks1–Skp1 contained wild type Skp1.

Given the substantial effect of Fbw7–Skp1 on deneddylation, we next sought to test whether binding of substrate to Fbw7 might further influence deneddylation of the associated HPN8-Cul1. There is good reason to think this might be the case – Cul1 co-precipitated from cells with SCF substrates is essentially 100% neddylated (e.g., see (Read, Brownell et al. 2000)), implying that substrate might either increase the rate of neddylation or decrease the rate of deneddylation above and beyond the effect of the F-box protein. Consistent with this possibility, the addition of the Skp2–Cks1 substrate $p27^{kip1}$ to $SCF^{Skp2\text{-}Cks1}$ complexes in fractionated cell lysate decreases Cul1 deneddylation (Bornstein, Bloom et al. 2003). However, because this experiment was carried out with undefined protein fractions, a clear explanation for this phenomenon remains lacking.

To test the effect of substrate in a defined system, we compared the rate of deneddylation of HPN8-SCF^{Fbw7} in the presence and absence of full-length phospho-cyclin E bound to Cdk2. Cyclin E must be phosphorylated on at least two sites (T380 and S384) to serve as a substrate for SCF^{Fbw7} (Welcker, Singer et al. 2003). Addition of phospho-cyclin E–Cdk2 further reduced the rate of deneddylation of HPN8-SCF^{Fbw7} by ~2.5-fold (Fig. 2*C*). The effect of substrate was specific, because phospho-cyclin E–Cdk2 had no effect on the rate of deneddylation of HPN8-Cul1 in the absence of Fbw7–Skp1 (Fig. 2*D*). Together, Fbw7 plus phospho-cyclin E reduced deneddylation by >10-fold. Note that this experiment was done with 50 nM substrate, in contrast to Fig. 2*A* which was done with 500 nM. Thus, the inhibitory effect of Fbw7–Skp1 on deneddylation of HPN8-Cul1 was similar when CSN was either sub-saturated or nearly saturated with substrate. To determine whether the effect of substrate applies to other SCF complexes, we tested the effect of phospho-p27–cyclin E–Cdk2 substrate on HPN8-$SCF^{Skp2–Cks1}$.

Addition of substrate reduced the rate of deneddylation by ~2.3-fold (Fig. 2*B*), similar to what was seen in Fig. 2*C*. A similar magnitude of substrate-mediated inhibition was observed when SCF^{Skp2} complexes were assayed in the presence of phospho-p27–cyclin E–Cdk2 under conditions that were permissive (+Cks1) or not permissive (-Cks1) for substrate binding and ubiquitylation (Fig. 2*E*). Taken together, these results imply that substrate reduced the rate of deneddylation equivalently regardless of whether or not it was undergoing ubiquitylation.

Cullin deneddylation *in vivo* must occur in the presence of a substantial concentration of unmodified cullins as well as a large constellation of factors that bind cullins, any one of which might have an impact on the rate of deneddylation. To address this issue, we evaluated deneddylation of HPN8-Cul1–Rbx1 in the presence of different recombinant proteins purified from *E. coli* and added at a fixed concentration of 1 μM. Neddylated substrate was mixed with each potential regulator and allowed to interact for 5 minutes at room temperature before CSN was added and the reaction progress was monitored. Interestingly, every single factor that was tested reduced the rate of deconjugation of HPN8 from substrate. The factors tested fell into two categories based on their ability to repress CSN deneddylase activity: moderate inhibitors (Ubc12, Dcn1, UbcH5C, Nedd8) which repressed deneddylation by 2.2 to 4.8 fold, and strong inhibitors (Cul1, Ubxd7, Cdc34, Cand1) which repressed deneddylation between 7.2 and 14.4 fold (Fig 3*A*). Supplemental Table 2 contains initial rates of deneddylation in the presence of each factor tested. Based on these results, we pursued in more detail the inhibition of deneddylation by Cand1 and unmodified Cul1–Rbx1.

Cand1 was previously reported to interact exclusively with unmodified cullins, including Cul1–Rbx1 (Liu, Furukawa et al. 2002, Zheng, Yang et al. 2002). Consistent with this, the co-crystal structure of Cul1–Rbx1–Cand1 showed that the Nedd8 conjugation site of Cul1 is partially obscured by Cand1 (Goldenberg, Cascio et al. 2004). Moreover, the crystal structure of Nedd8 conjugated to the C-terminal domain of Cul5 showed how a Nedd8-induced conformational change blocks binding of the N-terminal domain of Cand1 (Duda, Borg et al. 2008). Therefore, we were surprised to find Cand1 was a potent inhibitor of deneddylation (Fig. 3*A*). We investigated this property further in our *in vitro* deneddylation assay by keeping the concentrations of HPN8-Cul1–Rbx1 substrate (150 nM) and CSN enzyme (0.8 nM) constant and varying the concentration of Cand1. This experiment yielded an apparent inhibition constant of 160 nM (Fig. 3*B*). Two lines of evidence suggest that Cand1 inhibited deneddylation by binding substrate: addition of Cand1 increased the K_M but did not affect the k_{cat} for deneddylation of HPN8-Cul1 (Fig. 3*C*), and Cand1 exhibited no effect on the initial rate of deneddylation of HPN8-$SCF^{Skp2–Cks1}$ (Fig. 3*D*). These data suggest that binding of the C-terminal domain of Cand1 to the N-terminal domain of Cul1 (which is blocked by Skp1–Skp2–Cks1) interferes with recruitment of CSN. Notably, in *Aspergillus*, Cand1 is naturally split into two polypeptides, and the polypeptide corresponding to the C-terminal portion of human Cand1 can bind Cul1 in the absence of the N-terminal portion (Helmstaedt, Schwier et al. 2011).

CSN was also strongly inhibited by its reaction product, unmodified Cul1–Rbx1 (Fig. 3*A*). We determined the IC_{50} for Cul1to be 260 nM when assayed at 50 nM substrate (Fig. 3*E*) This suggests that the Nedd8 modification must not confer a large

amount of affinity for CSN, which is consistent with our observation that free Nedd8 was a weak inhibitor of deneddylation (Fig. 3*A*). The surprisingly strong apparent affinity of unmodified Cul1–Rbx1 product for CSN is consistent with our original discovery that CSN associates with a mutant Cul1 that lacks the extreme C-terminus including the Nedd8 conjugation site (Lyapina, Cope et al. 2001), and raises the possibility that product dissociation might be rate-limiting for substrate deneddylation.

To conclusively demonstrate that CSN can form a stable interaction with unmodified SCF, we mixed purified CSN with purified $SCF^{Skp2–Cks1}$ and fractionated the mixture on a Superdex 200 size exclusion column. $SCF^{Skp2–Cks1}$ that was not mixed with CSN was used for comparison purposes. In the presence of CSN, a fraction of the $SCF^{Skp2–Cks1}$ molecules were shifted to higher molecular weight fractions, corresponding to fractions that contained CSN (Fig. 4*A*).

To test whether unmodified full-length Cul1 (i.e. the product of deneddylation) exhibits significant binding to CSN in cells, we transiently transfected HA epitope-tagged wild type and K720R Cul1 expression constructs into HEK293 cells. K720R lacks the site on Cul1 to which Nedd8 is conjugated. Twenty-four hours post transfection, cells were lysed and the ^{HA}Cul1 was immunoprecipitated with HA antibody. The immunoprecipitates were then immunoblotted with antibodies to detect ^{HA}Cul1 as well as the endogenous Skp1, Rbx1, Csn5 and Cand1 proteins (Fig. 4*B*). Whereas wild type and K720R ^{HA}Cul1 were expressed at similar levels and bound similar amounts of Rbx1 and Skp1, the K720R mutant actually retrieved more Csn5 than wild type. By comparison, a recent proteomic study reported equivalent association of CSN with wild type and K720R-Cul1 in HEK293T cells (Bennett, Rush et al.). As independent confirmation of

this result, we examined the interaction of endogenous Cul1 with transiently-expressed FLAG-tagged Csn5. Cul1 co-immunoprecipitated with ^{FLAG}Csn5 was exclusively in the unconjugated form (Fig. 4*C*). Even if deconjugation occurred within the CSN–SCF complex *in vitro*, this result emphasizes the point that unlike traditional enzymes, CSN did not rapidly let go of its substrate upon deconjugating it. To more directly compare the association of CSN with neddylated and unmodified Cul1, we repeated this experiment with ^{FLAG}Csn5-ASA, which is mutated for two of the histidine residues that play a critical role in forming the active site that mediates deneddylation (Cope, Suh et al. 2002, Ambroggio, Rees et al. 2004). Although most of the endogenous Cul1 that co-immunoprecipitated with ^{FLAG}Csn5-ASA was modified with Nedd8, a substantial pool of unmodified Cul1 was recovered, confirming that unmodified cullin substrate can associate stably with CSN. Finally, to explore structure-activity relationships in greater depth, we also evaluated binding of endogenous CSN to ^{HA}Cul1 variants that could not bind to Skp1 and Rbx1. These mutants were generated by using the X-ray crystal structure of SCF as a guide (Zheng, Schulman et al. 2002). Both of these mutants bound less Csn5 (Fig. 4 *B*). The failure of the RING-deficient mutant to bind CSN is consistent with the original finding that Csn2 binds Rbx1 in a yeast 2-hybrid assay (Lyapina, Cope et al. 2001). Taken together, our data suggest that CSN exhibits a complex mode of interaction with Cul1 that is not dependent on Nedd8 and involves both ends of the elongated CRL complex.

Stable binding to substrate and/or product is unusual for an enzyme and suggested to us that CSN might regulate CRLs by mechanisms other than deconjugation of Nedd8. This possibility is further supported by our observation that multiple factors that interact

with Cul1, including the E2 enzymes UbcH5C and Cdc34, inhibited deneddylation of HPN8-Cul1–Rbx1. We therefore set out to test if CSN can inhibit SCF activity, independently of its effects on Nedd8 conjugation. An ubiquitylation reaction was set up that contained unmodified $SCF^{\beta TrCP}$ plus radiolabelled β-catenin peptide, ubiquitin, E1 and either UbcH5C or Cdc34. The ubiquitylation reaction was initiated by the addition of ATP and Mg^{2+} followed by the addition or omission of 300 nM CSN (which is slightly less than the estimated *in vivo* concentration of 500 nM in 293 cells; (Bennett, Rush et al. 2010)). The addition of CSN resulted in a 3.4 – 3.8-fold reduction in the rate of substrate conversion to products, independent of the E2 that was employed (Figs 5*A*, *B*). Inclusion of CSN affected both the extent of substrate conversion as well as the pattern of reaction products that were produced, indicating that CSN affected both ubiquitin chain initiation and elongation.

UbcH5 and Cdc34 catalyze SCF-dependent substrate ubiquitylation with K_M values that differ by about an order of magnitude (Saha and Deshaies 2008). Their equivalent sensitivity to inhibition by CSN suggested that CSN might not compete with E2 for binding to unmodified SCF. Consistent with this, 300 nM CSN exerted a similar fold inhibition of ubiquitylation in reactions that contained either 1 μM or 10 μM Cdc34 (Supplemental Fig. 4*A*). We also evaluated whether CSN might compete with substrate. Regardless of whether cyclin E peptide substrate was present at 0.1 μM or 1 μM, 300 nM CSN inhibited SCF^{Fbw7} to a similar degree (Supplemental Figure 4*B*).

Discussion

CSN mediates deneddylation of all cullins *in vivo*. However, the quantitative kinetic parameters of CSN-mediated deneddylation have remained largely unknown, owing in part to the complexity of the enzyme and its substrate. In this work, we developed reagents and methods that enabled us to measure quantitatively the deconjugation of radiolabeled Nedd8 from a purified Nedd8-Cul1–Rbx1 substrate. Here, we consider the implications of our quantitative measurements for the physiological function of CSN.

Affinity of CSN for substrate and product: Our studies reveal that CSN has high affinity (K_M = 212 nM) for Cul1 substrate. We do not know the K_D for the interaction, but given that k_{cat}/K_M is in the diffusion-limited range, it is possible that K_D is considerably lower than K_M. Contrary to what has been suggested elsewhere (Choo, Boh et al. 2011), we also show that deneddylated cullin binds tightly with CSN, although not quite as tightly as neddylated substrate. At least 4 lines of evidence support this claim: (1) CSN activity was significantly inhibited by unmodified Cul1–Rbx1, with an IC_{50} of 260 nM (Fig. 3E); (2) unmodified $SCF^{Skp2–Cks1}$ was shifted to higher molecular weight fractions on Sephadex 200 in the presence of CSN (Fig. 4A); (3) Csn5 stably co-precipitated with a mutant of Cul1 that cannot be neddylated (Fig. 4B); and (4) deneddylated Cul1 co-precipitated with both wild type Csn5 and a mutant that lacks deneddylase activity (Fig. 4C). These data add to a considerable body of evidence that CSN binds tightly to its reaction product. Indeed, the role of CSN in CRL biology was first discovered based on its efficient co-immunoprecipitation with a C-terminal truncation mutant of Cul1 that lacks the lysine 720 that Nedd8 is conjugated to (Lyapina, Cope et al. 2001). In the recent

quantitative proteomic study of Bennett et al, they reported that even in the absence of Nedd8 conjugation (brought about by the addition of the Nedd8 conjugation inhibitor MLN4924 to cells), nearly 50% of Csn6 remains associated with cullins 1 through 5 (Bennett, Rush et al. 2010).

Given the surprisingly tight binding of unmodified Cul1 to CSN and the total relative concentrations of CSN (500 nM) and Cul1-Cul5 (~1250 nM) in cells (Bennett, Rush et al. 2010), of which we estimate based on data shown in (39) that ~35% (~450 nM) is neddylated, it is plausible that the entire cellular pool of CSN is essentially saturated with neddylated and unmodified cullins. Indeed, based on the mole fraction of Csn6 that is bound to individual cullins, up to 60% of CSN remains associated with cullins following immunoprecipitation (Bennett, Rush et al. 2010). It is a reasonable possibility that most of the remaining 40% of CSN was also bound to cullins in cells but dissociated during the preparation and washing of the immunoprecipitates. Thus, it is possible that in cells, dissociation of CSN from CRLs is rate-limiting for deneddylation.

Catalytic rate of CSN: At saturating concentrations of Nedd8-modified Cul1 substrate, the maximal rate of CSN-mediated deneddylation is ~1 sec^{-1}, Although reasonably fast, this k_{cat} is ~100-fold slower than the maximal rate of cleavage of the model substrate CbzGly-L-Phe by the zinc metalloprotease carboxypeptidase A (Spilburg, Bethune et al. 1977). What is puzzling about the multi-turnover rate of 1 sec^{-1} is that it implies that the rate of product dissociation must be at least this fast. However, this is difficult to reconcile with the observations noted in the prior section that CSN binds to deneddylated CRLs with sufficient stability to survive gel filtration or immunoprecipitation. Resolution of this conundrum will require further experimentation.

A notable feature of the neddylation cycle is the rate at which it proceeds in cells. Application of the Nedd8 conjugation inhibitor MLN4924 to cells results in rapid loss of Nedd8 conjugates; although quantification was not reported, a conservative estimate is that 80% of neddylated cullins are consumed within 5 minutes (Soucy, Smith et al. 2009). This represents a minimal rate for deneddylation, since earlier time-points were not evaluated and it takes a finite amount of time for the drug to penetrate cells and effect depletion of the pre-existing pool of Ubc12~Nedd8 thioesters. Regardless, this rate is easily achievable. At the estimated cellular concentrations of CSN and total Nedd8-conjugated cullins (500 nM and 450 nM, respectively) and the k_{cat}/K_M for deneddylation reported here (~5 x 10^6 M^{-1} sec^{-1}), the pool of cullins could be extensively deneddylated within several seconds upon extinguishing Nedd8 conjugation activity.

Inhibition of deneddylation by F-box proteins, substrates, and other Cul1-binding factors: A key finding of this manuscript is that binding of F-box–Skp1 complexes to Cul1 can substantially reduce the rate of deneddylation. Fbw7–Skp1 slowed deneddylation by ~5-fold, and this effect was increased to >10-fold upon addition of phospho-cyclin E–Cdk2 substrate. Thus, in the environment of the cell where CSN is essentially saturated with neddylated and unmodified cullins, fully assembled SCF complexes that are engaged with substrate are expected to be comparatively immune to the action of CSN. This has important implications for the regulation of SCF complex deactivation and disassembly. Accumulation of substrate for a particular CRL complex would be expected to lead to accumulation of the Nedd8-conjugated form of that complex (Fig. 6, step 1). Upon consumption of the substrate (step 2), the CRL complex would either be subject to autoubiquitylation and degradation of the substrate receptor

(step 5) or recruit CSN and be deneddylated (step 3). Reappearance of substrate would lead to displacement of CSN (step 4) and re-formation of neddylated, active complex (step 1). By this mechanism, CRL complexes for which substrate is present would be preferentially neddylated and activated. In the absence of CSN (gray zone) this regulation would be undermined, and upon depletion of substrate for a particular CRL, the complex would remain conjugated to Nedd8 and active (step 2), leading to autoubiquitylation and ultimately degradation of the substrate receptor and inactivation of the CRL (step 5). We speculate that substrate adaptors that are most prone to become ubiquitinated in the absence of bound substrate will be the most sensitive to loss of CSN function. Several important questions remain unanswered by this model. For example, how do F-box proteins and substrates inhibit deneddylation? Why does Fbw7–Skp1 but not Skp2–Cks1–Skp1 potently inhibit deneddylation? How does Cand1 fit into this cycle?

In addition to Fbw7–Skp1, which interacts with the N-terminal domain of Cul1, every factor that is known to contact Rbx1 and/or the C-terminal domain of Cul1 that was tested here (UbcH5c, Cdc34, Ubc12, Dcn1, Ubxd7, Cand1) also inhibits deneddylation of Cul1 by CSN to some extent. We conclude that CSN is likely to make extensive contacts with Rbx1 and the C-terminal domain of Cul1. Our observation that Cand1 inhibits deneddylation is in direct conflict with a report to the contrary (Min, Kwon et al. 2005). We do not understand the reason for the discrepancy, but note that those authors measured deneddylation in a buffer that is completely lacking salt. We also draw attention to the inhibition of deneddylation by Ubxd7. Ubxd7 binds directly to the Nedd8 modification via an internal UIM domain (Bandau, Knebel et al. 2012, Besten, Verma et

al. 2012). Overexpression of Ubxd7 can cause accumulation of Nedd8-conjugated Cul2, suggesting that it can shield Cul2 from CSN *in vivo*.

CSN inhibits CRL activity by catalytic and non-catalytic mechanisms: CSN initiates deactivation of a neddylated CRL complex by reversing the Nedd8 modification. The deconjugated CRL has several fold less ubiquitin ligase activity (Read, Brownell et al. 2000, Kawakami, Chiba et al. 2001, Duda, Borg et al. 2008, Saha and Deshaies 2008). We suggest that in some instances, CSN remains stably bound to its product, and this reduces ubiquitin ligase activity even further. To investigate this possibility, we evaluated the effect of CSN on the basal activity of SCF that was not neddylated. Remarkably, 300 nM CSN (which is lower than its intracellular concentration) inhibited unmodified SCF by up to 3.5-fold. Equivalent inhibition of unmodified SCF occurred regardless of whether Cdc34 or UbcH5 was used as the E2, or whether Cdc34 was added at 0.1 (not shown), 1, or 10 μM. These observations suggest that the non-catalytic inhibitory activity of CSN was not competitive with respect to E2, even though E2 was able to inhibit deneddylation of HPN8-Cul1 by CSN. Likewise, CSN exhibited equivalent inhibition of $SCF^{Fbw7}$when assays were conducted with 0.1 or 1 μM cyclin E peptide substrate. We suggest that the E3 inhibition is a k_{cat} effect that arises because CSN restrains SCF in a low-activity conformation. Regardless of the exact mechanism, non-catalytic regulation is likely to be physiologically relevant, because nearly 30% of Cul1 and >40% of Cul4B are stably bound to CSN in 293T cells (Bennett, Rush et al. 2010). Indeed, genetic studies implicated fission yeast Csn1 and Csn2, but not Csn5, as being required for a specific function of CRL4 (Holmberg, Fleck et al. 2005), and a recent publication reported that

expression of catalytically inactive Csn5 partially restores proper CRL regulation in a Neurospora mutant that lacks Csn5 (Zhou, Wang et al. 2012).

While this manuscript was being drafted, it was reported that CSN potently inhibits autoubiquitylation of substrate receptor subunits within $CRL4A^{DDB2}$ and $CRL4A^{CSA}$ complexes (Fischer, Scrima et al. 2011). Remarkably, this inhibition was relieved by addition of a ligand for the substrate receptor. This suggests that binding of ligand/substrate to CSN–CRL4A complex activates CRL4A by facilitating dissociation of CSN. Interestingly, $CRL4A^{CSA}$ efficiently polyubiquitinates its substrate CSB in the presence of CSN. Although this is in apparent conflict with our results, the kinetics of CSB ubiquitylation were not evaluated in the presence and absence of CSN, so it is possible that CSN retards ubiquitylation of CRL4A substrates much as it does for SCF as shown here.

Improvements in biochemical assay methods (Saha and Deshaies 2008, Kleiger, Hao et al. 2009, Kleiger, Saha et al. 2009, Pierce, Kleiger et al. 2009) and mass spectrometry-based quantification (Bennett, Rush et al. 2010, Lee, Sweredoski et al. 2011) have begun to give us a much clearer picture of the numerical parameters that govern the ubiquitin ligase activity of CRLs and the mechanisms that regulate this activity. Systematic pursuit of these approaches, coupled with structural biology and enzymology, promises to reveal a detailed picture of how these enzymes work, how their activities are controlled, and how these features relate to their physiological roles in cells. We propose that this information will enable researchers to make good on the promise of basic science by developing novel medicines that target CRLs. Already, encouraging steps have been made in that direction (Ceccarelli, Tang et al. , Orlicky, Tang et al. ,

Soucy, Smith et al. 2009, Aghajan, Jonai et al.), and we can only hope, for the sake of patients, that there will be more to follow.

Materials and Methods

Purification of CSN

293F23V5 cells (gift from ZQ Pan, Mount Sinai School of Medicine, New York) stably expressing FLAG-Csn2 and Csn3-V5 (DTC# 56) were adapted to grow under suspension conditions in FreeStyle 293 Expression Medium (Invitrogen). When an approximate cell density of $5x10^5$ cells/mL was reached in a culture volume of 500 mL, cells were pelleted, washed once in cold PBS, pelleted again and flash frozen in liquid N_2. CSN was affinity purified using anti-FLAG M2 resin (Sigma) as previously described (Yamoah, Wu et al. 2005), except binding occurred over a 2 hour period, 1 mM EDTA was used, EGTA was omitted and Complete Mini EDTA-free Protease Inhibitor Cocktail (Roche) was used instead of individually adding different inhibitors. Following affinity purification, CSN was concentrated and immediately loaded onto a Superdex-200 gel filtration column equilibrated with 25 mM Tris, pH 7.5, 100 mM NaCl, 1 mM dithiothreitol, and 10% glycerol (storage buffer). Fractions containing CSN were pooled, concentrated with an Amicon Ultra-4 30k MWCO (Millipore), and aliquoted for storage at -80°C.

Purification of Nedd8

The artificial gene His8-PKA-Nedd8 was designed to aid in the purification of *in vitro* neddylated Cul1 and to be radiolabeled with ^{32}P for quantitative enzymatic analysis. The gene encoding the amino acid sequence

MHHHHHHHHRRGSLMLIKVKTLTGKEIEIDIEPTDKVERIKERVEEKEGIPPQQQR LIYSGKQMNDEKTAADYKILGGSVLHLVLALRGG, was purchased from DNA2.0 and put into their expression plasmid pJexpress414 (RDB# 2673). Expression was in BL21 (DE3) bacterial cells under ampicillin selection. 1 L cultures were grown at 37^{o}C until an OD_{600} of ~1.0 was reached. The temperature was dropped to 16°C before addition of isopropyl β-D-1-thiogalactopyranoside. Induction was carried out at 16°C overnight. Bacterial pellets were lysed by sonication in a buffer containing 50 mM Tris-HCl pH 7.6, 100 mM NaCl, 2 mM dithiothreitol and Complete Mini EDTA-free Protease Inhibitor Cocktail (Roche). The lysates were clarified by centrifugation and incubated with 1.5 mL of Ni Beads (Qiagen) per pellet from a 1 L culture. Binding to resin was allowed to occur for 2 h at 4^{o}C. The resin was washed two times with 50 column volumes of lysis buffer, followed by elution with 25 mM Tris, pH 7.5, 100 mM NaCl, and 200 mM imidazole. This mixture was then loaded onto a Superdex-75 gel filtration column equilibrated in storage buffer composed of 25 mM Tris, pH 7.5, 100 mM NaCl, 1 mM dithiothreitol, and 10% glycerol. Fractions with His8-PKA-Nedd8 were concentrated, and the purified protein was frozen at -80°C.

Expression and Purification of Recombinant Proteins

All proteins as outlined in Table S3, were expressed in either *E. coli* or Hi5 insect cells and purified using standard procedures. Ubxd7 was a gift from W. den Besten. Dcn1 was a gift from B. Schulman (St. Jude, Memphis). CSN expressed and purified from *E. coli* was a gift from N. Zheng (University of Washington, Seattle). Phosphorylated Cyclin E–Cdk2 was a gift from B. Larimore (Clurman laboratory, University of Washington, Seattle).

In Vitro Neddylation Reaction

Cul1–Rbx1 was neddylated with His8-PKA-Nedd8 (HPN8) using conditions previously described (Duda, Borg et al. 2008), with the exception that His8-PKA-Nedd8 was used at a concentration of 40 μM. Cul1–Rbx1 conjugated with HPN8 was purified by standard column chromatography techniques, using first S-sepharose, followed by binding to Ni-affinity matrix and then Superdex-200 gel filtration. For the experiments shown in Supplemental Figs. 1*C* and *D*, neddylation reactions were terminated by addition of 5 μM MLN4924 and then diluted directly into a deneddylation reaction.

In Vitro Deneddylation Reaction

Deneddylation reactions in Figs. 2*E* and 3 were carried out with 0.8 nM CSN in a 1X deneddylation buffer containing 25 mM Tris, pH 7.5, 100 mM NaCl, 1 mM dithiothreitol, 5% glycerol and 1ng/μl ovalbumin. Deneddylation reactions in Fig. 2*A* and Supplemental Figs. 1*C,* 1*D* and 3 were carried out with 1 nM CSN in deneddylation buffer containing 25 mM Tris pH7.5, 100 mM NaCl, 1 mM DTT, 1% glycerol, 1 ng/μl ovalbumin. Deneddylation reactions in Fig. 2*B, C,* and *D* were carried out with 1 nM CSN in deneddylation buffer containing 25 mM Tris pH7.5, 50 mM NaCl, 1 mM DTT, 1% glycerol, 15 ng/μl ovalbumin 25 mM trehalose. See figure legends for the time of reaction and the concentrations of the reaction components. All reactions were performed at room temperature (23-25^{o}C). Deneddylation reactions were quenched with reducing SDS-PAGE buffer and separated by SDS-PAGE on 16% gels. The gels were dried and exposed to a phosphor screen for analysis. Quantification was performed with ImageQuant (GE Healthcare) and plotted using GraphPad Prism. All values reported are the average of at least two independent experiments. Rates of deneddylation were

calculated by dividing the signal for free [^{32}P]-labeled HPN8 by the summed signals for [^{32}P]-labeled HPN8–Cul1 and free HPN8 to obtain % deneddylation. The amount of free Nedd8 formed was then calculated as: (% deneddylation) * (concentration of input HPN8-Cul1–Rbx1)/100. For the experiments shown in Figs. 2*A*-*D*, initial rates were calculated excluding the first 10 seconds, due to the apparent biphasic nature of some of the reactions, which we ascribe to a small fraction of Cul1 that did not assemble with F-box–Skp1 or substrate, and was therefore deneddylated more rapidly.

Ubiquitylation Reaction

All of the ubiquitylation reactions were carried out as previously described (Saha and Deshaies 2008) in a reaction buffer composed of 25 mM Tris, pH 7.5, 100 mM NaCl, 5 mM $MgCl_2$, 2 mM ATP, 1 mM dithiothreitol. All reactions were performed at room temperature (23^{o}C). See figure legends for the time of reaction and the concentrations of the reaction components. Ubiquitylation reactions were quenched with reducing SDS-PAGE buffer and separated on 16% Tris-glycine SDS-PAGE gels. The gels were dried and exposed to a phosphor screen for analysis. Quantification was performed with ImageQuant (GE Healthcare) and plotted using GraphPad Prism. All values reported are the average of at least two independent experiments, except Supplemental Fig 4.

Cell culture, Immunoprecipitation and Western Blot

HEK293T cells were obtained from A.T.C.C. and grown under standard cell culture conditions in DMEM supplemented with 10% FBS. For transfection, Lipofectamine2000 was used according to the manufacturer's instructions (Invitrogen). A description of the plasmids used in this study for transfection and immunoprecipitation is provided in Table S2. Twenty-four hours post transfection, cells were rinsed in cold phosphate-buffered

saline and lysed in 400 μM cold lysis buffer (50 mM Tris-HCl [pH 7.5], 150 mM NaCl, 1 mM EGTA, 0.1% NP-40, Complete Mini EDTA-free Protease Inhibitor Cocktail (Roche)). Lysates were cleared by centrifugation at 12,000 X g for 10 minutes at 4^{o}C, followed by incubation with either anti-HA (Covance), anti-M2 FLAG (Sigma), or anti-myc (Covance) and 30 μl Tris-Acryl protein A (Pierce) at 4^{o}C for 2 hours with rotation. Resins were washed four times with lysis buffer and resuspended in SDS sample buffer. Proteins bound to resin were resolved by SDS-PAGE on a 7, 10 or 12.5% gel. Immunodetection was performed with antisera to Cul1 and Skp1 (Invitrogen), Cand1 (Calbiochem), Cks1 (Invitrogen), Csn5 (Santa Cruz), myc (Covance) and Rbx1/Roc1 (Biosource).

Figure Legends

FIGURE 1. **Characterization of *in vitro* deneddylation assay components and enzymatic properties of human CSN.**

A, Purified CSN from HEK293 cells was fractionated by SDS-PAGE and analyzed by silver staining to check for purity and stoichiometry of enzyme subunits.

B, Purified Cul1–Rbx1 (50 nM) conjugated with [^{32}P]-labelled HPN8 was incubated with 1 nM CSN in a total reaction volume of 50 µl. At the indicated time points, aliquots were quenched and evaluated by SDS-PAGE followed by autoradiography.

C, Phosphorimager quantification of *B*.

D, The initial rate of deneddylation by 0.8 nM CSN at different concentrations of substrate is plotted. K_M and k_{cat} were estimated by fitting the curve to the Michaelis-Menten equation.

FIGURE 2. **F-box–Skp1 and substrate inhibit deneddylation by CSN.**

A, Purified Cul1–Rbx1 (500 nM) conjugated with [^{32}P]-labeled HPN8 was preincubated for 10 minutes with 600 nM of Fbw7–Skp1 or b-TrCP–Skp1, followed by the addition of 1 nM CSN. At the indicated time points, aliquots were quenched and evaluated by SDS-PAGE (left panel) followed by phosphorimager quantification (right panel). Rates (fmol Nedd8 released from Cul1/sec) are indicated to the right of each curve. The total reaction volume was 25 µl.

B, Same as *A*, except [^{32}P]-HPN8-Cul1–Rbx1 substrate at 50 nM was mock-incubated or preincubated with 100 nM Skp1–Skp2–Cks1 in the presence or absence of 1 µM

phospho-p27–cyclin E–Cdk2 (p27). Total reaction volume was 50 µl. The asterisk indicates [^{32}P] label incorporated into p27.

C, Same as *A*, except [^{32}P]-HPN8-Cul1–Rbx1 substrate was at 50 nM, Fbw7–Skp1 was at 100 nM, and phospho-cyclin E–Cdk2 (CycE) was at 500 nM.

D, Same as *C*, except that Fbw7–Skp1 was omitted.

E, [^{32}P]-HPN8-Cul1–Rbx1 substrate at 100 nM was preincubated 5 min. with 300 nM Skp2–Skp1 plus or minus Cks1. Following assembly of SCF^{Skp2} complexes, the reactions were supplemented with ubiquitylation components (1 µM ubiquitin, 400 nM E1, 100 nM Cdc34, plus or minus 500 nM phospho-p27–cyclin E–Cdk2), incubated for 10 minutes, supplemented with ATP and Mg^{2+} to initiate ubiquitylation, and incubated a further 20 minutes prior to addition of CSN (0.8 nM). Total reaction volume was 50 µl. At the indicated time points, aliquots were quenched and evaluated by SDS-PAGE followed by phosphorimaging (top panel). Quantification of the phosphorimager scans is shown in the bottom panel.

FIGURE 3. **Proteins that bind the C-terminal domain of Cul1 inhibit deneddylation**

A, [^{32}P]-labeled HPN8-Cul1–Rbx1 (25 nM) was incubated for 10 min with 1 µM of the indicated factor prior to addition of 0.8 nM CSN. At the indicated time points, aliquots were quenched and evaluated by SDS-PAGE followed by phosphorimager quantification. The total reaction volume was 40 µl.

B, Same as A, except that substrate was 150 nM and was preincubated with the indicated final concentration of Cand1 prior to adding CSN.

C, Same as B, except that Cand1 (250 nM) and CSN (0.8 nM) were held constant while the concentration of substrate was varied. The data were fitted to the Michaelis–Menten equation to estimate k_{cat} and K_M.

D, [^{32}P]-labeled HPN8-Cul1–Rbx1 (50 nM) was preincubated with 200 nM Skp1–Skp2–Cks1 for 10 minutes prior to addition of the indicated final concentrations of Cand1. Following a further 10 min precincubation, CSN (0.8 nM) was added. At the indicated time points, aliquots were quenched and evaluated by SDS-PAGE followed by phosphorimager quantification.

E, Same as *B*, except that substrate was 50 nM and Cul1–Rbx1 was titrated.

FIGURE 4. **CSN forms a stable complex with both neddylated and unmodified Cul1.**

A, Purified $SCF^{Skp2–Cks1}$ (600 nM) was incubated for 15 min either in the presence (top panel) or absence (bottom panel) of 300 nM purified CSN. Complexes were passed through a Sephadex-200 size exclusion column and every third fraction was separated by SDS-PAGE and Western blotted with antisera to the indicated proteins.

B, The indicated HA-tagged Cul1 constructs were transfected into HEK293 cells. Twenty-four hours post transfection, lysates were generated and ^{HA}Cul1 was immunoprecipitated with anti-HA antibody. IPs were fractionated by SDS-PAGE and western blotted with antisera to the indicated proteins. Cul1 was detected with anti-HA. xRING and xSkp1 refer to point mutants of Cul1 that were deficient in binding Rbx1 and Skp1, respectively. K720R has an arginine substitution at the Nedd8 conjugation site (lysine 720).

C, The indicated FLAG-tagged Csn5 constructs were transfected into HEK293 cells. Twenty-four hours post transfection, lysates were generated and ^{FLAG}Csn5 was immunoprecipitated with anti-FLAG antibody. IPs were fractionated by SDS-PAGE and Western blotted with antisera to Csn5 and Cul1 as indicated. EV refers to empty vector. ASA refers to a double point mutation that inactivates the JAMM domain of Csn5.

FIGURE 5. **CSN inhibits ubiquitylation by unmodified SCF**

A, $SCF^{\beta TrCP}$ (100 nM) and ubiquitylation components (1 μM ubiquitin, 400 nM E1, 100 nM UbcH5C, 600 nM [^{32}P]-labeled-phospho-β catenin peptide) were incubated either in the presence or absence of 300 nM CSN for 10 min, after which ubiquitylation reactions were initiated by addition of ATP and Mg^{2+}. Time points were harvested at the indicated times, fractionated by SDS-PAGE, and subjected to phosphorimager quantification. *B*, Same as *A*, except that 100 nM Cdc34 was used in place of UbcH5C.

FIGURE 6. **Regulation of CRLs by reversible neddylation**

See text for details. Transitions marked by single arrows are vectorial. Intermediates at steps 5 and 6 could re-form new CRL complexes by binding a different substrate receptor–adaptor module (dashed and curved lines, respectively)

Acknowledgements

We thank N. Zheng for recombinant CSN, B. Schulman for Dcn1, W. den Besten for recombinant Ubxd7, B. Larimore and B. Clurman for phosphorylated cyclin E–Cdk2, A. Saha and N. Pierce (Deshaies laboratory) for various purified proteins, NS Z-Q Pan for

the FLAG-Csn2 cell line, and R. Enchev for baculovirus-expressed CSN. We are indebted to M. Peter and B. Schulman for communicating results prior to publication. E.D.E. was supported in part by the Canadian Institutes of Health Research with a Post Doctoral Fellowship. Work on CSN in R.J.D's laboratory was supported by NIH grant GM065997. R.J.D. is an Investigator of the Howard Hughes Medical Institute. We thank Jost Vielmetter and members of the Caltech PEC for assistance with protein expression and members of the Deshaies lab for comments on the manuscript.

Figure 1

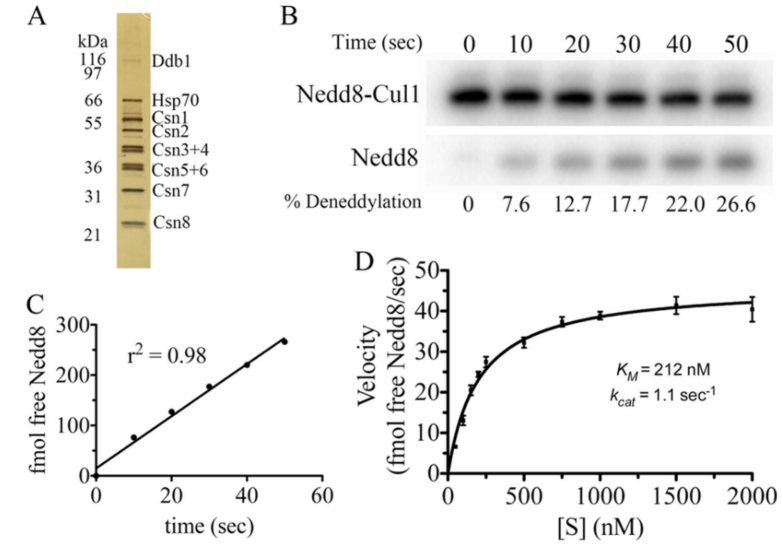
A
kDa
116
97
66
55
36
31
21
Ddb1
Hsp70
Csn1
Csn2
Csn3+4
Csn5+6
Csn7
Csn8
B
Time (sec) 0 10 20 30 40 50
Nedd8-Cul1
Nedd8
% Deneddylation 0 7.6 12.7 17.7 22.0 26.6
C
fmol free Nedd8
r2 = 0.98
time (sec)
D
Velocity (fmol free Nedd8/sec)
KM = 212 nM
kcat = 1.1 sec-1
[S] (nM)

Figure 2.

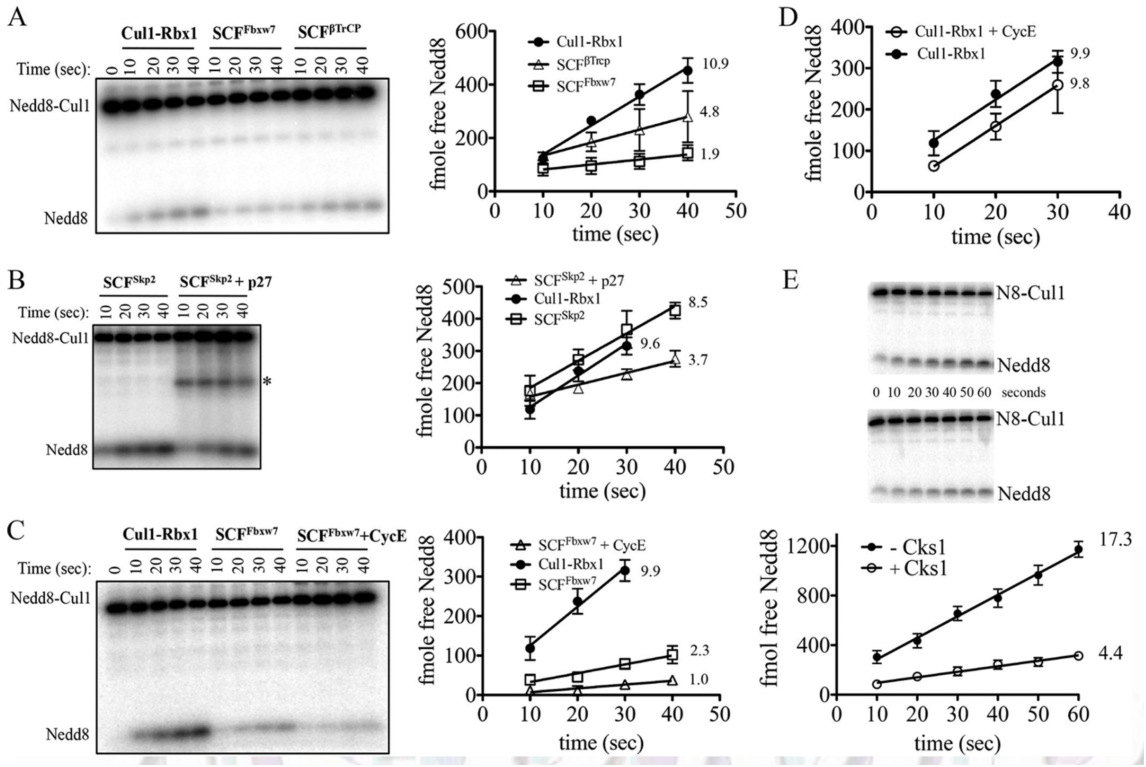
A
Cul1-Rbx1
SCF^Fbxw7
SCF^βTrCP
Time (sec):
Nedd8-Cul1
Nedd8
fmole free Nedd8
time (sec)
Cul1-Rbx1
SCF^βTrcp
SCF^Fbxw7
10.9
4.8
1.9
D
Cul1-Rbx1 + CycE
Cul1-Rbx1
9.9
9.8
B
SCF^Skp2
SCF^Skp2 + p27
SCF^Skp2 + p27
Cul1-Rbx1
SCF^Skp2
8.5
9.6
3.7
E
N8-Cul1
Nedd8
0 10 20 30 40 50 60 seconds
C
Cul1-Rbx1
SCF^Fbxw7
SCF^Fbxw7+CycE
SCF^Fbxw7 + CycE
SCF^Fbxw7
9.9
2.3
1.0
fmol free Nedd8
- Cks1
+ Cks1
17.3
4.4

Figure 3.

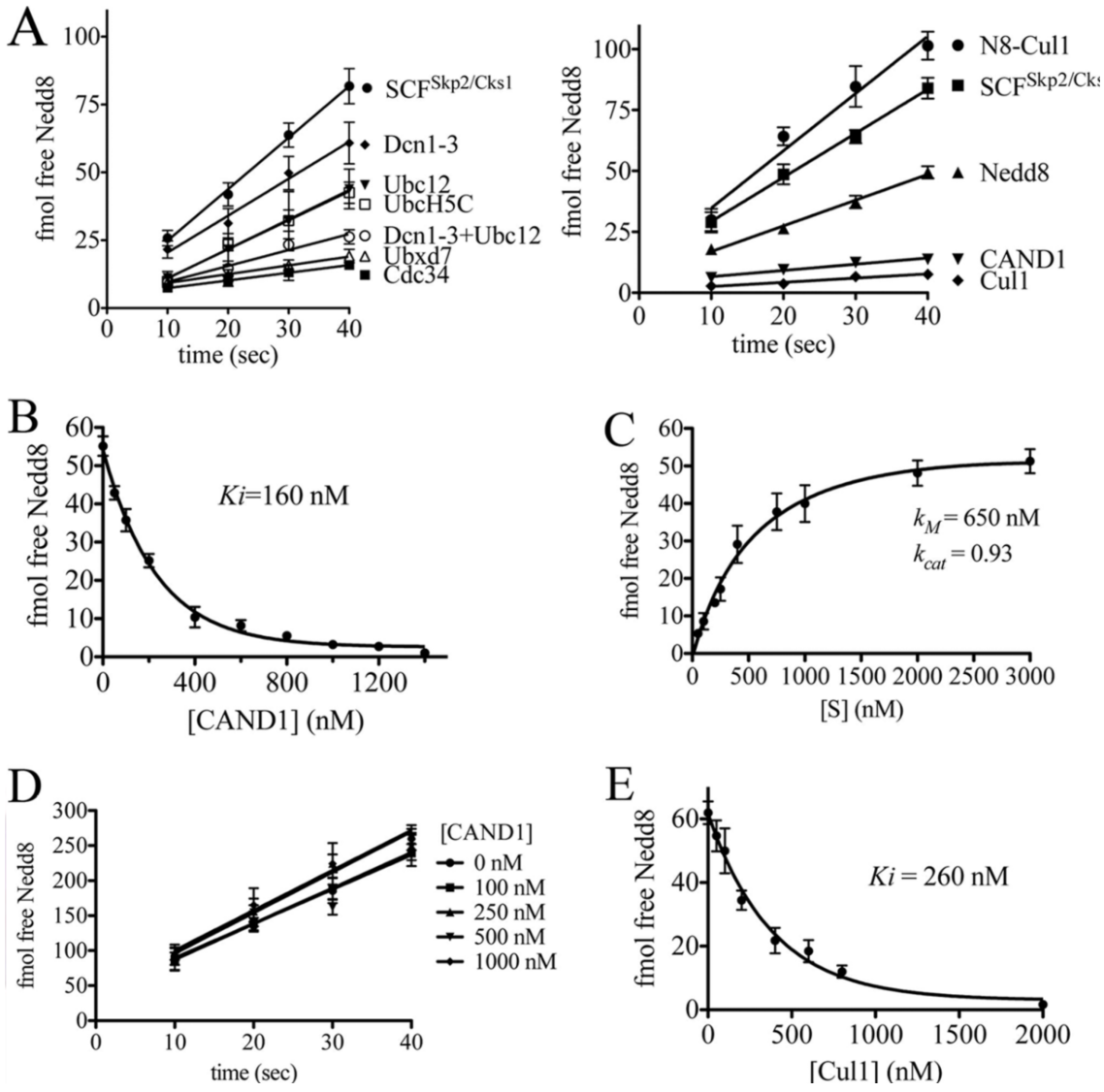
A
fmol free Nedd8
time (sec)
SCF^Skp2/Cks1
Dcn1-3
Ubc12
UbcH5C
Dcn1-3+Ubc12
Ubxd7
Cdc34
N8-Cul1
Nedd8
CAND1
Cul1
B
Ki=160 nM
[CAND1] (nM)
C
k_M = 650 nM
k_cat = 0.93
[S] (nM)
D
[CAND1]
0 nM
100 nM
250 nM
500 nM
1000 nM
E
Ki = 260 nM
[Cul1] (nM)

Figure 4.

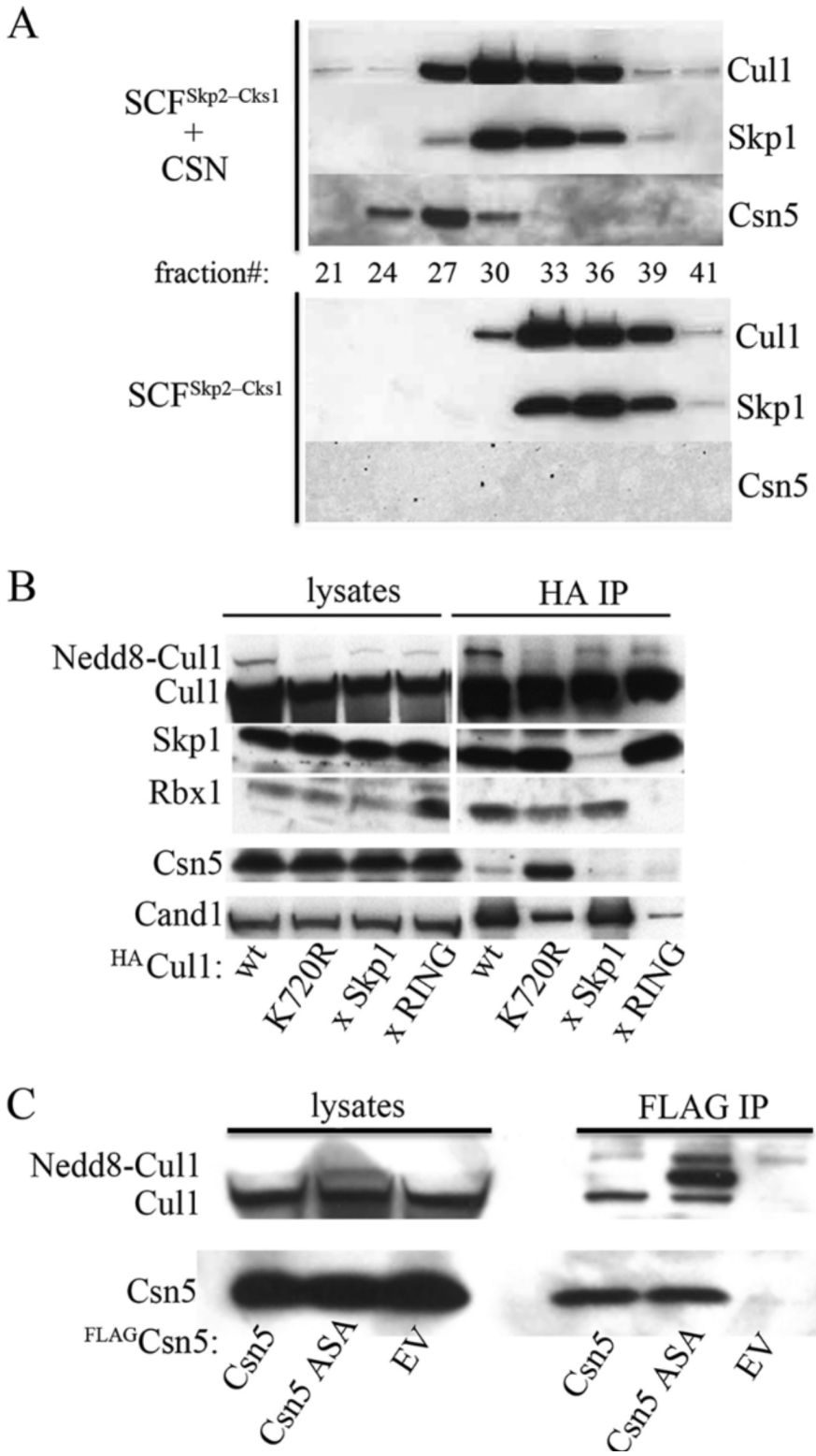
A
SCF^Skp2–Cks1 + CSN
Cul1
Skp1
Csn5
fraction#: 21 24 27 30 33 36 39 41
SCF^Skp2–Cks1
Cul1
Skp1
Csn5
B
lysates
HA IP
Nedd8-Cul1
Cul1
Skp1
Rbx1
Csn5
Cand1
HACul1: wt K720R x Skp1 x RING wt K720R x Skp1 x RING
C
lysates
FLAG IP
Nedd8-Cul1
Cul1
Csn5
FLAGCsn5: Csn5 Csn5 ASA EV Csn5 Csn5 ASA EV

Figure 5.

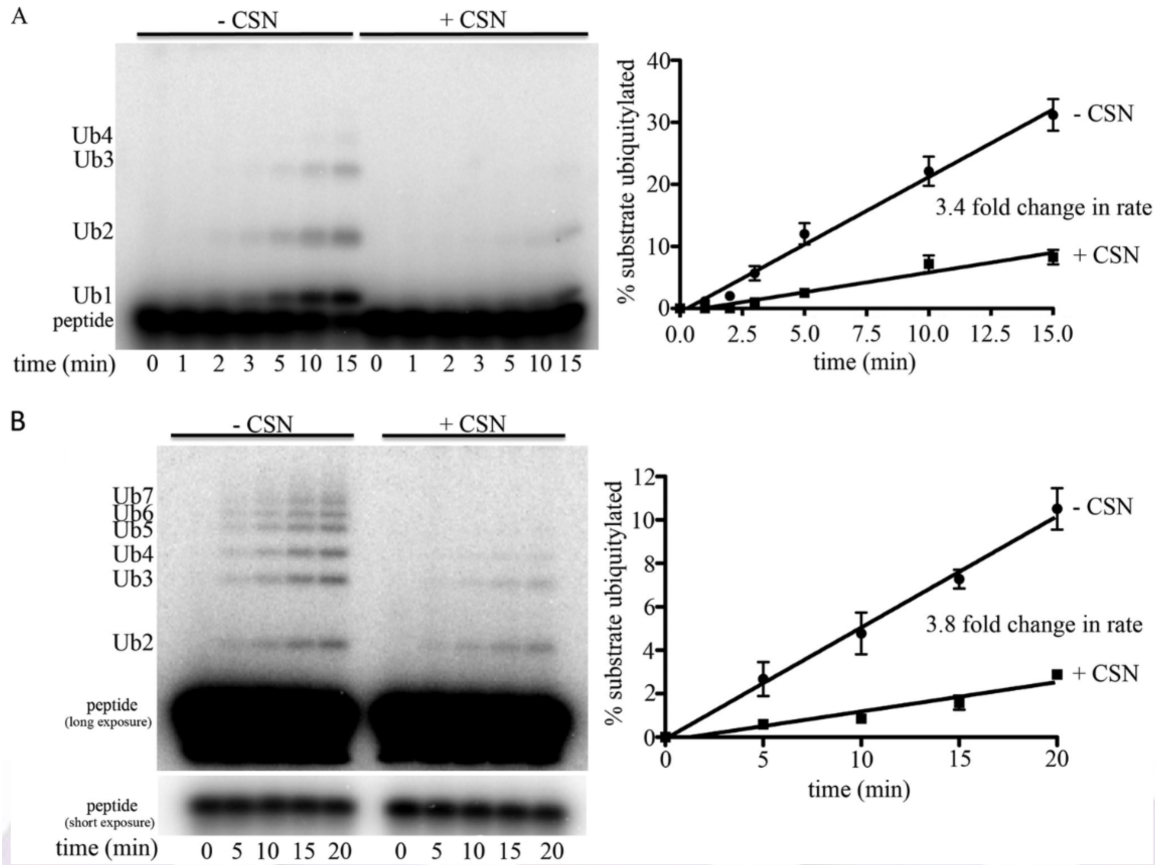
A
- CSN
+ CSN
Ub4
Ub3
Ub2
Ub1
peptide
time (min) 0 1 2 3 5 10 15 0 1 2 3 5 10 15
% substrate ubiquitylated
40
30
20
10
0
- CSN
3.4 fold change in rate
+ CSN
0.0 2.5 5.0 7.5 10.0 12.5 15.0
time (min)
B
- CSN
+ CSN
Ub7
Ub6
Ub5
Ub4
Ub3
Ub2
peptide
(long exposure)
peptide
(short exposure)
time (min) 0 5 10 15 20 0 5 10 15 20
% substrate ubiquitylated
12
10
8
6
4
2
0
- CSN
3.8 fold change in rate
+ CSN
0 5 10 15 20
time (min)

Figure 6.

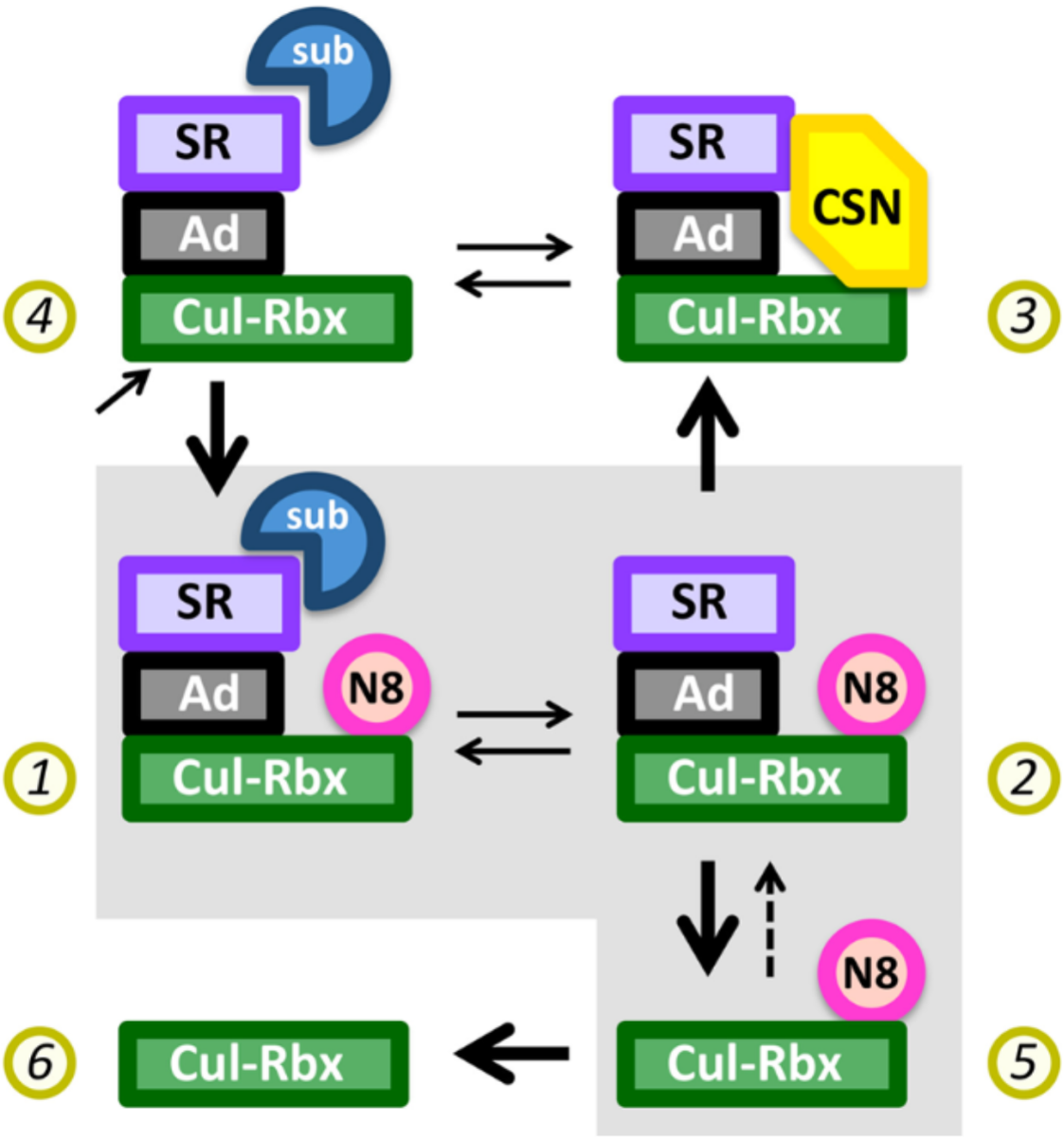
sub
SR
Ad
Cul-Rbx
4
SR
Ad
CSN
Cul-Rbx
3
sub
SR
Ad
N8
Cul-Rbx
1
SR
Ad
N8
Cul-Rbx
2
N8
Cul-Rbx
6
Cul-Rbx
5

SUPPLEMENTAL DATA

Deconjugation of Nedd8 from Cul1 is directly regulated by Skp1–F-box and substrate, and CSN inhibits deneddylated SCF by a non-catalytic mechanism

Ethan D. Emberley, Ruzbeh Mosadeghi, and Raymond J. Deshaies

Division of Biology, Howard Hughes Medical Institute, California Institute of Technology, Pasadena, CA 91125

Supplemental Fig 1

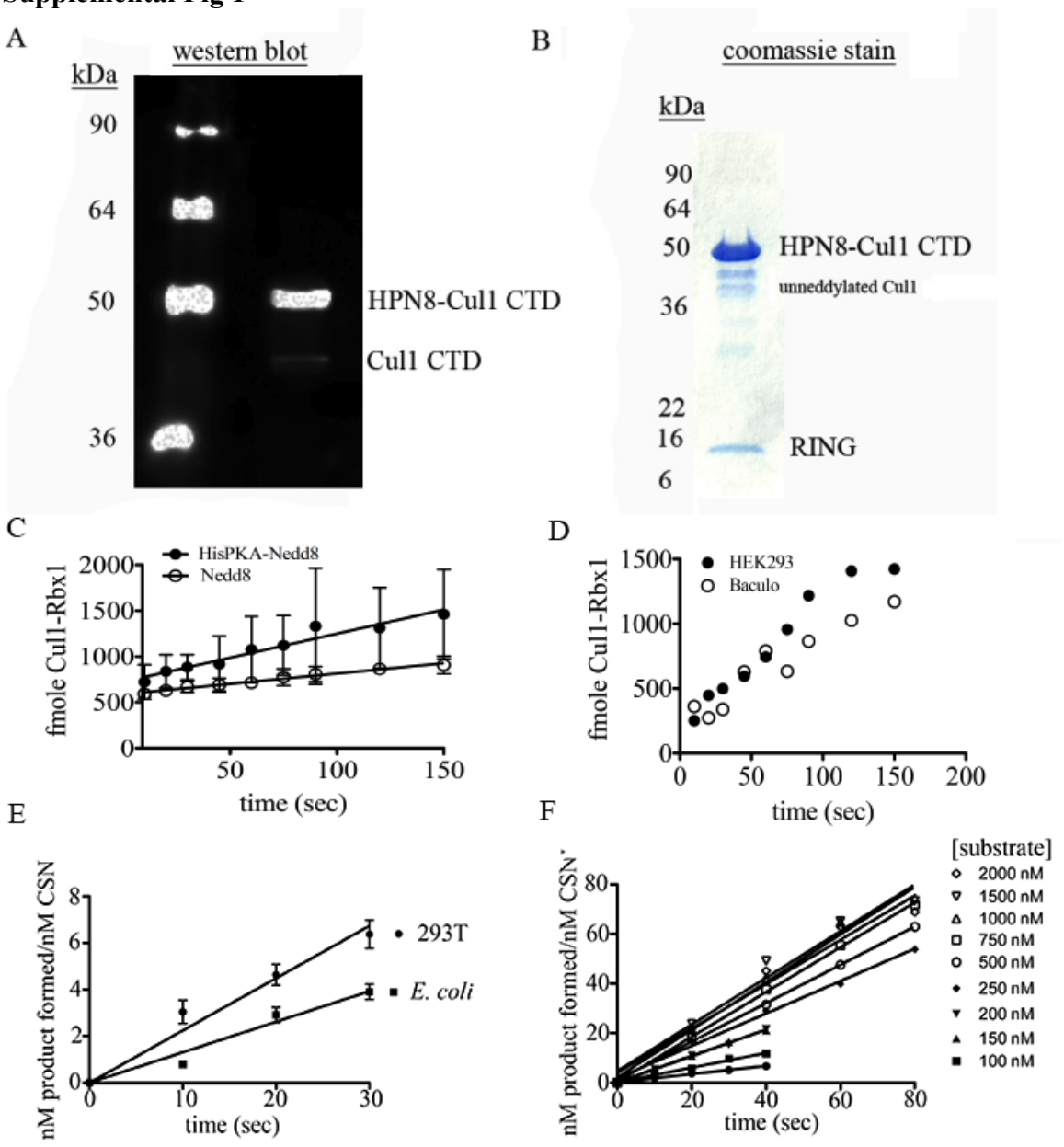

A,*B* Purified, Nedd8-conjugated Cul1 used for kinetic studies was fractionated by SDS-PAGE and either stained directly with Coomassie Blue (*B*) or transferred to nitrocellulose and immunoblotted with anti-Cul1 antibodies (*A*). CTD refers to the C-terminal domain of the split-n-coexpress Cul1 used in these studies.

C, Cul1 was conjugated with either wild type Nedd8 or tagged HisPKA-Nedd8 (HPN8). Neddylation was terminated with MLN4924 and substrates were diluted into a deneddylation reaction as described in Materials and Methods. The background of unmodified substrate was high because neddylated Cul1–Rbx1 was not enriched prior to the assay. The total reaction volume was 50 µl.

D, HPN8-Cul1–Rbx1 substrate (50 nM) was incubated with 0.5 nM of CSN purified from either 293 cells or baculovirus-infected insect cells. The total reaction volume was 50 µl.

E, Same as *D* except 0.8 nM CSN purified from 293 cells and *E. coli* were compared.

F, Rate curves for deneddylation at different concentrations of substrate. These curves were used to construct the graph in Fig. 1*D*.

Supplemental Fig 2

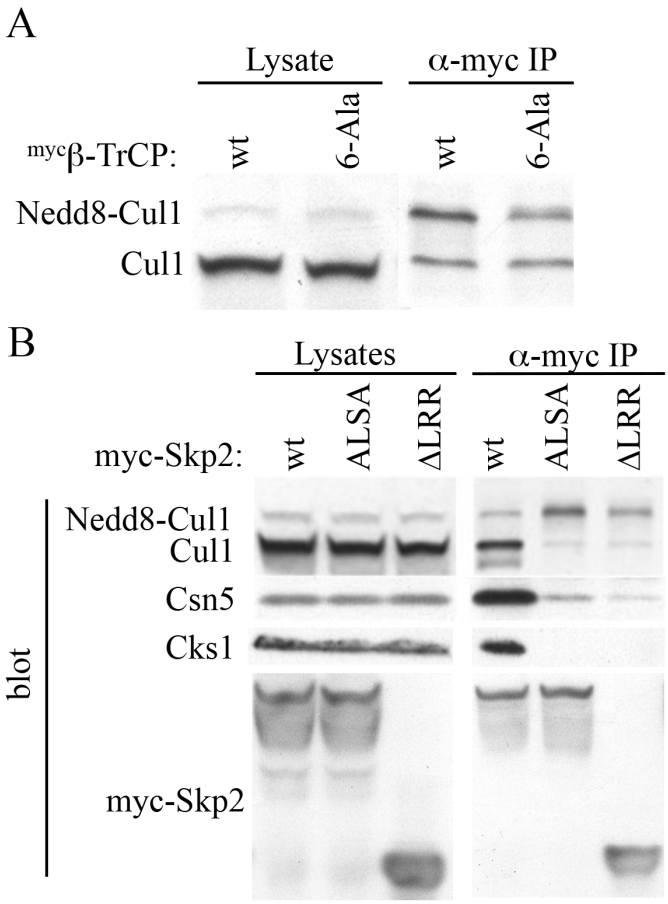

A, Plasmids encoding either wild type (wt) b-TrCP tagged with 5 copies of the myc epitope or a mutant (6-Ala) in which 6 residues that contact b-catenin phosphopeptide were mutated to alanine were transfected into 293 cells. After 24 hours, lysates were prepared and subjected to immunoprecipitation with anti-myc antibodies. Samples were fractionated by SDS-PAGE and immunoblotted for Cul1. Cul1 associated with b-TrCP was largely in the neddylated state, but this bias was modestly reduced for the mutant b-TrCP.

B, Plasmids encoding either wild type (wt) myc-tagged Skp2 or mutants in which the leucine rich repeats were deleted (ΔLRR) or the Cks1-binding site DLSD was converted to ALSA were transfected into 293 cells. After 24 hours, lysates were prepared and subjected to immunoprecipitation with anti-myc antibodies. Recovered proteins were fractionated by SDS-PAGE and immunoblotted for the indicated proteins. Note that contrary to b-TrCP, most of the Cul1 associated with Skp2 was in the deneddylated state. This may be due to an active ability of Skp2 to recruit functional CSN, because both the ALSA and ΔLRR mutants of Skp2 were associated primarily with neddylated Cul1 and exhibited a strong reduction in Csn5 binding.

Supplemental Fig 3

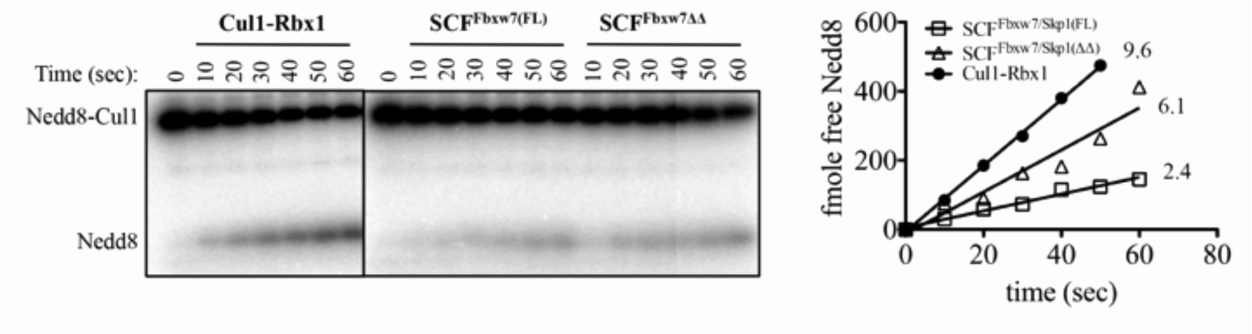

Effect of Skp1 loops on inhibition of CSN. Fbw7 was co-expressed with either wild type Skp1 to generate Fbw7(FL) or with Skp1 lacking the two internal acidic loops to generate Fbw7ΔΔ. The resulting proteins were mixed with [^{32}P]-labeled HPN8-Cul1–Rbx1. CSN (1 nM) was added to a total reaction volume of 50 µl and samples were withdrawn and quenched at the indicated time points. Reaction progress was evaluated by SDS-PAGE (left panel) followed by quantification on a phosphorimager (right panel). Reaction rates in fmol Nedd8 released from Cul1/sec are shown to the right of each curve.

Supplemental Fig. 4

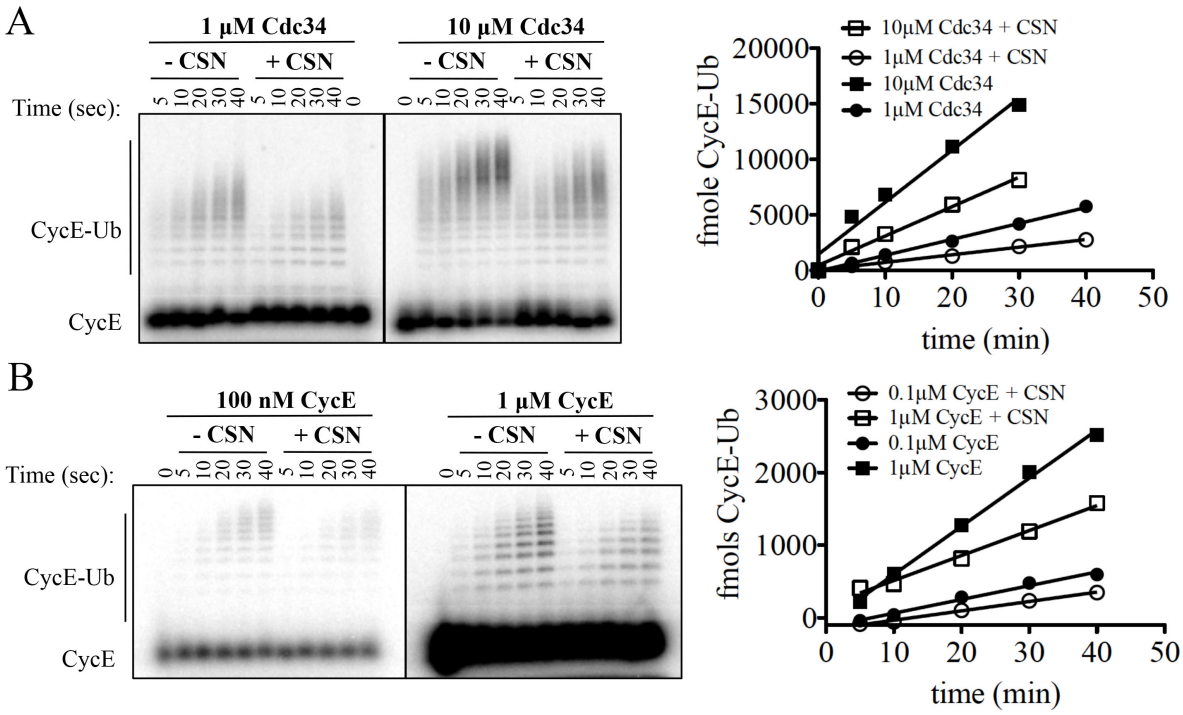

A, Effect of Cdc34 concentration on inhibition of SCF^{Fbw7} by CSN. Fbw7–Skp1, Cul1–Rbx1, and [^{32}P]-labeled cyclin E phosphopeptide were mixed together in either the absence or presence of CSN for 3 minutes at room temperature to generate a pair of samples referred to as 'set 1'. In parallel, different concentrations of Cdc34 were mixed with E1 enzyme, ubiquitin, and ATP at room temperature for 3 minutes to allow ubiquitin charging to occur, yielding samples referred to as, ' set 2'. An ubiquitylation reaction was initiated by mixing together a tube from set 1 with the appropriate tube from set 2. Samples were withdrawn at the indicated times, quenched, fractionated by SDS-PAGE, and evaluated by phosphorimaging. A gel image is shown on the left and quantification of the image on the right.

B, Effect of Cyclin E substrate peptide on inhibition of SCF^{Fbw7} by CSN. Fbw7–Skp1, Cul1–Rbx1, and varying concentrations of [^{32}P]-labeled cyclin E phosphopeptide were mixed together in either the absence or presence of CSN for 3 minutes at room temperature to generate samples referred to as 'set 1'. In parallel, Cdc34 was mixed with E1 enzyme, ubiquitin, and ATP at room temperature for 3 minutes to allow ubiquitin charging to occur, yielding a sample referred to as reaction 2. An ubiquitylation reaction was initiated by mixing together a tube from set 1 with an aliquot of reaction 2. Samples were withdrawn at the indicated times, quenched, fractionated by SDS-PAGE, and evaluated by phosphorimaging. A gel image is shown on the left and quantification of the image on the right.

Supplemental Table 1

[S] (nM)	Rate (nM product formed/nM CSN/second)	Rate (fmol free Nedd8/second)
50	0.16	6.6
100	0.29	13.1
150	0.50	20.5
200	0.53	24.4
250	0.65	27.5
500	0.77	32.2
750	0.90	37.4
1000	0.95	38.9
1500	0.96	41.4
2000	0.94	40.4

Supplemental Table 2

Substrate	Initial Rate (nM product/nM CSN/sec)	Initial Rate (fmol free Nedd8/sec)
N8-Cul1	0.13	2.4
N8-$SCF^{Skp2/Cks1}$	0.10	2.4
N8-Cul1 + Dcn1-3	0.06	1.4
N8-Cul1 + Nedd8	0.06	1.4
N8-Cul1 + Ubc12	0.04	1.1
N8-Cul1 + UbcH5C	0.04	1.1
N8-Cul1 + Dcn1-3 + Ubc12	0.02	0.59
N8-Cul1 + Ubxd7	0.02	0.32
N8-Cul1 + Cand1	0.02	0.30
N8-Cul1 + Cdc34	0.02	0.28
N8-Cul1 + Cul1	0.01	0.17

Supplemental Table 3

List of proteins used in this study

Protein	Construct	Strain	Expression	Purification	Comments	Reference
Cdc34b	pET11 His TEV Cdc34	RDB 2222	*E. coli*	Ni-NTA, TEV digest, S200	-	(Saha and Deshaies 2008)
UbcH5c	pGEX TEV UbcH5c	RDB 1973	*E. coli*	GST, TEV digest (on beads), S75	-	(Saha and Deshaies 2008)
Cul1 NTD Rbx1-Cul1 CTD	pAL Cul1 NTD, pCool Rbx1 Cul1 CTD	RDB 2080 RDB 2081	*E. coli*	GST, Thrombin digest, Mono S, S200	Co-expression	(Li, Pavletich et al. 2005)
b-TrCP-Skp1 (139-569)	GST bTrCP-Skp1	-	Hi5 insect cell	GST, thrombin digest, Mono Q, S200	Co-expression	(Li, Pavletich et al. 2005)
Fbw7-Skp1	GST Fbw7-Skp1	-	Hi5 insect cells	GST, thrombin digest, S200	Co-expression	(Pierce et al., submitted)
His8-PKA-Nedd8	pJexpress414	RDB 2673	*E. coli*	Ni-NTA, S75		(this study)
Nedd8 E1	GST-Nedd8 E1	RDB 2037	*E.coli*	GST, thrombin digest, S200	Co-expression	

Ubc12	GST-Ubc12	RDB 2036	*E. coli*	GST, thrombin digest, S75		
Cand1	GST-Cand1	RDB 2049	*E. coli*	GST, thrombin, Mono Q, S200		
Skp1-Skp2	GST-Skp1 Skp2	RDB 2047	*E. coli*	GST, thrombin, Mono Q, S200	Co-expression	
Cks1	GST-Cks1	RDB 2046	*E. coli*	GST, thrombin, S75		
Fbw7-Skp1ΔΔ	GST Fbw7-Skp1	-	Hi5 insect cells	GST, thrombin, S200	Co-expression	
phospho-cyclin E-Cdk2						B. Clurman
phospho-p27	GST-p27	-	*E. coli*			(Saha and Deshaies 2008)
cyclin E-Cdk2	GST-Cdk2-Cyclin E		Hi5 insect cells	GST, thrombin, S75	Co-expression	(Saha and Deshaies 2008)
CSN	FLAG-Csn2		293 cells	GST, thrombin, S200		(this study)
CSN			*E.coli* Insect cells	FLAG, S200		N. Zheng
CSN						R. Enchev

Supplemental Table 4

List of plasmids used for transfection in this study

Protein	Construct	Mutation	RDB	Tag
Cul1	pCS2	-	942	N-term 5Xmyc
Cul1K720R	pCS2	K720R	2713	N-term 5Xmyc
Cul1xRING	pCS2	535DFSIQVL→RRSIQEE	2712	N-term 5Xmyc
Cul1xSkp1	pCS2	M43S, Y46K, Y50K, Y139A, R142D	2710	N-term 5Xmyc
Csn5	pcDNA	-	1419	N-term FLAG
Csn5 ASA	pcDNA	H118A, H120A	1500	N-term FLAG
Myc-b-TrCP	pcDNA	-	865	N-term 5Xmyc
Myc-b-TrCP-6Ala	pcDNA	Y271A, R285A,R431A S448A, R474A, Y488A	1985	N-term 5Xmyc
Myc-Skp2	pCS2	-	939	N-term 5Xmyc
	pCS2	D316A, D319A	1983	
Myc-Skp2-ALSA	pCS2	Stop codon after codon 210	1982	N-term myc
Myc-Skp2-ΔLRR				N-term myc
				N-term myc

Chapter 3: Kinetic Analysis of CSN mediated SCF Deneddylation

Abstract

In this work, we sought to better understand the mechanisms regulating how Cullin-RING Ligases (CRL) are deactivated by the deneddylation activity of the Cop9 Signalosome (CSN). Using a series of fluorescent and biochemical assays we developed for this work,to measure the biochemical characteristics of CSN, we have discovered that a conformation change in the catalytic subunit of CSN, CSN5, dramatically increases the affinity for CRLs and activates the isopetidase activity. Our data show that while contacts with the N-terminus of CSN4 do indeed increase the substrate binding affinity and activity of CSN, the majority of the binding energy comes from CSN5 itsself. The dramatic shift in affinity is controlled by the Ins-1 in both This is achieved by the binding of the E104 residue of Ins-1 to the catalytic zinc in the inactive, low affinity state of CSN, and T103 and E104 to some undetermined residues in the active, high affinity state. Furthermore, my data suggests we have shown that the inhibition of deneddylation comes primarily from competitive inhibition by E2 enzymes as opposed to the current model that substrates sterically block the binding of CSN.

Introduction

Cellular homeostasis is dependent on an intricate control of both the small molecules bathing cells in their environment as well as regulation of the macromolecules derived from the cells themselves. In particular, constant turnover of proteins within a cell is required for the maintenance of a properly folded and fully functional repertoire as well as limiting the expression of certain proteins to distinct periods of time when their activities are necessary. One of the major mechanisms by which cells achieve homeostatic regulation of their proteins is through the marking and degradation of proteins by the Ubiquitin-Proteasome System (UPS). When the fate of a protein has been decided by any of a variety of factors, ubiquitin E1 and E2 enzymes aid in the transfer of ubiquitin molecules, as a post-translation modification, to substrates through E3 Ligases which serve to both recognize substrates and catalyzes their ubiquitination (Deshaies and Joazeiro 2009).

One of the largest classes of ubiquitin E3 ligases is the family of Cullin-RING Ligases (CRLs), which constitute a heterometric complex capable of transferring ubiquitin to many hundreds of substrates. The cullin family of proteins provide a long flat functional scaffold upon which the system is based. On their c-termini they are intimately bound to a RING domain protein (Rbx1/Roc1/Hrt1), which serves to activate the E2 Ubiquitin Conjugating enzymes to directly transfer ubiquitin to its substrates. On their n-termini they bind adaptor molecules that mediate the binding of substrate receptors and substrates. Although mechanistically unclear, the modification of CRLs by Nedd8 (the closest homolog of ubiquitin) appears to alter the quaternary conformation of the CRL to close the gap between the substrate and E2 to dramatically increase the rate of ubiquitin

transfer (Duda, Borg et al. 2008) (Saha and Deshaies 2008) (Deshaies and Joazeiro 2009, Echalier, Pan et al. 2013).

Although the activation of CRLs by neddylation is required for their catalytic activity *in vivo,* it has long been understood that negatively regulating CRL activity through deneddylation by the Cop9 Signalosome (CSN) is required to maintain appropriate levels of substrate receptors and efficiently degrade CRL substrates (Cope and Deshaies 2006). In fact, the ability of many substrates of CRLs such as c-myc, β-catenin and Hif1α to serve as proto-oncogenes, as well as the known roles of CRL substrate receptors such as Fbw7, β-TrCP, and VHL as tumor suppressor, implies that maintaining efficient CRL function plays a critical role in cellular homeostasis (Skaar, Pagan et al. 2013).

At the time of its discovery in the last decade, the effect on both substrate receptors and their respective substrates upon the loss of deneddylation by CSN appeared paradoxical. However, the mechanisms behind this phenomenon became clearer with the recent discovery that efficient exchange between substrate receptors is mediated by a protein exchange factor CAND1 (Pierce, Lee et al. 2013). It was found that in order for CAND1 to perform its biochemical activity to allow new substrate receptors to bind, the CRL must first be deneddylated. Thus, in the absence of CSN activity to remove and deactivate CRLs, substrate receptors are less capable of dissociating from the CRL and become substrates for ubiquitination. This cannibalism of substrate receptors by the complex increases the cellular levels of CRL substrates by two mechanisms: 1) the levels of substrate receptors scouting and bringing substrates to the E3 are reduced and 2)

without proper deneddylation, free substrate receptor bound to substrates cannot gain access to the scaffold.

Since the initial reports of the discovery of CSN and its role in regulating the organismal response of *A. thaliana* to cycles of dark and light conditions and the demonstration of its definitive catalytic function as a deneddylase, very little had been elucidated about its enzymatic activity (Wei and Deng 1992). Over the last few years, however, there has been a rapid ramp up of tools and structural determinations that have given new insight into the mechanisms of CSN's deneddylation activity. Recently published crystal structures have given us a structural understanding of why CSN is inactive against fluorescence UBLs and model deubiquitinase (DUB) substrates, which have been crucial in the study of other isopeptidases. The highly conserved Ins-1 loop of CSN5 appears to be bound to, or near, its catalytic site and thus precludes the positioning of the isopeptide bond in the catalytic core of CSN in the absence of some sort of conformational change (Echalier, Pan et al. 2013) (Lingaraju, Bunker et al. 2014).

We now understand that a major contact for CSN is the N-terminus of CSN2 binding the C-terminus of Cul1 (Enchev, Scott et al. 2012). However, there is some evidence to suggest that CSN4 might also be making contacts with the Rbx1 protein and thus forcing a conformational change in the quaternary structure of CSN allowing the Ins-1 loop of CSN5 to shift out and open up its catalytic center (Lingaraju, Bunker et al. 2014). With the development of new biochemical assays that have allowed determination of CSN's kinetic parameters as well as structural insights, we can now use mutagenesis to perturb the portions of its subunits to better understand their role in regulating CSN's functional regulation.

Results

In order to mechanistically understand how the Cop9 Signalosome activity is regulated, we sought out to measure the microscopic kinetic rates of the entire reaction deneddylation reaction. We, and others, have published data on the kinetic parameters of Cul1 deneddylation, including k_{cat} and K_m, it is clear from the data that the reaction is either diffusion-limited or nearly diffusion-limited and thus may not follow classic Michalis-Menton kinetics. The strict definition for diffusion limited reactions is k_{cat}/K_m of 10^9 M^{-1} sec^{-1} for reactions involving small molecules, but for interactions involving large protein complexes a k_{cat}/K_m on the order of 10^6 M^{-1} sec^{-1}, as has been reported for the deneddylation of Cul1 and Cul4a, is considered diffusion limited (Emberley, Mosadeghi et al. 2012) (Lingaraju, Bunker et al. 2014). The reported k_{cat}/K_m of 5x10^6 M^{-1} sec^{-1}, in the case of CSN deneddylating Cul1, implies that after binding, there is greater chance of a reaction occurring rather than the two proteins dissociating. This implies that we cannot make the assumption that $K_m=K_d$. In order to be able to measure the affinity of CSN for different SCF complexes we sought to develop an assay with an optical read-out to measure both equilibrium binding constants and the kinetic binding rates between the two complexes.

We developed an environmentally sensitive assay by using sortase-mediated transpeptidation to conjugate to the C-terminus of split'n'co-express Cul1-Rbx1, a peptide of sequence GGGGK that was modified with a dansyl fluorophore, to yield C1D (Popp, Antos et al. 2007). The binding of CSN to the C-terminal domain of Cul1 alters the local environment of the dansyl dye, resulting in an increase in its quantum yield, which can be used to assay binding (Fig. 1A). After affirming that CSN could in fact

increase the fluorescence C1D, we sought to validate the assay by testing buffer conditions and attempting to chase away the signal increase upon CSN binding. Neither the addition of the Hepes buffer our CSN was purified in (data not shown) nor increasing amounts of Ovalbumin altered the fluorescence of C1D (Fig S1B). Unfortunately, we were not able to chase away the signal increase by CSN with the addition of unlabeled Cul1-Rbx1 (data not shown). Since it has been reported that some RING domain ligases, including CRL3, proteins might act as dimers, we sought to test whether Cul1 dimerization, through Cul1 or Rbx1, was obscuring our results by binding CSN but also binding and increasing the fluorescence of C1D (Fig. S1A). Indeed, we found that this was the case when we added Cul1-Rbx1 alone to C1D and observed a binding affinity of 652.2 nM. In the case of neddylated Cul1, C1ND, unlabeled Cul1-Rbx1, bound with an apparent affinity of 110.7 nM (Fig S1C). We then sought to determine whether another cullin, Cul3-Rbx1, or another cullin assembled with different RING protein, Cul5-Rbx2, could outcompete CSN for binding to C1D. Cul3-Rbx1 was able to heterodimerize with an increase the fluorescence of C1D and thus was not suitable as a chase. Cul5-Rbx2 did not appear to bind with C1D, but unfortunately, Cul5-Rbx2 also did not chase away CSN (Fig. S1D). This is perhaps due to the poor binding affinity between CSN and unneddylated Cul5 (Fig. 3C). In fact, we do not see a great deal of Cul5 binding CSN in our mass spectroscopic assays.

Given the observation that C1D was able to dimerize with Cul3-Rbx1, but not to Cul5-Rbx2, we hypothesized that the ability of cullins could be partially mediated by the RING domains. When we added a large surplus of Cul1-Rbx1$^{\Delta RING}$, we were no longer able to increase the fluorescence signal of dansyl (Fig. 1A). When added in excess, Cul1-

Rbx1$^{\Delta RING}$ was able to chase away the signal increase of C1D binding to CSN. It remains to be determined whether Cul1-Rbx1 can dimerize in the absence of the RING domain, or whether binding to a Cul1-Rbx1$^{\Delta RING}$ is incapable of increasing the fluorescence of the dansyl fluorophore in the dimerized state.

To start our characterization of the deneddylation reaction we first set out to measure the equilibrium binding of CSN to different states of SCFs. We titrated increasing amounts of wild-type CSN against C1D and determined that they bind with a K_d of 305 nM (Fig. 1C and Table 1). In order to account for the effects that Nedd8 might have on the off-rate of the complex immediately after the cleavage of the isopeptide bond we repeated this experiment with the addition of 5 μM Nedd8 and found a slight shift of the K_d to 230 nM (Fig. S2 and Table 1). Both 305 nM and 230 nM closely match the reported K_i (250 nM) of unneddylated Cul1-Rbx1 for inhibiting the deneddylation of Cul1 of 250 nM (Emberley, Mosadeghi et al. 2012). The implication is that CSN binds its Cul1-Rbx1product with fairly high affinity and that Nedd8's surface contributes very little to the binding energy to the binding of CSN. The minor effect of Nedd8 also agrees with the Emberley et al. finding that Nedd8 on its own was a poor inhibitor of deneddylation.

Next, we wanted to measure the affinity of CSN for its substrate. In order to do this, we substitute one the zinc chelating residues to alanine, H138A. The absence of the zinc molecule in this conformation renders the CSN inactive, but we found it otherwise normal in assembly into complex and purifying off of ion exchange and size exclusion chromatography columns. The binding affinity between CSN^{H138A} and C1ND is incredibly tight at 1.64 nM (Fig. 4A). In fact, the K_d for CSN^{H138A} binding to C1ND was

two orders of magnitude lower than that of wild-type enzyme to C1D and the K_d for binding of CSN^{E76A} to C1ND at 119 nM. This led us to test whether the catalytic zinc was required for maintaining CSN in a low affinity confirmation for Cul1. Indeed, when we tested the ability of CSN^{H138A} to bind unneddylated C1D, we found that the binding affinity was 10.1 nM (Fig. 4B), representing ~30-fold increase in binding affinity to its product as compared to wild-type enzyme, but less than 10-fold worse compared to its substrate.

In order to determine the equilibrium binding constants of CSN for its substrate, N8-Cul1-Rbx1, we performed analogous experiments to those above, but with a catalytically dead JAMM domain mutant CSN^{E76A} instead of the zinc chelating mutant (Echalier, Pan et al. 2013). We found that the K_d of CSN^{E76A} for C1ND was 119 nM (Fig. 1E and Table 1). This mutant also had a subtle effect when binding to C1D at 182 nM (Fig. 1D and Table 1). The contributions of Nedd8 and the conformational changes in Cul1 and Rbx1 in response to neddylation appear to confer only subtle increases in binding energy regardless of which mutant we are testing. In contrast to this, the catalytic core of CSN5 appears to have a great influence on the binding of the entire complex to Cul1-Rbx1 by two orders of magnitude or more.

In order to better understand how CSN5, the catalytic subunit of CSN, contributes to bind, we produced CSN complex missing CSN5, $CSN^{\Delta 5}$. We found that $CSN^{\Delta 5}$ was dramatically in the K_d of that $CSN^{\Delta 5}$ and C1D was at least 1178 nM (Table 1), >3-fold weaker than the weakest interaction studied with wild-type enzyme. This number might in fact be even high given that we did not have enough protein to properly saturate the binding between these two protein complexes. Because this enzyme was catalytically

dead, it allowed us to measure its affinity for C1ND, which we found to be nearly identical to the K_d between $CSN^{\Delta 5}$ and unneddylated Cul1 at 1086 nM (Table 1.). Thus it appears that $CSN^{\Delta 5}$ cannot distinguish between the neddylated and unneddylated form of Cul1-Rbx1, meaning that CSN5 plays a crucial role recognizing and binding to Cul1 in all states.

Based on the complete CSN crystal structure, the catalytic zinc of the JAMM domain is bound in an inactive state by glutamate 104 of the critical regulatory loop Ins-1, while the structure of monomeric CSN5 shows that arginine 106 was mediating binding to aspartate 151 to sterically block an isopeptide bond from entering the catalytic groove. The authors even reported that an E104A mutation was active against a model substrate, ubiquitin-rhodamine, while monomeric CSN5 with a R106A mutation was able to deneddylated Cul1-Rbx1. In order to systematically look at the role of this loop, we developed a cell-based assay by which we could quickly test if any mutations in Ins-1 could lead to changes in cullin neddylation. Specifically, if binding of the autoinhibitory loop to the active site of CSN was lost we expected to see activation of CSN and a reduction in cullin neddylation *in vivo*. We did this by making stable 293T cell lines expressing Flag-tagged MSCV vectors harboring point mutations for each of the four highly conserved residues in Ins-1: T103I, E104A, T105A and R106A. We decided to make T103I because this mutant is known to cause severe developmental defects in drosophila (Suh, Poeck et al. 2002). In order to better incorporate our point mutants into intact CSN complexes, we then created CRISPR vectors to knockout endogenous CSN5, but not our mutants, by targeting upstream sequence that are not present in the MSCV construct. Strikingly, we noticed that two mutations, $CSN5^{T103I}$ and $CSN5^{E104A}$, appeared

to behave oppositely to what we expected. Both of those mutants led to a hyperneddylation of cullins under asynchronous growth conditions (Fig. 3A). $CSN5^{T105A}$ and $CSN5^{R106A}$, although highly conserved, did not show this phenotype under our assay conditions.

Since we knew that the loss of a zinc atom could lead to a significant increase in the affinity between CSN and Cul1, we wondered if the hyperneddylation we saw *in vivo* was caused by product inhibition. Specifically, does a loss of binding of the autoinhibitory loop, Ins-1, lead to a tight binding between CSN and Cul1, thus reducing the rate of deneddylation under multi-turnover conditions in the cell? To test this hypothesis, we treated our cell lines with the neddylation inhibitor MLN4924 (Soucy, Smith et al. 2009) to completely deneddylate all cullins and test whether CSN^{T103I} and CSN^{E104A} mutants were able to immunoprecipitate more unneddylated Cul1-Rbx1 than wild-type. Much to our surprise, the two mutations behaved oppositely. The CSN^{E104A} lead to a remarkable increase in co-immunoprecipitated Cul1-Rbx1, while $CSN5^{T103I}$ co-immunoprecipitated slightly less Cul1 out of lysate (Fig. 3B). Interestingly, The T103I mutation was epistatic to E104A, because the T103I/E104A double mutant behaved the same as T103I and did not confer increased binding affinity to unneddylated Cul1.

To better quantify this effect and evaluate its generality, we set out to compare both of these mutants under these conditions by using SILAC Mass Spectroscopy. Of all of the species, it appears that Cul4 bound the largest fraction of CSN, while Cul1 bound the least. As expected, we saw a prominent increase in Cul1 and Cul2 bound to CSN^{E104A} and a smaller, but consistent, increase in Cul3, Cul4A and Cul4B (Fig. 3C). The milder effects on these latter cullins might be due to the fact that a high mole fraction of each is

alrady bound to wild-type CSN. Much like the IP western data, we saw a reduction in binding of $CSN5^{T103I}$ to all cullins except Cul5. There were significant differences in which substrate receptors that each mutant preferred to bind to, but we were unable to discern any obvious patterns with out current knowledge.

To build upon our cell lysate assay, we sought to elucidate the kinetic parameters contributed by the binding of E104 to the zinc atom that is required for the lower affinity, autoinhibited, state of CSN. We tested the binding affinity between CSN^{E104A} for unneddylated C1D and indeed found that it was significantly tighter than the K_d of wild-type enzyme at 25.8 nM (Fig 4C). This finding suggests that since loss of either binding partner keeping Ins-1 in the active groove of CSN5 will lead to a higher affinity for CSN's product, and that the binding of E104 to the catalytic zinc is required for the low affinity state. Unfortunately, because this mutant is still active, we were unable to determine the equilibrium binding of constants for Nedd8-conjugated Cul1-Rbx1.

Next, we sought to test the effects of CSN^{E104A} *in vitro* and address two assumptions. First, based on the cellular data we hypothesized that we might see a reduction in multi-turnover deneddylation due to product inhibition. When we compared wild-type CSN to CSN^{E104A} at saturating concentrations of substrate to measure the multi-turnover k_{cat} for N8-Cul1-Rbx1 deneddylation, we saw that the CSN^{E104A} was indeed slower than wild-type enzyme (Table 2). We also increased the concentration of substrate with both enzymes to see if the point mutant appeared to be slower because of a shift in K_m, but saw that no appreciable difference (Fig. 4D). This result establishes two points: 1) that the E104A point mutant has reduced deneddylation activity and 2) that the

difference is not due to differences in on-rate, since the reaction was done with saturating concentrations of substrate.

In order to test whether E104A was product inhibited or whether E104 is involved in stabilizing other conformations of Ins-1, we then tested the single-turnover k_{cat} by deneddylating low concentrations of N8-Cul1-Rbx1 by saturating concentrations of CSN in molar excess over N8-Cul1-Rbx1. Unexpectedly, we saw that the single-turnover k_{cat} of E104A mutant was a) slower than wild-type and b) the same as the k_{cat} for multit-urnover conditions (Table 2). The implication of this result is that E104 may also helping to stabilize the activate conformation.

Next, we sought to test the proposed hypothesis, based on interpretations of the available crystal and cryoEM structures, that the activation of CSN is mediated through the binding of the N-terminal domain of Csn4 to Rbx1 (or some portion of the C-terminus of Cul1) to alter the quaternary structure of CSN by sterically moving a loop in Csn6, forcing it to shift and rearrange Csn5. In this rearrangement, it is proposed that Ins-1 is pulled out of the catalytic cleft of Csn5 and this activates the enzyme. Indeed, the removal of the loop in CSN6 was reported to increase the k_{cat} of CSN by about six-fold (Lingaraju, Bunker et al. 2014)). In order to test how much binding energy the N-terminus of CSN4 was contributing to the activation of CSN, we set out to test the kinetic parameters of a CSN complex missing the N-terminus of CSN4 ($CSN^{4\Delta n}$). While the activity of this mutant was reduced, we found that the enzyme was still active. Although we could not measure its affinity for N8-Cul1, we did establish that its K_m N-Cul1-Rbx1 was 562 nM. Clearly, this mutant is a less effective enzyme with significant catalytic and binding defects compared to wild-type CSN, but the effects were much less dramatic than

that of $CSN^{\Delta 5}$. Taken together, our results suggest that while the N-terminus of CSN4 makes contact with the SCF, this binding is not the main trigger for activating CSN, because in the absence of CSN5, it cannot maintain CSN in an active conformation.

We next sought to test whether assembly of Cul1 with different classes of Fboxes would have large effects on binding. We tested the binding of CSN to both unneddylated SCF^{Skp2} and SCF^{Fbw7} and found that neither complex was able to increase the binding affinity to CSN by more than a few fold (Fig. 2A, 2B and Table 1). This was also the case when neddylated SCFs were tested with a catalytically dead mutant, CSN^{H138A}, which is incapable of chelating the catalytic zinc and neddylated SCFs (Fig 2C and 2D).

Since we could not see an appreciable effect of CSN binding under equilibrium binding conditions, we sought to determine their effect on on-rates and catalysis. Using a Stopped-flow apparatus, we determined that both mutant and wild-type CSNs bound all forms of Cul1-Rbx1 with a k_{on} value within two-fold of 2x10^7 M^{-1} sec^{-1}, implying that the any difference in the K_d between SCFs and N8-SCFs was primarily influenced by off-rate rather than on-rate (Table 1). Interestingly, all of the complexes bind CSN very quickly and nearly at a diffusion-limited rate. While it is possible to for proteins to bind more quickly than we report here, those instances generally require electrostatic interactions that help reduce the dimensionality of the search during formation of a stable complex, as is the case for the acidic tail of Cdc34 and the basic canyon of Cul1 (Kleiger, Saha et al. 2009).

Next, we measured the k_{cat} under single-turnover conditions to test whether Fboxes could affect. Under single-turnover conditions the off-rate is not relevant. In addition, because the reaction contains a 50-fold excess of enzyme at a saturating

concentration, the on-rate of the enzyme should not be rate-limiting. Thus, the single-turnover k_{cat} determined under these conditions should reflect of the slowest step in the interval immediately following binding of enzyme and substrate through the chemical catalysis, i.e., potential conformational changes after binding and the cleavage of the isopeptide bond. The measured k_{cat} values for all of the SCF complexes were approximately 1.1 sec^{-1}, which is the same as that for N8-Cul1-Rbx1 under multi-turnover conditions (Table 2). This suggests that either conformational change or proteolysis is the rate-determining step in N8-Cul1 neddylation and is not significantly affected by the presence of Fboxes.

Finally, we sought to use our new set of assays to test the popular hypothesis that the regulation of CRL neddylation state was primarily through steric hindrance of CSN binding by CRL substrates. This model has some very attractive aspects because it is accepted that CSN should not inactivate a CRL while it is performing its proper enzymatic activity. Also, there was an interesting result published by Hershko and colleagues that showed that addition of an F-box and its substrates could maintain Cul1-Rbx1 in a more neddylated form by the addition of Fboxes and substrates (Bornstein, Ganoth et al. 2006). It should be noted, however, that these experiments were done with relatively crude proteins fractions from lysates and that theses fractions contained CAND1 and neddylation machinery in addition to Cul1 and CSN. In our own work, we also showed that substrates had a marginal ~2-fold effect on cullin deneddylation under multi-turnover conditions. Our largest effect with Cylclin E-Cdk2 had the caveat that the substrates were still attached to a GST-tag and the status of their phospho-degron was unknown. Thus we set out to test what role substrates played in CSN regulation.

To elucidate the role of substrate in our experiments, we sought to purify a complex of Cyclin E/Cdk2 (EK2) that contained 100% phosphorylated degron by virtue of conjugating the complete degron by a sortase-mediate transpeptidation reaction. Our substrate was capable of being ubiquitinated *in vitro*, albeit slower than the short peptide substrate previously described (data not shown). In multi-turnover assays, our sortase-modified version of EK2 did not decrease the rate of deneddylation of SCF^{Fbw7}, while the GST-EK2 behaved the same as in our previous results (Fig 5A). In fact, when we made more of the GST-EK2 protein and cleaved the GST tag, we found that the inhibition of CSN by EK2 was also lost.

While many things can occur in complex biochemical experiments we sought to test the ability of EK2 to displace CSN, as has been proposed. In order to be compatible with our fluorescence-based assays, we made a version without a fluorophore. We carried out ubiquitination assays on this latter form to determine at which point our substrate was saturating our cullin by titrating the concentration of substrate and measuring the total amount of Cyclin E-Ub species until we not could appreciably see an increase in modified Cyclin E species. Based on this experiment, we carried out our experiments up to 1 μM Cyclin E-Cdk2. We titrated EK2 up to 1 μM and found that it was incapable of outcompeting CSN for binding to SCF^{Fbw7} (Fig. 5B and 5C), although it was fully capable of being ubiquitinated by SCF^{Fbw7}. While other substrates might behave differently and steric obstruction by some substrates might be a means of regulating CSN-mediated deneddylation of specific CRLs, we concluded that perhaps given the heterogeneity of CRL substrates there is a distinct mechanism thay regulates CSN more broadly.

To address how CSN-mediated deneddylation of multiple CRLs might be regulated, we set out to find what must be a common component of all CRLs. Given that the role of CRLs is to modify their substrates by catalyzing the transfer of ubiquitin from an E2, we assumed that every substrate-bound CRL would interact with an E2-Ub unless otherwise regulated. Thus, we hypothesized that a bound E2 could inhibit CSN from deneddylating a cullin engaged in substrate ubiquitination. Three previously published observations provide critical support for this hypothesis: 1) Cdc34, which binds Rbx1 and the C-terminus of Cul1inhibits deneddylation (Emberley, Mosadeghi et al. 2012), 2) the E2 must come into close to proximity to the substrate to transfer the ubiquitin molecule and 3) after the first transfer of ubiquitin, the commitment of the substrate to ubiquitination, the rate of ubiquitin transfer dramatically increases until the many ubiquitins are added (10-15), qualifying the substrate for proteasomal degradation, and the E2 becomes inefficient at adding more (Pierce, Kleiger et al. 2009). It is thought that this is due to docking of the distal-most ubiquitin attached to substrate to a noncovalent 'acceptor' binding site on Cdc34 (Petroski 2005 Cell paper). Thus we reasoned that the E2 enzyme might be able to sense that a substrate undergoing ubiquitination is bound to a CRL, precluding CSN binding until until the ubiquitinated protein dissociates.

To test our hypothesis, we set out to determine the ability of Cdc34-Ub (oxy ester), which cannot transfer its conjugated ubiquitin, to inhibit deneddylation of SCF^{Fbw7}. For SCF^{Fbw7} and SCF^{Fbw7} in the presence of CycE peptide we found the K_i of Cdc34-Ub to be in the low micromolar range at 1.99 μM and 4.28 μM, respectively (Fig. 6A and 6B). When we repeated this experiment with CycE peptide that was modified with a single ubiquitin, CycE-Ub, we found that the K_i of the reaction dropped to 565 nM

(Fig. 6C). While this showed that commitment of CycE to ubiquitination does indeed inhibit the ability of CSN to deactivate the complex, our hypothesis would only be relevant if the cellular concentration of Cdc34 was not dramatically greater than 4 μM or lower than 565 nM. To determine the cellular concentration of Cdc34 in 293T cells, we quantified the concentration by mass spec with and found it to be ~500 nM (data not shown). Thus, in the context of the cell, the K_d of Cdc34 is approximately the same as its K_i for SCF^{Fbw7}-CycE-Ub, while it is 4-8-fold lower than the K_i for the same SCF not rapidly involved in ubiquitination.

Discussion

Our investigations into the microscopic rates constants for different steps of the deneddylation reaction have elucidated several novel facts about the function and regulation of CSN. Most clearly we see that CSN does not differentiate between its own conformations or that of C1D in binding, since all of our measured on-rates were in the ballpark of the diffusion limit. Given that the off-rate of CSN from C1D appears to be slower than its k_{cat}, ~1 sec^{-1}, a majority of these interactions will lead to the deneddylation of the cullin, as is suggested by the near-diffusion-limited multi-turnover k_{cat}/K_ms previously published for both Cul1 and Cul4A (Emberley, Mosadeghi et al. 2012) (Lingaraju, Bunker et al. 2014). In the context of the cell, this implies that CSN is policing CRLs as quickly as possible by binding any available cullins and quickly deneddylating them.

As opposed to what was previously published, by others, and us that CSN could bind cullins tightly and be product inhibited, our data show that the binding of SCF complexes to CSN is incredibly dynamic. The tight affinity between CSN and its product

is driven by a high on-rate rather than a slow off-rate. The calculated off-rate of 4.7 sec^{-1} implies that CSN:CRL complexes rapidly dissociates following deneddylation. While the *in vitro* experiments did show that CSN inhibited ubiquitination, in the context of a cell with other regulators cells and much higher concentrations of total CRLS (~1.2 μM) (Bennett, Rush et al. 2010), this may not be a significant effect. Given this insight, the true regulation role of CSN in regulating CRLs is still solely due to its ability to deneddylate cullins rather than sequester its product.

Our data also cast doubt on the model that cullin deneddylation is regulated by CRL substrates physically obstructing the binding of CSN. While this may be an additional mechanism for some large substrates, which bind CRLs in particular conformations that can interfere with CSN binding, it does not appear to be the case for every single one of the hundreds to thousands of heterogeneous CRL substrates. The results that Cdc34-Ub can recognize a substrate committed to ubiquitination and inhibit CSN from deneddylating Cul1-Rbx1 that is bound to a monoubiquitinated substrate, implies that active ubiquitination of substrates precludes CSN activity rather than the steric bulk of substrates themselves. According to this model, the deneddylation of every CRL could be regulated by this generalized mechanism regardless of its size and three-dimensional structure, and the identity of its bound substrate. Further work is required to test this model in a cellular context, although these studies might prove tricky given the ability of multiple different E2s to ubiquitinate CRL substrates.

While the specificity of CSN for its substrate appears to be through affinity binding, its intramolecular activation appears to be highly regulated and rather complex. It has long been observed that unbound CSN appears to travel through the cell in an

autoinhibited state until forming a complex with a CRL. CSN is then rapidly activated such that the isopeptide bond linking Nedd8 to cullin is cleaved before the substrate can dissociate. Our data sheds light on why CSN is in an autoinhibtited state and how its activation is achieved.

In order to reconcile the perplexing observation that E104 is both required for the autoinhibition of CSN, as well as the full manifestation of CSN's catalytic activity, we proposed a model in which switching between active and inactive conformations of CSN occur stochastically and is biased by the presence of an neddylated CRL. First, we propose that activation/deactivation of CSN is regulated by the catalytic zinc binding either E104 (inactive state) or water (sandwiched between the zinc and E76; active state) by what we refer to as a 'glutamate-swap' (e-swap) mechanism. As drawn in Figure 7B, this hypothesis relies on three postulates: 1) that the published crystal structure is a representation of the low affinity, inactive conformation (State A) stabilized by the binding of E104 to the active site zinc 2) that binding of SCF to CSN forms the high affinity and active conformation (State B), in which E104 is turned away and E76 can be properly positioned to activate the hydrolytic water molecule and 3) that the presence of Nedd8 and the isopeptide bond in the active site stabilizes the high affinity, active conformation (State B) and precludes E104 from flipping back to bind the zinc until the reaction is complete and Nedd8 disassociates from the complex (State C). At this point, the low affinity binding between CSN and the SCF allows it to rapidly dissociate and for CSN to return to State A.

Postulate 1 is supported fact that both the loss of the catalytic zinc ion and its reversible binding partner E104 lead to a tight binding of Cul1 (States D and E). While

the zinc metal is absolutely required for a functional JAMM domain an E104A mutant is still an active enzyme. This implies that both of these elements are required for CSN to return to its low affinity state, as seen in the crystal structure. Postulate 2 and 3 are supported by the fact that both the CSN^{H138A} and CSN^{E76A} appear to bind more tightly to N8-$Cul1^{d}$ as opposed to unneddylated $Cul1^{d}$. Those results suggest that even with CSN^{H138A}, which is generally in a high affinity state, the binding of N8-$Cul1^{d}$ does impart some, albeit relatively little, binding energy.

The second part of our model suggests that E104 is required not only for maintaining the low affinity state, but also for stabilizing high affinity, active state of the enzyme. This hypothesis is supported by two facts. First, the single-turnover k_{cat} implies that with a loss of E104, the conformational change, the catalysis or both are disfavored. Second, because the multi and single-turnover k_{cat}s are the same, the major reason for a loss in activity is due to slower catalysis. Whatever effect E104A has on the off-rate of CSN is not enough to render the reaction product inhibited.

The third part of our model is that the majority of the binding energy required to establish the high affinity, active conformation of CSN is imparted by CSN5, in large part through the action of residues T103 and E104. This hypothesis is strongly supported by three pieces of data. First, the binding affinity of $CSN^{\Delta 5}$ for N8-$Cul1^{d}$ is over an order of magnitude weaker than any other catalytically dead mutants, meaning it is largely deficient in stabilizing the high affinity conformation. Second, $CSN^{\Delta 5}$ binds unneddylated cullin with less affinity than wild-type CSN, suggesting wild-type CSN5 imparts binding energy, and that in the presence of E104, T103 is heavily favored to remain in the low affinity conformation. Third, within the dynamic range of our assays, $CSN^{\Delta 5}$ is incapable

of differentiating between its substrates and products. The implication of this result is that while other interactions between CSN and N8-Cul1 might contribute some binding energy, they are dwarfed compared that of the energy imparted by CSN5 and the Ins-1 residues T103 and E104.

The final aspect of our model for the activation of CSN is that the role imparted by the binding of CSN4 is significant, but marginal. Although it has been proposed that CSN is activated by a conformational change caused by the binding of CSN4, $CSN^{4\Delta n}$ is still capable of bind and catalysis. Also, we find that the affinity of $CSN^{4\Delta n}$ for $Cul1^{d}$ is significantly reduced by a factor of two, but less than that of $CSN^{\Delta 5}$. A deletion of CSN5 shows at least twice of an effect, implying that it contributes significantly more binding energy.

Lastly, we set out to test the model that the deneddylation of CRLs is predominately regulated by the presence of substrate. Both our biochemical data with a true SCF^{Fbw7} substrate, as well equilibrium binding data, imply that this is not the case for all substrate. We would like to put forth a new model based on the fact that the role of CRLs is to mediate substrate ubiquitination by E2s. We show that the ability of Cdc34-Ub to inhibit deneddylation is increased once the substrate is committed to being ubiquitinated. Moreover, given the cellular concentrations of both cullins and Cdc34, we feel that this is physiologically relevant in the context of a cell.

For decades, researchers have known the significance of CSN's role in cell biology. Given the large size of CSN and its substrates, as well as their complexity, studying CSN has been difficult and the mechanisms of how it is regulated have been elusive. Through this series of experiments, we set out understand how this mysterious

complex is regulated. By measuring many of the individual microscopic rates of the reaction we are now able to gain incredible insight into its recognition of substrates as well as the conformation changes that regulate its activity. While there are still many things to learn about CSN biochemistry, including the binding partners of T103 and E104 in the active conformation, we can now set out to study CSN role in cell biology with a better understanding of its function.

Materials and Methods

Protein Purification and modifications CSN and all mutants were purified as described in (Enchev, Scott et al. 2012). Call Cullin constructs were expressed and neddylated as describe in (Emberley, Mosadeghi et al. 2012). EK2 was purified out of *Sf*9 cells and lysed in 25 mM Tris pH 7.6, 100 mM NaCl, 5% Glycerol, 1 mM DTT, 0.5 mM EDTA and Roche cOmplete Protease Inhibitor Tablets. After sonications, the lysates were cleared at 14,000 rpm for 45 minutes at 4°C in a Sorval SS-34 rotor. The proteins were affinity purified with Glutathione for 3 hours at 4°C with rotation. After washing in batch, the tag was cleaved off by overnight Thrombin digestions. All sortase reactions were done at 30°C overnight in 50 mM Tris pH 7.6, 150 mM NaCl and 0.5 mM EDTA.

Deneddylation Assays Deneddylation reactions were done as described in (Emberley, Mosadeghi et al. 2012) except that the Ovalbumin was increased to 0.1 mg/ml. Multi-turnover assays were done with 50 nM Cullin substrate and 2 nM CSN unless otherwise noted. Single-turnover reactions were done with 25 nM Cullin substrates and 1 μM CSN. Substrates were added at 500 nM for Fig. 5A and 700 mM for Cdc34 K_i measurements.

Fluorescence Assays All assays were performed in a buffer containing 30 mM Tris pH 7.6, 100 mM NaCl, 0.25 mg/ml Ovalbumin and 0.5 mM DTT. All assays were measured with 30 nM dansyl-labeled Cul1-Rbx1 and titrated concentrations of CSN. Equilibrium binding assays were performed on a Fluorolog-3 (Jobin Yvon) while on-rate measurements were performed on a Kintec Stopped-flow Apparatus. The fluorophore was excited at 340 nM and emissions were scanned between 450 and 600 nM, while a peak of 515 nM was used for the assessment of binding. All data points were fitted to a quadratic (Y = M3+M4*(K_d+A+X-sqrt((K_d +30+X)^ 2-4A*X))/2*A) where A equals concentration of labeled protein using Prism (Graph Pad).

Cell Culture and Mass Spectroscopy Cells were grown in Lonza DMEM containing 10% FBS (Invitrogen). Transfections were done with FugeneHD per the manufacturers instructions (Roche). Flag-tagged CSN was inserted into a pBABE multiple cloning site engineered into an MSCV-GFP vector, and expressed a non-linked GFP. SILAC labeling was in Invitrogen DMEM containing 10% FBS and Lys8 and Arg8 from Immunoprecipitations were done in Pierce Lysis Buffer containing cOmplete Protease Inhibitor Cocktail (Roche) and sonicated for 15 seconds. After a 5 minute clearing at 16000 rpm at 4°C, proteins were immunoprecitiates and with M2 Flag agarose beads (Sigma) for 30 minutes and prepared for mass spectroscopy by (Pierce, Lee et al. 2013). Sample were run on an OrbiTrap Fusion and analyzed by MaxQuant. CRISPR constructs were made as described by (Shalem, Sanjana et al. 2014)

Figures Legends

Figure 1. Validation of Dansy Environmental Sensitivity Assay. A) Background subtracted fluorescence traces of the dansyl dye bound to Cul1-Rbx1 alone or in solution with CSN, CAND1 or both. B) Fluorescence traces of neddylated Cul1-Rbx1 bound to excess Skp1/Skp2 in solution with CSN^{H138A}, CAND1 or both. C) Titration curve of wild-type CSN binding to Cul1-Rbx1. D) titration curve of catalytically dead CSN^{E76A} binding to Cul1-Rbx1. E) titration curve of CSN^{E76A} binding to neddylated Cul1-Rbx1.

Figure 2. Effect of Fboxes on CSN binding and kinetics. A and B) titration curve of wild-type CSN binding to SCF^{Skp2} and SCF^{Fbw7}. C and D) Titration curve of CSN^{H138A} zinc binding point mutant binding to neddylated Cul1-Rbx1. E) k_{obs} for increasing concentrations of wild-type CSN and CSN^{H138A}, binding Cul1-Rbx1 or neddylated Cul1-Rbx1 respectively. F) k_{obs} for increasing concentrations of CSN^{H138A} binding to neddylated Cul1-Rbx1, neddylated SCF^{Skp2} and SCF^{Fbw7}. G) single-turnover deneddylation of neddylated Cul1-Rbx1, neddylated SCF^{skp2} and neddylated SCF^{Fbw7}.

Figure 3. Cellular Asses of the Role of Ins-1. A) Western blots of 293T cell lines stably expressing either vector alone (GFP), flag tagged wild-type CSN5, $CSN5^{T103I}$, $CSN5^{E104A}$, $CSN5^{T105A}$, or $CSN5^{R106A}$ lysed with 2% SDS lysis buffer. B) Western blots of inputs and Immunoprecipitation of flag-CSN5 constructs after 30 minute treatment with MLN4924. C) Efficiency of different CSN5 CRSPR constructs for decreasing cellular concentration of CSN5. D) SILAC ratios comparing binding partners of either $CSN5^{T103I}$ or $CSN5^{E104A}$ (light) to wild-type CSN5 (heavy).

Figure 4. Equilibrium and kinetics effects of mutating zinc chelating residues. A) Titration curve of CSN^{H138A} to neddylated Cul1-Rbx1. B) Titration curve of CSN^{H138A} binding to Cul1-Rbx1. C) Titration of CSN^{E104A} binding to Cul1-Rbx1. D) Multi-turnover deneddylation reactions of Cul1-Rbx1 by CSN^{E104A} or wild-type enzyme at 1 or 1.3 μM substrate. E) Single-turnover deneddylation of Cul1-Rbx1 by CSN^{E104A}.

Figure 5. A) Multi-turnover deneddylation of SCF^{Fbw7} in the presence of excess EK2, GST-EK2 or EK2 with a sortased degron. B) Fluorescence traces of SCF^{Fbw7} binding CSN^{H138A} in the presence of increasing EK2 with a sortased degron. C) Ubiquitination of EK2 with a sortased degron. D) Plot of the peak absorbances of dansyl measured in 5B against the concentration of EK2.

Figure 6. Effect of Substrate or ubiquitinated substrate of Cdc34's ability to inhibit deneddylation. A) K_i of Cdc34-Ub for the inhibition of the deneddylation of SCF^{Fbw7} without Cyclin E peptide, with Cyclin E peptide or with mono-ubiqtuitinated Cyclin E peptide.

Figure 7. Models incorporating the measured rates of CSN's biochemical parameters. A) Model representing the microscopic rates of a deneddylation reactions. B) Model of how CSN switches between an inactive, low affinity state to an active, high affinity state through an E-swap. C) Model of how the residues in Ins-1 play a role in stabilizing both active and inactive conformations of CSN.

Table 1. Compilation of all determined binding rate constants.

Table 2. Compilation of all calculated k_{cat}.

Figure S1. Controls for the Environmental Sensitivity Assay. A) Fluorescence traces of dansyl-conjugated Cul1-Rbx1 with or without unlabeled Cul1-Rbx1. B) Fluorescence traces of dansyl-conjugated to Cul1-Rbx1 with different concentrations of Ovalbumin carrier protein. C) Titration curves of unlabeled Cul1-Rbx1 binding to dansyl-conjugated Cul1-Rbx1 or N8-Cul1-Rbx1. D) Fluorescence traces of Cul1-Rbx1 in the presence of Cul5-Rbx2, Cul3-Rbx1, CSN or CSN and Cul3-Rbx1.

Figure S2. Effect of free Nedd8 on binding Cul1-Rbx1 to wild-type CSN. Wild-type CSN was titrated against 30 nM Cul1-Rbx1 in the presence of 5 μM free Nedd8.

Figure S3. Validation of CSN5 CRiSPR cell lines. Cells were transduced with a lentiviral cell virus and selected with Puromycin

Figure S4. Validation of Substrates. A) Western blot of ubiquitination assay of EK2 with a sortased degron without a fluorophore..

Figures

Figure 1.

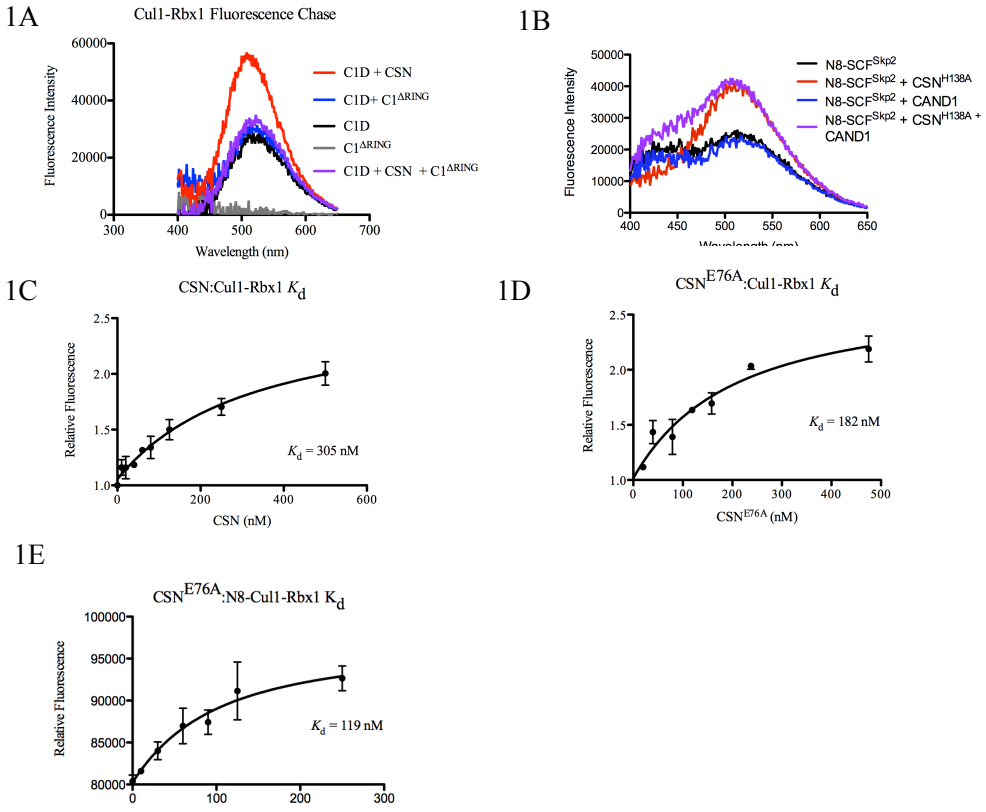

Figure 2.

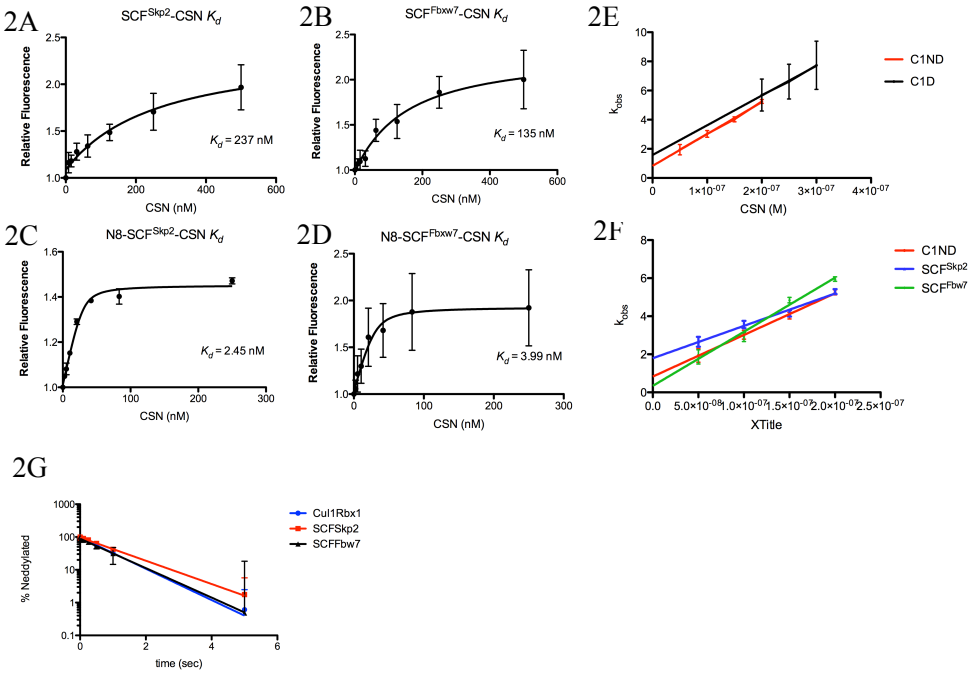
2A
SCF^Skp2-CSN K_d
Relative Fluorescence
K_d = 237 nM
CSN (nM)
2B
SCF^Fbxw7-CSN K_d
Relative Fluorescence
K_d = 135 nM
CSN (nM)
2E
k_obs
C1ND
C1D
CSN (M)
2C
N8-SCF^Skp2-CSN K_d
Relative Fluorescence
K_d = 2.45 nM
CSN (nM)
2D
N8-SCF^Fbxw7-CSN K_d
Relative Fluorescence
K_d = 3.99 nM
CSN (nM)
2F
k_obs
C1ND
SCF^Skp2
SCF^Fbw7
XTitle
2G
% Neddylated
Cul1Rbx1
SCFSkp2
SCFFbw7
time (sec)

Figure 3.

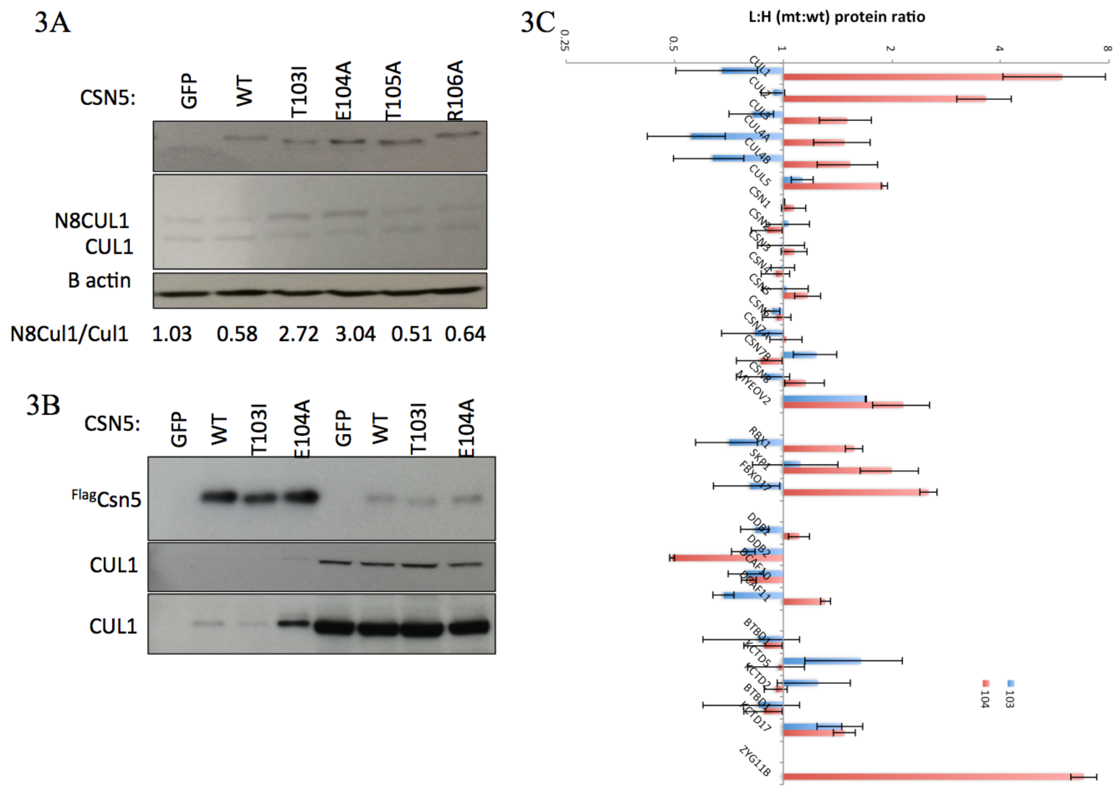
3A
CSN5:
GFP
WT
T103I
E104A
T105A
R106A
N8CUL1
CUL1
B actin
N8Cul1/Cul1
1.03
0.58
2.72
3.04
0.51
0.64
3B
CSN5:
GFP
WT
T103I
E104A
GFP
WT
T103I
E104A
FlagCsn5
CUL1
CUL1
3C
L:H (mt:wt) protein ratio
0.25
0.5
1
2
4
8
103
104

Figure 4.

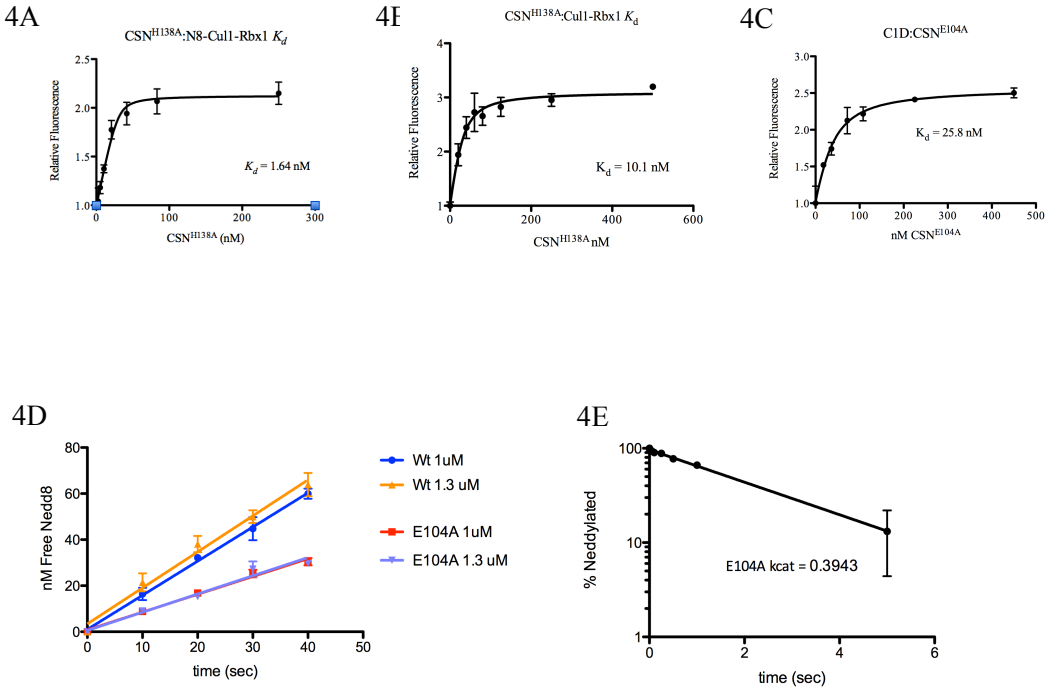
4A
CSN^H138A:N8-Cul1-Rbx1 K_d
Relative Fluorescence
K_d = 1.64 nM
CSN^H138A (nM)
4B
CSN^H138A:Cul1-Rbx1 K_d
Relative Fluorescence
K_d = 10.1 nM
CSN^H138A nM
4C
C1D:CSN^E104A
Relative Fluorescence
K_d = 25.8 nM
nM CSN^E104A
4D
nM Free Nedd8
time (sec)
Wt 1uM
Wt 1.3 uM
E104A 1uM
E104A 1.3 uM
4E
% Neddylated
E104A kcat = 0.3943
time (sec)

Figure 5.

5A

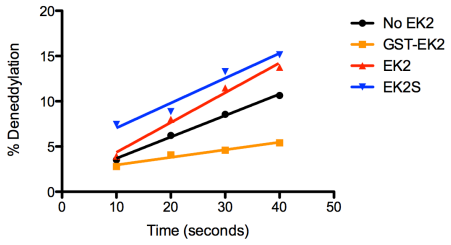

5B

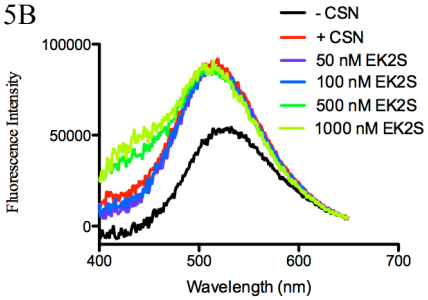

5C

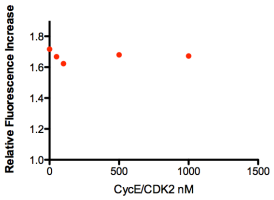

Figure 6.

6A

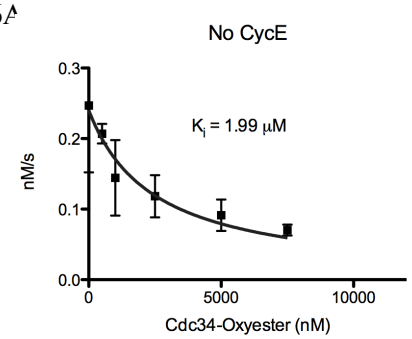

6B

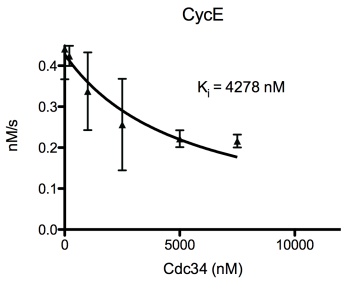

6C

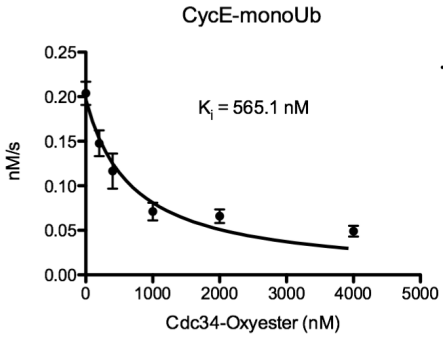

Figure 7.

7A

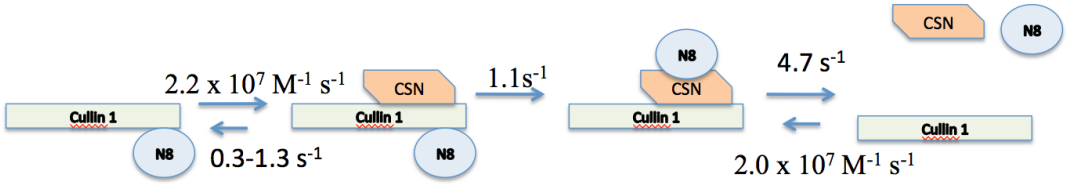

7B

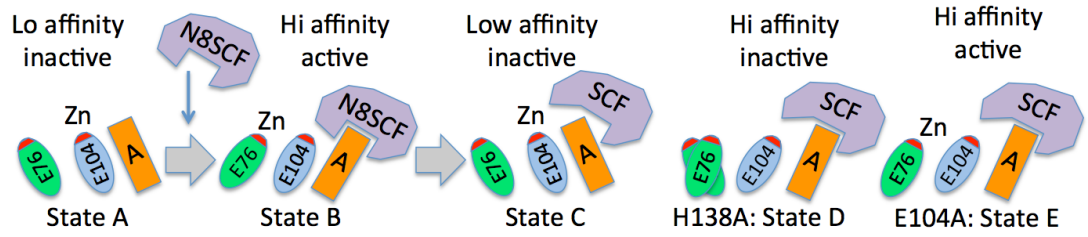

Figure S1.

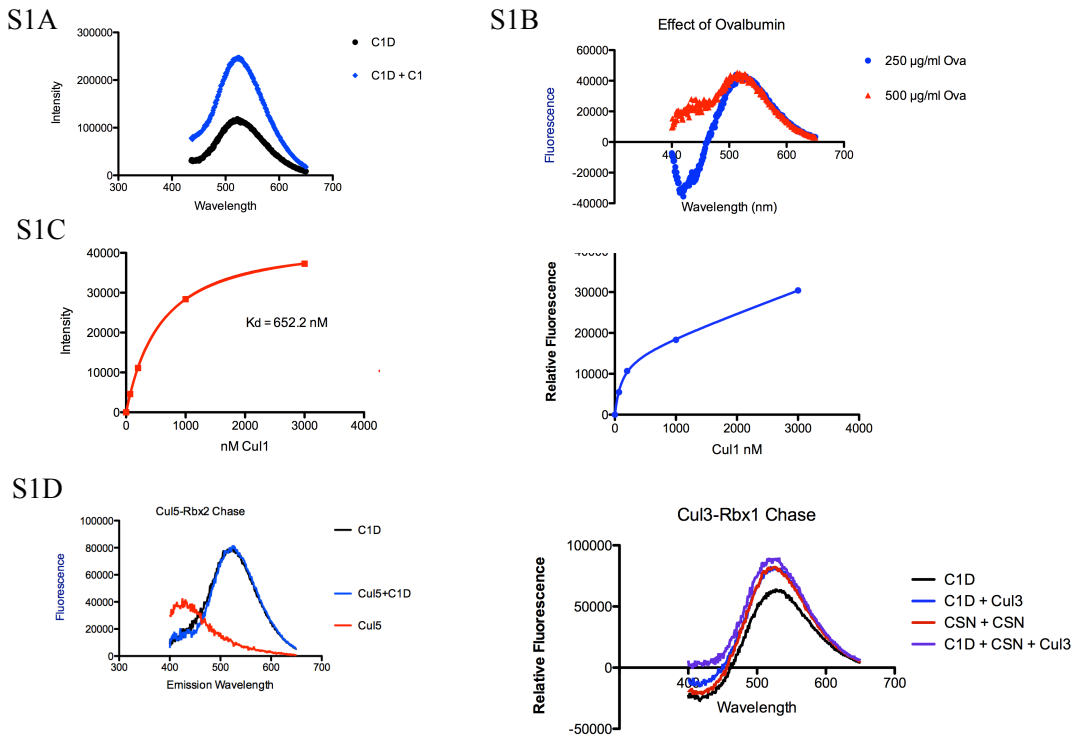
S1A
Intensity
Wavelength
C1D
C1D + C1
S1B
Effect of Ovalbumin
Fluorescence
Wavelength (nm)
250 µg/ml Ova
500 µg/ml Ova
S1C
Intensity
Kd = 652.2 nM
nM Cul1
Relative Fluorescence
Cul1 nM
S1D
Cul5-Rbx2 Chase
Fluorescence
Emission Wavelength
C1D
Cul5+C1D
Cul5
Cul3-Rbx1 Chase
Relative Fluorescence
Wavelength
C1D
C1D + Cul3
CSN + CSN
C1D + CSN + Cul3

Figure S2.

S2

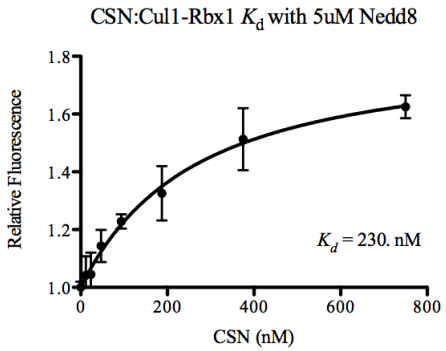
CSN:Cul1-Rbx1 K_d with 5uM Nedd8
Relative Fluorescence
1.8
1.6
1.4
1.2
1.0
0
200
400
600
800
CSN (nM)
K_d = 230. nM

Figure S3.

S3

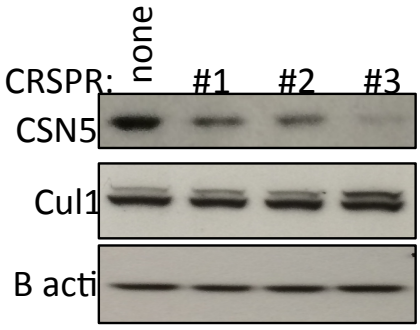

Figure S4.

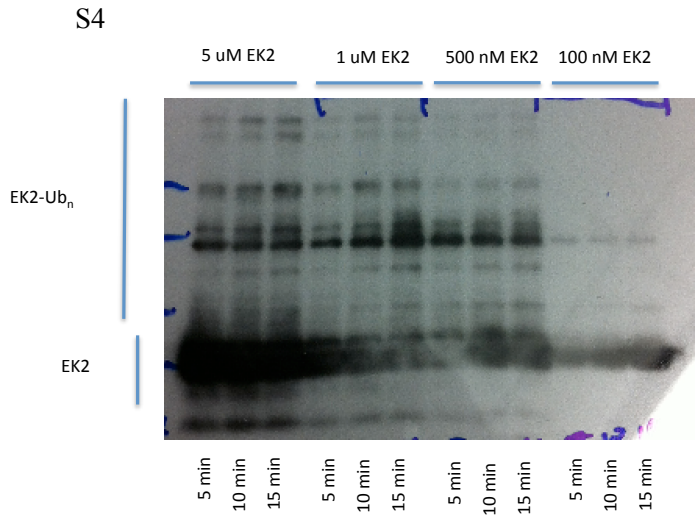

Ubi Assay with different concentrations of substrate

Table 1.

Substrate	K_d (nM)					k_{on} (x10^7 M-1 sec-1)					k_{off} (sec-1) (calculated))				
	CSN	CSN^{H138A}	CSN^{E76A}	$CSN_{\Delta 5}$	CSN^{E104A}	CSN	CSN^{H138A}	CSN^{E76A}	$CSN^{\Delta 5}$	CSN_{E104A}	CSN	CSN^{H138A}	CSN^{E76A}	$CSN^{\Delta 5}$	CSN^{E104A}
Cul1-Rbx1	305	10.1	180	1180	25.8	-	TBD	TBD	TBD	TBD	-	TBD	TBD	TBD	TBD
Cul1-Rbx1 + N8	230	-	-	-	-	2	-	-	-	-	4.7	-	-	-	-
N8-Cul1-Rbx1	NA	1.64	119	1090	NA	NA	2.2	TBD	TBD	NA	NA	0.036	TBD	TBD	NA
SCF^{Skp2}	236	-	-	-	-	-	-	-	-	-	-	-	-	-	-
SCF^{Fbw7}	135	-	-	-	-	-	-	-	-	-	-	-	-	-	-
N8-SCF^{Skp2}	NA	2.45	-	-	NA	NA	1.7	-	-	NA	NA	0.042	-	-	NA
N8-SCF^{Fbw7}	NA	3.99	-	-	NA	NA	2.8	-	-	NA	NA	0.113	-	-	NA

Table 2.

	Wild-type	CSN^{E104A}
N8-Cul1-Rbx1	1.1	0.4
Single-turnoever	1.1	0.4
Multi-turnover		
N8SCFSkp2		
Single-turnoever	0.82	-
Multi-turnover	-	
N8-SCFFbw7		
Single-turnoever	1.0	-
Multi-turnover	-	-

Chapter 4: Unpublished Work

CSN Cell Lysate Assay

There has long been an association with CSN5 upregulation and cancer. We set out to develop a lysate-based assay to quantify the amount of CSN deneddylation activity within different cell types. Although most of this overexpression has been coupled to c-myc associated gene amplification (the two genes are very near each other), there has long been an unanswered question (arising mainly form two-hybrid screen hits and transfection experiments) of whether CSN5 can act as a monomeric pro-oncogenic protein. Our goals were numerous. We wanted to 1) quantify total CSN activity 2) understand whether different cell lines had different amounts of activity, 3) know whether activity was correlated to protein level (or a post-translation modification), 4) test whether overexpression of Csn5 could enhance total CSN activity, and 5) test for associations with disease. To this end, we developed a fluorescence polarization assay compatible with lysate to measure deneddylation.

The lysates were diluted serially dilutions initial rates within the linear range of 1.5-25 ng total protein/µl were plotted. In this way, we can compare the slope of the lines (Fig. 1A and 1B). To speed up the assay, they were completed before protein quantification was performed, and only points within the assay window were plotted. Comparing plate to plated, the results were highly precise (Fig. 1C). By the use of the JAMM domain inhibitor 8-quinolinethiol and knocking down a subunit of CSN, CSN1, we showed that the activity was highly specific for not just JAMM domain proteins but also CSN (Fig. 1D and E). On ice, the lysates could stay active over the course of hours (Fig 2C). The rate of deneddylation in lysates proved to be highly sensitive to both NaCl concentrations and pH, preferring low salt buffers at a pH of 7.5 (Fig. 2A and B). We did

not tirate below 50 mM, which gave the fast rates, but without salt, the assay the activity of reduced (data not shown). We also showed by use of an ATP regenerating enzyme, that our assay could be used to also study neddylation, which was easily inhibited by the neddylation inhibitor MLN4924 (Fig. 2D and 2E).

Through our assays we found that CSN activity as compared to total protein varied to different extents among different cell lines (Fig. 3A-D). This change in activity either completely, or partially corrected by normalizing to CSN1 or CSN5 by western blots. Also, the T antigen in used in 293T did not have an effect on CSN activity, nor did overexpression of CSN5 alone.

Von Hippel Lindau Protein (VHL)

During the course of trying to find a cell-based assay we turned to other cullins and fell across some very interesting results with VHL. We first discovered that in cell lysates, one must always control for both neddylation and deneddylation even at 4°C. Our results showed that cullins bound to both VHL or a truncation mutant incapable of binding its substrate Hif1α could be both fully neddylated or deneddylated during an hour IP (Fig. 5A and 5B). We also noticed that in the absence of substrate, substrate receptors bound far less cullin (Fig. 5B), implying that substrates might play some role in complex assembly. This will be discussed later in this section. Beyond substrates, we used a cullin incapable of binding substrate receptors and found that they too were capable of being both neddylated and deneddylated, implying that substrate and substrate receptors are not required per se for this pathway.

VHL disease itself is broken down into several forms of diseases. Type 1 is caused by deletion or a loss of substrate binding, leads to massive Hif1α stabilization and multiple cancers including renal cell carcinoma (RCC) and hemanigoblastomas, but does not lead to pheochromocytomas. Type 2 diseases have varying levels of binding and ubiquitination and thus different risks for RCC and hemangioblastomas, but all (2A, 2B and 2C) do lead to pheochromocytomas. VHL Type 2C, which barely stabilized Hif1α *only* leads to pheochromocytomas. This finding that loss of substrate binding or deletion does not lead to pheochromocytomas, but that mild missense mutations do implies that pheochromocytomas are caused by gain of function of the VHL mutations.

Since VHL is a tumor suppressor, we used this set of mutations to test whether we could find interesting mutations since this is a mutational hotspot. What we found surprisingly was that certain mutations designed to ablate binding to substrate, led to hyperneddylation (Fig. 5D)! They all were also Type 2 mutations, implying that through some mechanism, either disrupting normal Cul2 cycling or through degrading a neosubstrates, Type 2 disease mutations are causing pheochromocyotmas.

Substrate and CAND1's Roles in Neddylation and Fbox Exchange

Two insights led us to take on the next set of experiments. First, was the published result that CAND1 is an exchange factor, which can exchange substrate receptors on non-neddylated cullins. Second was our VHL result that substrate receptors incapable of binding their substrates were significantly less bound to cullins. Our assessment was that perhaps substrate played a role in CAND1-meadiated bound exchange. Perhaps CAND1 could sense a CRL was bound to a substrate and would thus

not exchange its substrate receptor, but rather exchange empty substrate receptors to allow substrate bound ones an opportunity to bind a cullin.

While we knew that in the absence of CSN and CAND1, fboxes and substrates had no effect on the rate of neddylation (unpublished data), we knew that Fbox proteins could relieve CAND1 mediated inhibition of neddylation (Pierce, Lee et al. 2013). First, we attempted to test this theory by pulling down Cul1 and seeing how much TAMRA-labeled Fbw7 could be pulled down (Fig. 6A). In the presence of CAND1, we bound less Fbw7, which was further diminished by the addition of a competing Fbox, Skp2. Exactly as suspected, the addition of Fbw7's substrate CyclinE/Cdk2 (EK2) partially overcame the effects of Skp2 and CAND1, implying that an Fbox bound to a substrate would be more likely to bind Cul1 in the presence of CAND1 as opposed to one which was unbound. We next attempted to neddylate Cul1-Rbx1 and SCF^{Fbw7} in the presence of CAND1 with or without EK2 (Fig. 6A). We found that while Cul1-Rbx1 could not be neddylated, even in the presence of substrate (data not shown), that EK2 could increase the rate of neddylation by about two-fold. Although these effects are modest, they lend support for the idea that substrates can affect CAND1 function and thus provide a potential mechanism by which CRL complex assembly can be mediated.

In our control experiments for neddylation, we tested a few extra conditions. What we found while attempting to both neddylate and deneddylate was that regardless of substrate being around or not, CSN inhibited neddylation. Surprisingly, CAND1 actually relieved the inhibition of neddylation by CSN (Fig. 7A). This made us think that CAND1 could act as a Neddylation Priming Factor (NPF). We knew from the development of our assay in chapter three that CAND1 can out compete CSN for Cul1

binding but that Fboxes bind with CSN in a complex. Thus we assayed whether Fboxes could relieve CAND1's inhibition of CSN binding. Fbw7 could in fact relieve the sequestering of Cul1 by CAND1 (Fig. 7B) . To finalize our hypothesis of the CRL cycle, we tested whether CAND1 could act as a NPF by neddylating Cul1-Rbx1 in the presence of CSN, CAND1 and Fbox. We found that while CAND1 did slow down neddylation on the millisecond time scale, it was not nearly as efficient as CSN. But interestingly, CAND1 in the presence of CSN behaved identically to CAND1 alone (Fig. 7C). This means that CAND1 was completely neutralizing CSN's inhibition of neddylation.

Materials and Methods

All Cell lines were gown in DMEM with 10% FBS and lysed in 25 mM Tris pH 7.6, 150 mM NaCl, 1 mM DTT and 0.2% Triton X-100 with cOmplete Protease Inhibitor Tablet (Roche). Lysates were then diluted 7-fold into Assay Buffer containing 25 mM Tris pH 7.6, 50 mM NaCl, 0.1% Triton X-100 1% Glycerol, 1 mM DTT, 25 mM Trehalose and 3 ng/µl Ovalbumin and then serial diluted 11 times. 5 µl of each concentration was mixed into a total volume of 15 µl containing 2.5 nM Cul1-Rbx1-N8(Oregon Green). The linear range of this assay was 1.5-25 ng/µl of protein.

All VHL IPs were done in the buffer describe by (Alexandru, Graumann et al. 2008). Any modification in time and conditions are noted in the figures.

Fbox competition assays were all done in 25 mM Tris pH 7.6, 100 nM NaCl, 0.5 mg/ml Ovalbumin and 1 mM DTT. All protein concentrations were 200 nM, except for CycE/Cdk2, which was at 500 nM.

Neddylation Assays were all performed on the Kinetic Quench Flow Apparatus with 25 nM Tris pH 7.6, 100 nM NaCl, 12.5 mM ATP, 5 mM $MgCl_2$ and 1 mM DTT. Cul1-PKA-Rbx1 was at 100 nM, while Fboxes were at 275 nM, CAND1 was at 300 nM CSN variants were at 300 nM and EK2 was at 500 nM. These proteins were neddylated with 1 μM NAE, 10 μM Ubc12 (from *Sf*9 cells), 300 nM DCN1 and 25 μM Nedd8.

Figures Legends

Figure 1. Validation of Fluorescence Polarization (FP) Assay of CSN in Lysate. A) Traces of FP over time for a serial dilutions of lysate (concentrations in A and B refer to dilutions not protein concentration). B) Plot of initial rates of deneddylation versus an arbitrary concentration. C) Plot of two technical replicates from separate plates versus concentration. Dilutions were made and assayed before protein concentrations were determined. D) Taces of FP over time. Assay was run using identical lysates +/- the JAMM domain inhibitor 8-thioquininol (B10). E) Plot of rates comparing control versus CSN1 knockdown cells to reduce level of full complex.

Figure 2. Assessment of Various Conditions effecting CSN Activity. A) Rates of deneddylation plotted against increasing concentrations of NaCl. B) Rates of deneddylation plotted against pH. C) Rates of deneddylation of lysates that were placed on ice for varying lengths of time from 0 to 270 minutes. D and E) Traces of FP showing neddylation and deneddylation over time in the presence of an ATP Regenerating System (ARS) with or without the neddylation inhibitor MLN4924, respectively.

Figure 3A. Comparing CSN Activity across cell lines. A-D) Comparison of CSN Activity in different cell lysates compared to 293T cell lysate. CSN1 and CSN5 refer to lysates of the tested cell lines normalized to either Western blots of CSN1 or CSN5 of 293T cells.

Figure 4. Effect of Large T-antigen and CSN5 overexpression on CSN Activity. A) Plot comparing 293 and 293T cell lysates. 4) Plots comparing Control versus myc-CSN5 overexpression in 293T cell lines.

Figure 5. Effects of VHL Binding and Mutations on the Neddylation Status of Cul2. A) Western blot for Hif1α bound to immunoprecipitated Flag-VHL with or with out the substrate-binding domain (β domain). B) Western blot of Cul2 bound to immunoprecipitated Flag-VHL or mutants. IPs were done for 1 hour at 4°C with various inhibitors as noted in the figure. C) Western blots of Cul2 incubated with various inhibitors for 1 hour at 4°C as noted in the figure after lysates were cleared. D) Same B but with specific point mutants.

Figure 6. Effect of Substrate on competition between Fboxes and CAND1 for Cul1 Binding. 1) Pull-down of GST-Rbx1-Cul1 comparing ratio of bound and unbound TAMRA-Fbw7/Skp1 in the presence of CAND1, Skp2/Skp1 and CycE/Cdk2. B) Phosho-image of the neddylation of radiolabeled Cul1-PKA-Rbx1 prebound to excess CAND1 with or without the addition of Fbw7/Skp1 or GST-EK2. C) Quantification of B.

Figure 7. Effect of CAND1 and CSN on the Neddylation of Cul1-Rbx1. A) Neddylation of Cul1-PKA-Rbx1 in the presence of Fbw7/Skp1. Cul1-PKA-Rbx1 was prebound to wild-type CSN +/- CAND1. b) Fluorescence traces of dansyl-conjugated Cul1-Rbx1 in the presence of wild-type CSN and CAND1 +/- Fbw7/Skp1. 7) Phosphoimage of the millisecond neddylation of Cul1-PKA-Rbx1 in the presence of CAND1, catalytically inactive CSN^{H138A} and Skp2/Skp1 as noted in the figure.

Figures

Figure 1.

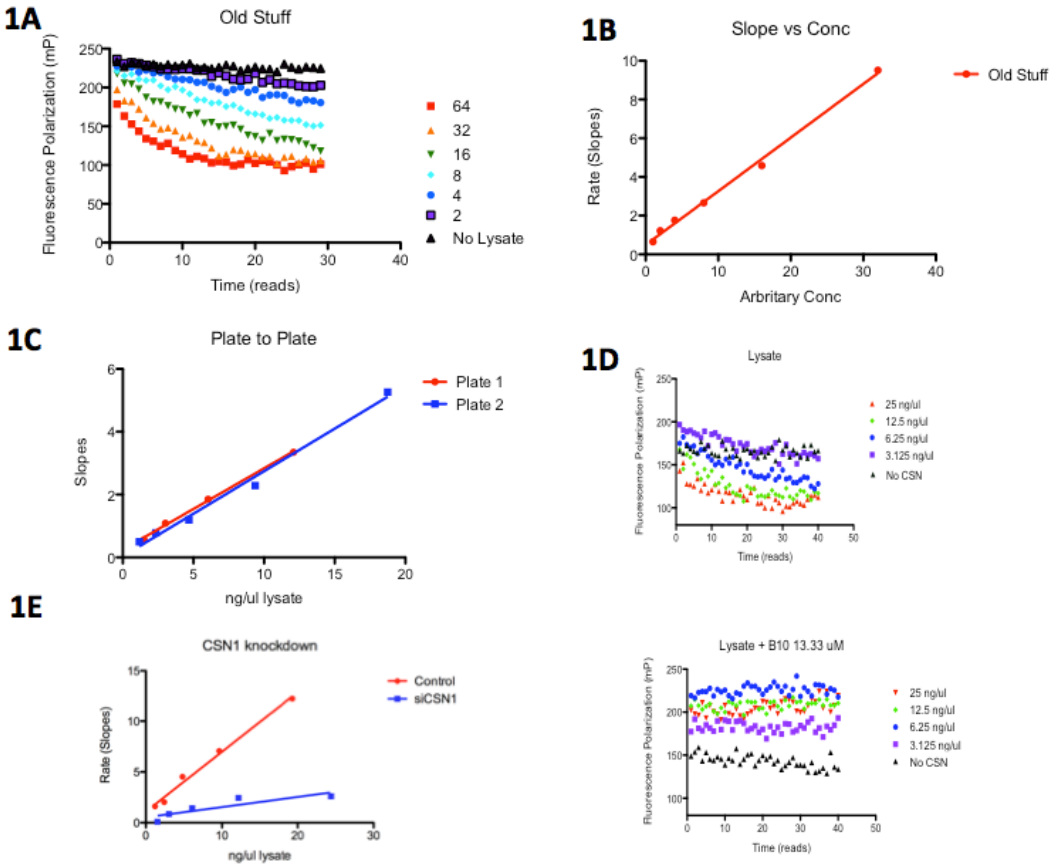

Figure 2.

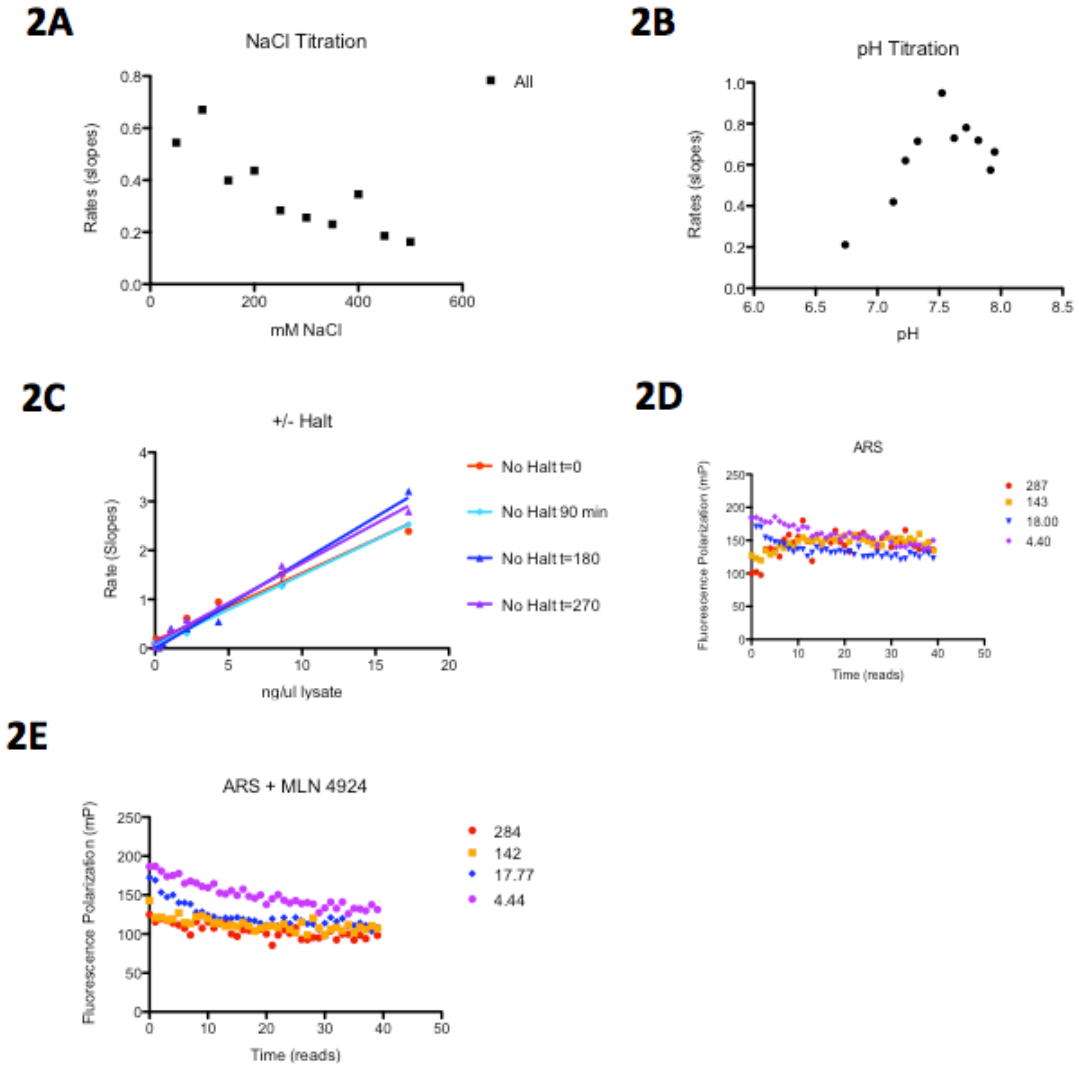
2A
NaCl Titration
All
Rates (slopes)
mM NaCl
2B
pH Titration
Rates (slopes)
pH
2C
+/- Halt
No Halt t=0
No Halt 90 min
No Halt t=180
No Halt t=270
Rate (Slopes)
ng/ul lysate
2D
ARS
287
143
18.00
4.40
Fluorescence Polarization (mP)
Time (reads)
2E
ARS + MLN 4924
284
142
17.77
4.44
Fluorescence Polarization (mP)
Time (reads)

Figure 3.

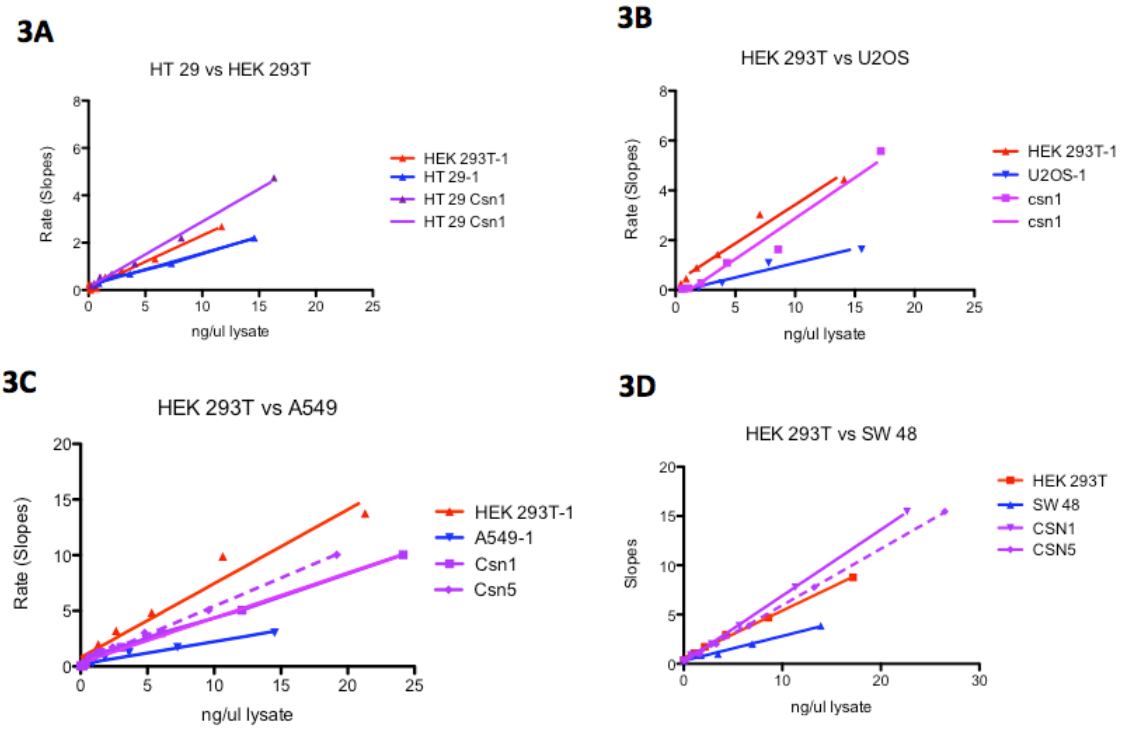

Figure 4.

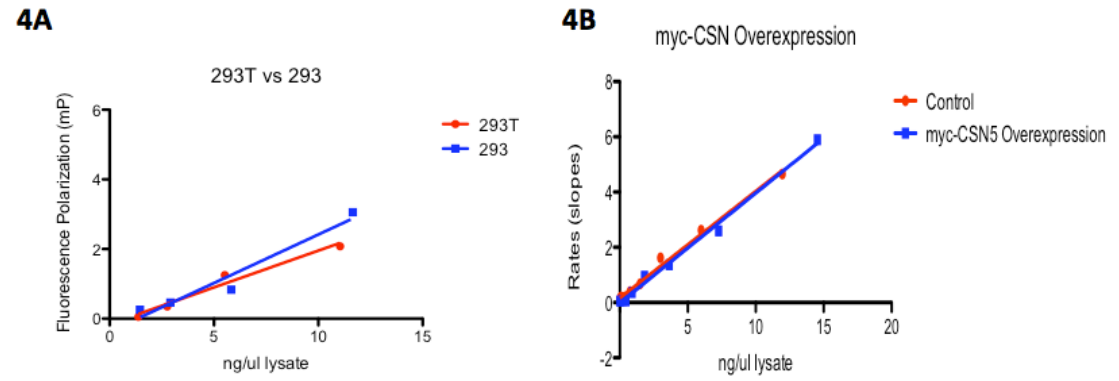

Figure 5.

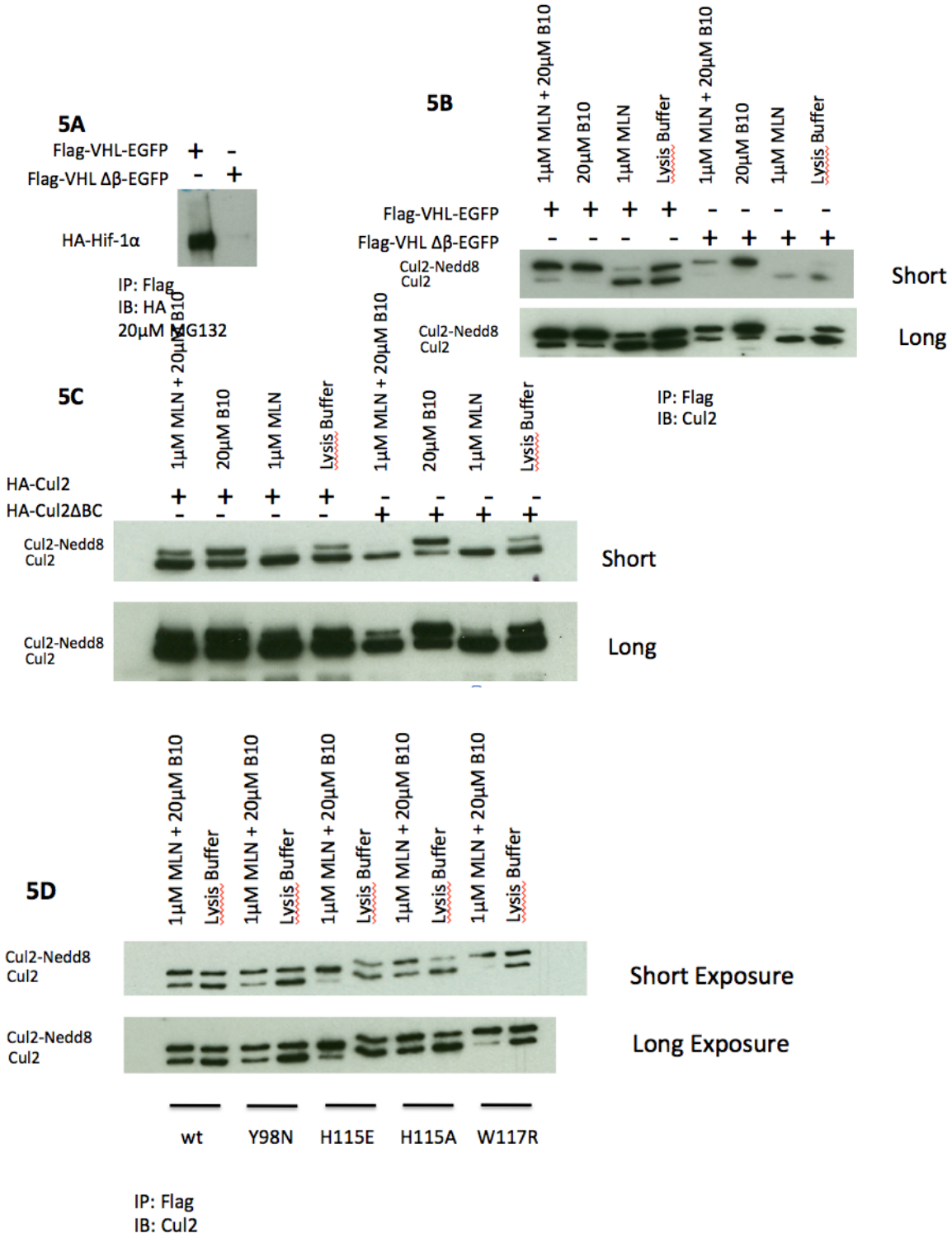
5A
Flag-VHL-EGFP + -
Flag-VHL Δβ-EGFP - +
HA-Hif-1α
IP: Flag
IB: HA
20μM MG132
5B
1μM MLN + 20μM B10
20μM B10
1μM MLN
Lysis Buffer
Flag-VHL-EGFP
Flag-VHL Δβ-EGFP
Cul2-Nedd8
Cul2
Short
Long
IP: Flag
IB: Cul2
5C
HA-Cul2
HA-Cul2ΔBC
Cul2-Nedd8
Cul2
Short
Long
5D
Short Exposure
Long Exposure
wt
Y98N
H115E
H115A
W117R
IP: Flag
IB: Cul2

Figure 6.

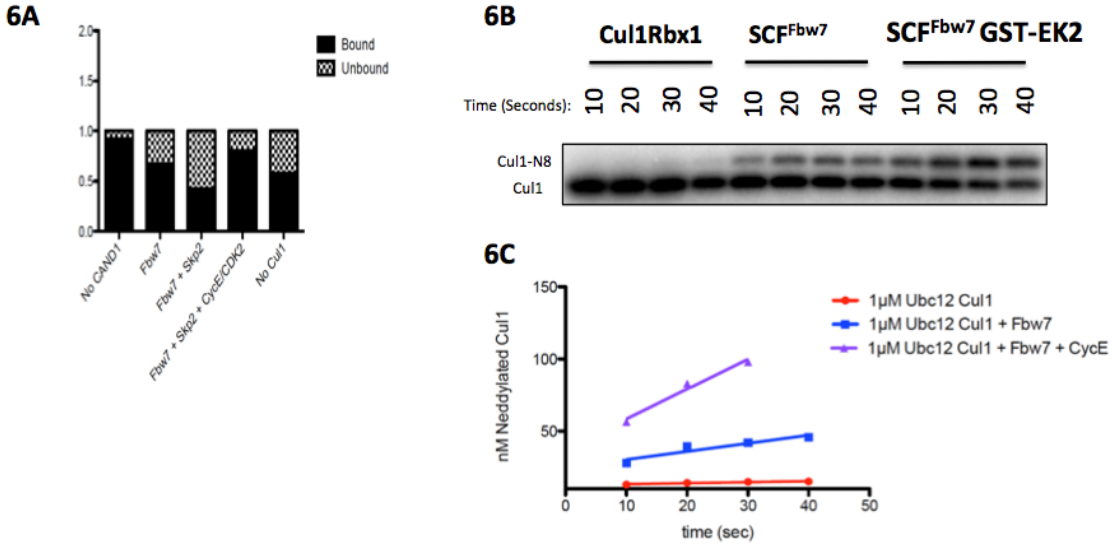

Figure 7.

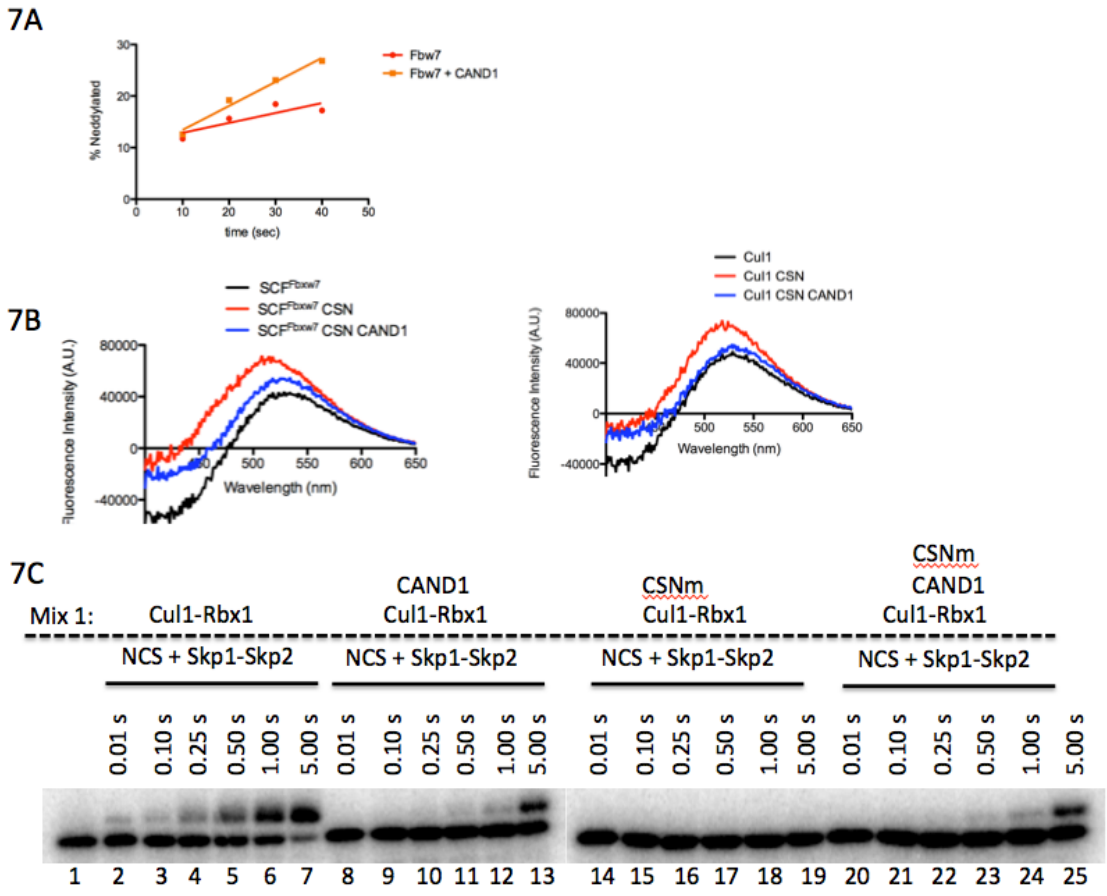

Bibliography

Adler, A. S., M. Lin, H. Horlings, D. S. Nuyten, M. J. van de Vijver and H. Y. Chang (2006). "Genetic regulators of large-scale transcriptional signatures in cancer." Nat Genet **38**(4): 421-430.
Adler, A. S., L. E. Littlepage, M. Lin, T. L. Kawahara, D. J. Wong, Z. Werb and H. Y. Chang (2008). "CSN5 isopeptidase activity links COP9 signalosome activation to breast cancer progression." Cancer Res **68**(2): 506-515.
Aghajan, M., N. Jonai, K. Flick, F. Fu, M. Luo, X. Cai, I. Ouni, N. Pierce, X. Tang, B. Lomenick, R. Damoiseaux, R. Hao, P. M. Del Moral, R. Verma, Y. Li, C. Li, K. N. Houk, M. E. Jung, N. Zheng, L. Huang, R. J. Deshaies, P. Kaiser and J. Huang (2010). "Chemical genetics screen for enhancers of rapamycin identifies a specific inhibitor of an SCF family E3 ubiquitin ligase." Nat Biotechnol **28**(7): 738-742.
Alexandru, G., J. Graumann, G. T. Smith, N. J. Kolawa, R. Fang and R. J. Deshaies (2008). "UBXD7 binds multiple ubiquitin ligases and implicates p97 in HIF1alpha turnover." Cell **134**(5): 804-816.
Ambroggio, X. I., D. C. Rees and R. J. Deshaies (2004). "JAMM: A Metalloprotease-Like Zinc Site in the Proteasome and Signalosome." PLoS Biol **2**(1): E2.
Bandau, S., A. Knebel, Z. O. Gage, N. T. Wood and G. Alexandru (2012). "UBXN7 docks on neddylated cullin complexes using its UIM motif and causes HIF1alpha accumulation." BMC Biol **10**: 36.
Bennett, E. J., J. Rush, S. P. Gygi and J. W. Harper "Dynamics of cullin-RING ubiquitin ligase network revealed by systematic quantitative proteomics." Cell **143**(6): 951-965.
Bennett, E. J., J. Rush, S. P. Gygi and J. W. Harper (2010). "Dynamics of cullin-RING ubiquitin ligase network revealed by systematic quantitative proteomics." Cell **143**(6): 951-965.
Besten, W., R. Verma, G. Kleiger, R. S. Oania and R. J. Deshaies (2012). "NEDD8 links cullin-RING ubiquitin ligase function to the p97 pathway." Nat Struct Mol Biol **19**(5): 511-516.
Bornstein, G., J. Bloom, D. Sitry-Shevah, K. Nakayama, M. Pagano and A. Hershko (2003). "Role of the SCFSkp2 ubiquitin ligase in the degradation of p21Cip1 in S phase." J Biol Chem **278**(28): 25752-25757.
Bornstein, G., D. Ganoth and A. Hershko (2006). "Regulation of neddylation and deneddylation of cullin1 in SCFSkp2 ubiquitin ligase by F-box protein and substrate." Proc Natl Acad Sci U S A **103**(31): 11515-11520.
Bosu, D. R. and E. T. Kipreos (2008). "Cullin-RING ubiquitin ligases: global regulation and activation cycles." Cell Div **3**: 7.
Cardozo, T. and M. Pagano (2004). "The SCF ubiquitin ligase: insights into a molecular machine." Nat Rev Mol Cell Biol **5**(9): 739-751.
Ceccarelli, D. F., X. Tang, B. Pelletier, S. Orlicky, W. Xie, V. Plantevin, D. Neculai, Y. C. Chou, A. Ogunjimi, A. Al-Hakim, X. Varelas, J. Koszela, G. A. Wasney, M. Vedadi, S. Dhe-Paganon, S. Cox, S. Xu, A. Lopez-Girona, F. Mercurio, J. Wrana, D. Durocher, S.

Meloche, D. R. Webb, M. Tyers and F. Sicheri "An allosteric inhibitor of the human Cdc34 ubiquitin-conjugating enzyme." Cell **145**(7): 1075-1087.
Chew, E. H. and T. Hagen (2007). "Substrate-mediated regulation of cullin neddylation." J Biol Chem **282**(23): 17032-17040.
Choo, Y. Y., B. K. Boh, J. J. Lou, J. Eng, Y. C. Leck, B. Anders, P. G. Smith and T. Hagen (2011). "Characterization of the role of COP9 signalosome in regulating cullin E3 ubiquitin ligase activity." Mol Biol Cell **22**(24): 4706-4715.
Cope, G. A. and R. J. Deshaies (2006). "Targeted silencing of Jab1/Csn5 in human cells downregulates SCF activity through reduction of F-box protein levels." BMC Biochem **7**: 1.
Cope, G. A., G. S. Suh, L. Aravind, S. E. Schwarz, S. L. Zipursky, E. V. Koonin and R. J. Deshaies (2002). "Role of predicted metalloprotease motif of Jab1/Csn5 in cleavage of Nedd8 from Cul1." Science **298**(5593): 608-611.
Crusio, K. M., B. King, L. B. Reavie and I. Aifantis "The ubiquitous nature of cancer: the role of the SCF(Fbw7) complex in development and transformation." Oncogene **29**(35): 4865-4873.
Dennissen, F. J., N. Kholod, D. J. Hermes, N. Kemmerling, H. W. Steinbusch, N. P. Dantuma and F. W. van Leeuwen (2011). "Mutant ubiquitin (UBB+1) associated with neurodegenerative disorders is hydrolyzed by ubiquitin C-terminal hydrolase L3 (UCH-L3)." FEBS Lett **585**(16): 2568-2574.
Denti, S., M. E. Fernandez-Sanchez, L. Rogge and E. Bianchi (2006). "The COP9 signalosome regulates Skp2 levels and proliferation of human cells." J Biol Chem **281**(43): 32188-32196.
Deshaies, R. J., E. D. Emberley and A. Saha (2010). Control of cullin–RING ubiquitin ligase activity by Nedd8. Conjugation and Deconjugation of Ubiquitin Family Modifiers. M. Groettrup, Landes Bioscience**:** 41-56.
Deshaies, R. J. and C. A. Joazeiro (2009). "RING domain E3 ubiquitin ligases." Annu Rev Biochem **78**: 399-434.
Dou, H., L. Buetow, G. J. Sibbet, K. Cameron and D. T. Huang (2012). "BIRC7-E2 ubiquitin conjugate structure reveals the mechanism of ubiquitin transfer by a RING dimer." Nat Struct Mol Biol **19**(9): 876-883.
Duda, D. M., L. A. Borg, D. C. Scott, H. W. Hunt, M. Hammel and B. A. Schulman (2008). "Structural insights into NEDD8 activation of cullin-RING ligases: conformational control of conjugation." Cell **134**(6): 995-1006.
Duda, D. M., L. A. Borg, D. C. Scott, H. W. Hunt, M. Hammel and B. A. Schulman (2008). "Structural insights into NEDD8 activation of cullin-RING ligases: conformational control of conjugation." Cell **134**: 995-1006.
Echalier, A., Y. Pan, M. Briol, N. Tavernier, L. Pintard, F. Hoh, C. Ebel, N. Galophe, F. X. Claret and C. Dumas (2013). "<Proc. Natl. Acad. Sci. U.S.A. 2013 Echalier-1.pdf>." Proc Natl Acad Sci U S A **110**(4): 5.
Emberley, E. D., R. Mosadeghi and R. J. Deshaies (2012). "Deconjugation of Nedd8 from Cul1 is directly regulated by Skp1-F-box and substrate, and the COP9 signalosome inhibits deneddylated SCF by a noncatalytic mechanism." J Biol Chem **287**(6): 9.

Enchev, R. I., D. C. Scott, P. C. da Fonseca, A. Schreiber, J. K. Monda, B. A. Schulman, M. Peter and E. P. Morris (2012). "Structural basis for a reciprocal regulation between SCF and CSN." Cell Rep **2**(3): 616-627.
Fischer, E. S., A. Scrima, K. Bohm, S. Matsumoto, G. M. Lingaraju, M. Faty, T. Yasuda, S. Cavadini, M. Wakasugi, F. Hanaoka, S. Iwai, H. Gut, K. Sugasawa and N. H. Thoma (2011). "The Molecular Basis of CRL4(DDB2/CSA) Ubiquitin Ligase Architecture, Targeting, and Activation." Cell **147**(5): 1024-1039.
Frescas, D. and M. Pagano (2008). "Deregulated proteolysis by the F-box proteins SKP2 and beta-TrCP: tipping the scales of cancer." Nat Rev Cancer **8**(6): 438-449.
Goldenberg, S. J., T. C. Cascio, S. D. Shumway, K. C. Garbutt, J. Liu, Y. Xiong and N. Zheng (2004). "Structure of the Cand1-Cul1-Roc1 complex reveals regulatory mechanisms for the assembly of the multisubunit cullin-dependent ubiquitin ligases." Cell **119**(4): 517-528.
Helmstaedt, K., E. U. Schwier, M. Christmann, K. Nahlik, M. Westermann, R. Harting, S. Grond, S. Busch and G. H. Braus (2011). "Recruitment of the inhibitor Cand1 to the cullin substrate adaptor site mediates interaction to the neddylation site." Mol Biol Cell **22**(1): 153-164.
Holmberg, C., O. Fleck, H. A. Hansen, C. Liu, R. Slaaby, A. M. Carr and O. Nielsen (2005). "Ddb1 controls genome stability and meiosis in fission yeast." Genes Dev **19**(7): 853-862.
Kawakami, T., T. Chiba, T. Suzuki, K. Iwai, K. Yamanaka, N. Minato, H. Suzuki, N. Shimbara, Y. Hidaka, F. Osaka, M. Omata and K. Tanaka (2001). "NEDD8 recruits E2-ubiquitin to SCF E3 ligase." Embo J **20**(15): 4003-4012.
Kim, H. C. and J. M. Huibregtse (2009). "Polyubiquitination by HECT E3s and the determinants of chain type specificity." Mol Cell Biol **29**(12): 3307-3318.
Kleiger, G., B. Hao, D. A. Mohl and R. J. Deshaies (2009). "The acidic tail of the Cdc34 ubiquitin-conjugating enzyme functions in both binding to and catalysis with ubiquitin ligase SCFCdc4." J Biol Chem **284**(52): 36012-36023.
Kleiger, G., A. Saha, S. Lewis, B. Kuhlman and R. J. Deshaies (2009). "Rapid dynamics of Cdc34-SCF assembly and disassembly enable processive polyubiquitylation of CRL substrates." Cell **139**: 957-968.
Kleiger, G., A. Saha, S. Lewis, B. Kuhlman and R. J. Deshaies (2009). "Rapid E2-E3 assembly and disassembly enable processive ubiquitylation of cullin-RING ubiquitin ligase substrates." Cell **139**(5): 957-968.
Komander, D. and M. Rape (2012). "The ubiquitin code." Annu Rev Biochem **81**: 203-229.
Koyano, F., K. Okatsu, H. Kosako, Y. Tamura, E. Go, M. Kimura, Y. Kimura, H. Tsuchiya, H. Yoshihara, T. Hirokawa, T. Endo, E. A. Fon, J. F. Trempe, Y. Saeki, K. Tanaka and N. Matsuda (2014). "Ubiquitin is phosphorylated by PINK1 to activate parkin." Nature **510**(7503): 162-166.
Lee, J. E., M. J. Sweredoski, R. L. Graham, N. J. Kolawa, G. T. Smith, S. Hess and R. J. Deshaies (2011). "The steady-state repertoire of human SCF Ubiquitin ligase complexes does not require ongoing Nedd8 conjugation." Mol Cell Proteomics.
Lee, Y. H., A. D. Judge, D. Seo, M. Kitade, L. E. Gomez-Quiroz, T. Ishikawa, J. B. Andersen, B. K. Kim, J. U. Marquardt, C. Raggi, I. Avital, E. A. Conner, I. Maclachlan, V. M. Factor and S. S. Thorgeirsson (2011). "Molecular targeting of CSN5 in human

hepatocellular carcinoma: a mechanism of therapeutic response." Oncogene **30**(40): 4175-4184.
Li, T., N. P. Pavletich, B. A. Schulman and N. Zheng (2005). "High-level expression and purification of recombinant SCF ubiquitin ligases." Methods Enzymol **398**: 125-142.
Lingaraju, G. M., R. D. Bunker, S. Cavadini, D. Hess, U. Hassiepen, M. Renatus, E. S. Fischer and N. H. Thoma (2014). "Crystal structure of the human COP9 signalosome." Nature **512**(7513): 161-165.
Liu, J., M. Furukawa, T. Matsumoto and Y. Xiong (2002). "NEDD8 modification of CUL1 dissociates p120(CAND1), an inhibitor of CUL1-SKP1 binding and SCF ligases." Mol Cell **10**(6): 1511-1518.
Luo, J., M. J. Emanuele, D. Li, C. J. Creighton, M. R. Schlabach, T. F. Westbrook, K. K. Wong and S. J. Elledge (2009). "A genome-wide RNAi screen identifies multiple synthetic lethal interactions with the Ras oncogene." Cell **137**(5): 835-848.
Lyapina, S., G. Cope, A. Shevchenko, G. Serino, T. Tsuge, C. Zhou, D. A. Wolf, N. Wei and R. J. Deshaies (2001). "Promotion of NEDD-CUL1 conjugate cleavage by COP9 signalosome." Science **292**(5520): 1382-1385.
Lydeard, J. R., B. A. Schulman and J. W. Harper (2013). "Building and remodelling Cullin-RING E3 ubiquitin ligases." EMBO Rep **14**(12): 1050-1061.
Min, K. W., M. J. Kwon, H. S. Park, Y. Park, S. K. Yoon and J. B. Yoon (2005). "CAND1 enhances deneddylation of CUL1 by COP9 signalosome." Biochem Biophys Res Commun **334**(3): 867-874.
Morikawa, H., M. Kim, H. Mimuro, C. Punginelli, T. Koyama, S. Nagai, A. Miyawaki, K. Iwai and C. Sasakawa (2010). "The bacterial effector Cif interferes with SCF ubiquitin ligase function by inhibiting deneddylation of Cullin1." Biochem Biophys Res Commun **401**(2): 268-274.
Nouspikel, T. and P. C. Hanawalt (2006). "Impaired nucleotide excision repair upon macrophage differentiation is corrected by E1 ubiquitin-activating enzyme." Proc Natl Acad Sci U S A **103**(44): 16188-16193.
O'Connell, B. C. and J. W. Harper (2007). "Ubiquitin proteasome system (UPS): what can chromatin do for you?" Curr Opin Cell Biol **19**(2): 206-214.
Orlicky, S., X. Tang, V. Neduva, N. Elowe, E. D. Brown, F. Sicheri and M. Tyers "An allosteric inhibitor of substrate recognition by the SCF(Cdc4) ubiquitin ligase." Nat Biotechnol **28**(7): 733-737.
Petroski, M. D. and R. J. Deshaies (2005). "Function and regulation of cullin-RING ubiquitin ligases." Nat Rev Mol Cell Biol **6**: 9-20.
Pierce, N. W., G. Kleiger, S. Shan and R. J. Deshaies (2009). "Detection of sequential polyubiquitylation on a millisecond timescale." Nature **462**: 615-619.
Pierce, N. W., G. Kleiger, S. O. Shan and R. J. Deshaies (2009). "Detection of sequential polyubiquitylation on a millisecond timescale." Nature **462**(7273): 615-619.
Pierce, N. W., J. E. Lee, X. Liu, M. J. Sweredoski, R. L. Graham, E. A. Larimore, M. Rome, N. Zheng, B. E. Clurman, S. Hess, S. O. Shan and R. J. Deshaies (2013). "Cand1 promotes assembly of new SCF complexes through dynamic exchange of F box proteins." Cell **153**(1): 206-215.
Popovic, D., D. Vucic and I. Dikic (2014). "Ubiquitination in disease pathogenesis and treatment." Nat Med **20**(11): 1242-1253.

Popp, M. W., J. M. Antos, G. M. Grotenbreg, E. Spooner and H. L. Ploegh (2007). "Sortagging: a versatile method for protein labeling." Nat Chem Biol **3**(11): 707-708.
Read, M. A., J. E. Brownell, T. B. Gladysheva, M. Hottelet, L. A. Parent, M. B. Coggins, J. W. Pierce, V. N. Podust, R. S. Luo, V. Chau and V. J. Palombella (2000). "Nedd8 modification of cul-1 activates SCF(beta(TrCP))-dependent ubiquitination of IkappaBalpha." Mol Cell Biol **20**(7): 2326-2333.
Saha, A. and R. J. Deshaies (2008). "Multimodal activation of the ubiquitin ligase SCF by Nedd8 conjugation." Mol Cell **32**(1): 21-31.
Saha, A. and R. J. Deshaies (2008). "Multimodal activation of ubiquitin ligase SCF by Nedd8 conjugation." Mol Cell **32**: 21-31.
Schulman, B. A., A. C. Carrano, P. D. Jeffrey, Z. Bowen, E. R. Kinnucan, M. S. Finnin, S. J. Elledge, J. W. Harper, M. Pagano and N. P. Pavletich (2000). "Insights into SCF ubiquitin ligases from the structure of the Skp1-Skp2 complex." Nature **408**(6810): 381-386.
Schulman, B. A. and J. W. Harper (2009). "Ubiquitin-like protein activation by E1 enzymes: the apex for downstream signalling pathways." Nat Rev Mol Cell Biol **10**(5): 319-331.
Schwechheimer, C., G. Serino, J. Callis, W. L. Crosby, S. Lyapina, R. J. Deshaies, W. M. Gray, M. Estelle and X. W. Deng (2001). "Interactions of the COP9 signalosome with the E3 ubiquitin ligase SCFTIRI in mediating auxin response." Science **292**(5520): 1379-1382.
Shackleford, T. J. and F. X. Claret (2010). "JAB1/CSN5: a new player in cell cycle control and cancer." Cell Div **5**(1): 26.
Shalem, O., N. E. Sanjana, E. Hartenian, X. Shi, D. A. Scott, T. S. Mikkelsen, D. Heckl, B. L. Ebert, D. E. Root, J. G. Doench and F. Zhang (2014). "Genome-scale CRISPR-Cas9 knockout screening in human cells." Science **343**(6166): 3.
Sharon, M., H. Mao, E. Boeri Erba, E. Stephens, N. Zheng and C. V. Robinson (2009). "Symmetrical modularity of the COP9 signalosome complex suggests its multifunctionality." Structure **17**(1): 31-40.
Skaar, J. R., J. K. Pagan and M. Pagano (2013). "Mechanisms and function of substrate recruitment by F-box proteins." Nat Rev Mol Cell Biol **14**(6): 369-381.
Soucy, T. A., P. G. Smith, M. A. Milhollen, A. J. Berger, J. M. Gavin, S. Adhikari, J. E. Brownell, K. E. Burke, D. P. Cardin, S. Critchley, C. A. Cullis, A. Doucette, J. J. Garnsey, J. L. Gaulin, R. E. Gershman, A. R. Lublinsky, A. McDonald, H. Mizutani, U. Narayanan, E. J. Olhava, S. Peluso, M. Rezaei, M. D. Sintchak, T. Talreja, M. P. Thomas, T. Traore, S. Vyskocil, G. S. Weatherhead, J. Yu, J. Zhang, L. R. Dick, C. F. Claiborne, M. Rolfe, J. B. Bolen and S. P. Langston (2009). "An inhibitor of NEDD8-activating enzyme as a new approach to treat cancer." Nature **458**(7239): 732-736.
Soucy, T. A., P. G. Smith, M. A. Milhollen, A. J. Berger, J. M. Gavin, S. Adhikari, J. E. Brownell, K. E. Burke, D. P. Cardin and C. A. Cullis (2009). "An inhibitor of NEDD8-activating enzyme as a novel approach to treat cancer." Nature **458**: 732-736.
Spilburg, C. A., J. L. Bethune and B. L. Valee (1977). "Kinetic properties of crystalline enzymes. Carboxypeptidase A." Biochemistry **16**(6): 1142-1150.
Suh, G. S. B., T. C. Poeck, E. Oron and S. L. Zipursky (2002). "Drosophila JAB1/CSN5 acts in photoreceptor cells to induce glial cells." Neuron **33**(1): 11.

van Wijk, S. J. and H. T. Timmers (2010). "The family of ubiquitin-conjugating enzymes (E2s): deciding between life and death of proteins." FASEB J **24**(4): 981-993.
Wee, S., R. K. Geyer, T. Toda and D. A. Wolf (2005). "CSN facilitates Cullin-RING ubiquitin ligase function by counteracting autocatalytic adapter instability." Nat Cell Biol **7**(4): 387-391.
Wei, N. and X. W. Deng (1992). "<Plant Cell 1992 Wei.pdf>." Plant Cell **4**(12): 11.
Wei, N., G. Serino and X. W. Deng (2008). "The COP9 signalosome: more than a protease." Trends Biochem Sci **33**: 592-600.
Wei, N., G. Serino and X. W. Deng (2008). "The COP9 signalosome: more than a protease." Trends Biochem Sci **33**(12): 592-600.
Welcker, M. and B. E. Clurman (2008). "FBW7 ubiquitin ligase: a tumour suppressor at the crossroads of cell division, growth and differentiation." Nat Rev Cancer **8**(2): 83-93.
Welcker, M., J. Singer, K. R. Loeb, J. Grim, A. Bloecher, M. Gurien-West, B. E. Clurman and J. M. Roberts (2003). "Multisite phosphorylation by Cdk2 and GSK3 controls cyclin E degradation." Mol Cell **12**(2): 381-392.
Wu, G., G. Xu, B. A. Schulman, P. D. Jeffrey, J. W. Harper and N. P. Pavletich (2003). "Structure of a beta-TrCP1-Skp1-beta-catenin complex: destruction motif binding and lysine specificity of the SCF(beta-TrCP1) ubiquitin ligase." Mol Cell **11**(6): 1445-1456.
Wu, K., K. Yamoah, G. Dolios, T. Gan-Erdene, P. Tan, A. Chen, C. G. Lee, N. Wei, K. D. Wilkinson, R. Wang and Z. Q. Pan (2003). "DEN1 is a dual function protease capable of processing the C terminus of Nedd8 and deconjugating hyper-neddylated CUL1." J Biol Chem **278**(31): 28882-28891.
Yamoah, K., K. Wu and Z. Q. Pan (2005). "In vitro cleavage of Nedd8 from cullin 1 by COP9 signalosome and deneddylase 1." Methods Enzymol **398**: 509-522.
Yang, X., S. Menon, K. Lykke-Andersen, T. Tsuge, X. Di, X. Wang, R. J. Rodriguez-Suarez, H. Zhang and N. Wei (2002). "The COP9 signalosome inhibits p27(kip1) degradation and impedes G1-S phase progression via deneddylation of SCF Cul1." Curr Biol **12**(8): 667-672.
Zheng, J., X. Yang, J. M. Harrell, S. Ryzhikov, E. H. Shim, K. Lykke-Andersen, N. Wei, H. Sun, R. Kobayashi and H. Zhang (2002). "CAND1 binds to unneddylated CUL1 and regulates the formation of SCF ubiquitin E3 ligase complex." Mol Cell **10**(6): 1519-1526.
Zheng, N., B. A. Schulman, L. Song, J. J. Miller, P. D. Jeffrey, P. Wang, C. Chu, D. M. Koepp, S. J. Elledge, M. Pagano, R. C. Conaway, J. W. Conaway, J. W. Harper and N. P. Pavletich (2002). "Structure of the Cul1-Rbx1-Skp1-F boxSkp2 SCF ubiquitin ligase complex." Nature **416**(6882): 703-709.
Zhou, Z., Y. Wang, G. Cai and Q. He (2012). "Neurospora COP9 Signalosome Integrity Plays Major Roles for Hyphal Growth, Conidial Development, and Circadian Function." PLoS Genet **8**(5): e1002712.